LIVE LOAD RELIABILITY INDEX EVALUATION
FOR
POST TENSIONED BALANCED CANTILEVER BRIDGES


A THESIS SUBMITTED TO
THE GRADUATE SCHOOL OF NATURAL AND APPLIED SCIENCES
OF
MIDDLE EAST TECHNICAL UNIVERSITY


BY

BERK BORA ÇAKIR


IN PARTIAL FULFILLMENT OF THE REQUIREMENTS
FOR
THE DEGREE OF MASTER OF SCIENCE
IN
CIVIL ENGINEERING


DECEMBER 2015

Approval of the thesis:

## LIVE LOAD RELIABILITY INDEX EVALUATION
## FOR
## POST TENSIONED BALANCED CANTILEVER BRIDGES

submitted by **BERK BORA ÇAKIR** in partial fulfillment of the requirements for the degree of **Master of Science in Civil Engineering Department, Middle East Technical University** by,

Prof. Dr. Gülbin Dural Ünver
Dean, Graduate School of **Natural and Applied Sciences**

Prof. Dr. İsmail Özgür Yaman
Head of Department, **Civil Engineering**

Assoc. Prof. Dr. Alp Caner
Supervisor, **Civil Engineering Dept., METU**


**Examining Committee Members:**

Prof. Dr. Ahmet Türer
Civil Engineering Dept., METU

Assoc. Prof. Dr. Afşin Sarıtaş
Civil Engineering Dept., METU

Assoc. Prof. Dr. Alp Caner
Civil Engineering Dept., METU

Assoc. Prof. Dr. Ayşegül Askan Gündoğan
Civil Engineering Dept., METU

Asst. Prof. Dr. Burcu Güldür
Civil Engineering Dept., Hacettepe University

*Date:*    28.12.2015

**I hereby declare that all information in this document has been obtained and presented in accordance with academic rules and ethical conduct. I also declare that, as required by these rules and conduct, I have fully cited and referenced all material and results that are not original to this work.**

Name, Surname:     Berk Bora ÇAKIR

Signature:

# ABSTRACT

LIVE LOAD RELIABILITY INDEX EVALUATION
FOR
POST TENSIONED BALANCED CANTILEVER BRIDGES

Çakır, Berk Bora

M. Sc., Department of Civil Engineering

Supervisor : Assoc. Prof. Dr. Alp CANER

December 2015, 140 pages

The purpose of this study is to determine the level of safety of the segmental post tensioned bridges designed according to AASHTO LRFD. Main span lengths are 90, 120, 150, 180 are studied in this paper. Four types of trucks are used; H30-S24T and L (currently be in use to design bridges in Turkey), HL-93(AASHTO), KGM-45 (is a new type of load consisting both axle load and lane load). Statistical parameters of truck loads are determined according to the data gathered from the Division of Transportation and Cost Studies of the General Directorate of Highways of Turkey. Target reliability index for ultimate state is chosen as 4.5 at first, then Service 3 stresses with corresponding reliability indices for ultimate capacities are computed. Moreover, this study shows if it is suitable to use the AASHTO LRFD tension limit stress for Service 3 Load Combination. Computing the uncertainties of live load models, extrapolation factors are calculated for 75 years and results are compared whether the

corresponding live load models are adequate for the service life of infrastructures. The most critical reaction is considered in reliability index calculations, the negative moment of pier zone. In addition, reliability indices are calculated for different level of stresses for Service 3 and optimum tensile limit stress is rearranged for Turkish Design Code.

**Keywords:** Segmental Post Tensioned Bridge, Reliability Index, Live Load Models, Statistical Evaluation of Load and Resistance Parameters, Tensile Stress Limit for Service 3

# ÖZ

DENGELİ KONSOL METODU İLE YAPILAN

ARDGERMELİ KÖPRÜLERİN

KAMYON YÜKÜ İÇİN GÜVENİLİRLİK ENDEKSİNİN HESAPLANMASI

Çakır, Berk Bora

Yüksek Lisans, İnşaat Mühendisliği Bölümü

Tez Yöneticisi : Assoc. Prof. Dr. Alp CANER

Aralık 2015, 140 sayfa

Bu çalışma kapsamında, AASHTO LRFD teknik şartnamesine göre tasarımı yapılan ardgermeli dengeli konsol köprülerin, Türkiye şartlarındaki güvenilirlik endeksleri incelendi. Köprü ana açıklıkları 90, 120, 150 ve 180 metre olan 4 adet köprü üzerinde çalışmalar yapıldı. 3 tip kamyon yükü kullanıldı; H30-S24 (şu anda Türkiye'deki köprülerin tasarımında kullanılmakta), HL-93 (AASHTO köprü teknik şartnamesinden), KGM-45 (hem aks hem yayılı yük içeren yeni bir yük tipi). Kamyon yüklerinin istatistiksel parametreleri, Karayolları Genel Müdürlüğünden alınan kamyon yükü dataları ile hesaplandı. Hedef güvenilirlik endeksi, dayanım durumu için 4.5 olarak belirlendi ve daha sonra Servis 3 yük kombinasyonu sonucunda oluşan gerilme değerleri hesaplandı. Buna ek olarak AASHTO LRFD şartnamesindeki Servis 3 yük kombinasyonu için verilen çekme gerilme limitlerinin uygunluğu incelendi.

Köprü tasarımında aktif olarak kullanılan kamyon yüklerinin istatiksel parametreleri çıkarıldı ve bu parametreler kullanılarak 75 yıl sonraki kamyon yüklerinin, kullanılan tasarım kamyonları ile kıyaslanması yapıldı. Ardgermeli dengeli konsolların en kritik bölgesi olan kolon yakınlarındaki negatif eğilme dikkate alınarak güvenilirlik endeksi hesapları tamamlandı. Ayrıca, farklı güvenilirlik endesklerine karşılık oluşan Servis 3 gerilmeleri hesaplanarak, Türk Tasarım Şartnamesine uygun Servis 3 limit gerilmesi elde edildi.

**Anahtar Kelimeler:** Balanced Cantilever Post Tensioned Bridge, Güvenilirlik Endeksi, Kamyon Yükleri, Yük ve Dayanım Parametrelerinin Belirsizlikleri, Servis Durumundaki Çekme Gerilme Limiti

*To my family and my friends*

# ACKNOWLEDGEMENTS

# TABLE OF CONTENTS

# LIST OF TABLES

# LIST OF FIGURES

FIGURES

# CHAPTER 1

# INTRODUCTION

In modern transportation systems like highway and railway network systems, bridges have an important role. As a result of this, bridges must ensure the required strength according to design specifications. Throughout the world, there are many different specifications to determine the certain rules for bridge design. For example, American Association of State Highway and Transportation Officials (AASHTO) is widely used in worldwide and Eurocode is another popular design specifications. Moreover, some countries have their own design specifications such as Germany (DIN), Russia (SNIP).

Since 1971 AASHTO LFD has been used as design specifications for bridges in US. After 1993, the Load Resistance Factor Design specifications are developed including probabilistic approach. Uncertainties of loads and resistance parameters are considered in LRFD specification to obtain probability based calibration. In Turkey a modified version of AASHTO specifications is in use to determine proper design vehicular load system. H30S24 Truck and H30S24 Lane Loads have been used in design according to Turkish Highway Specifications. Recently, there is a new load model named as KGM-45 which consists of three axle load weighing 50 kN, 200 kN, 200 kN and 10 kN/m lane load.

AASHTO Load Factor Design (LFD) design specifications was established based on deterministic methods and engineering judgement. Load Resistance Factor Design (LRFD) is usually based on probabilistic approach. With the new code LRFD load

combinations, impact factors and live load models were defined according to new probabilistic data gathered from US. Hence, this probabilistic approach will be used for Turkey, to compute the calibration factors according to uncertainty in material characteristics, variation in current truck loads, construction errors and similar uncertainties involved in engineering practice in Turkey.

Nowadays, most preferred probabilistic bridge safety parameter is reliability index. As the reliability index of design increases survival probability of the bridge increases. Target reliability index should be specified according to cost of the infrastructure and the optimum safety level.

## 1.1 AIM

There is limited study on reliability indices on design of concrete bridges constructed with balanced cantilever method. Therefore, the purpose of this study is to determine the load and resistance factors for the design and construction of balanced cantilever bridges. In this scope, superstructure closer to pier regions are investigated where the most critical negative moment occurs. Construction stages are also investigated through this study. Moreover, new truck load model of Turkish Highway Specifications KGM-45 is investigated according to 28054 recorded truck data. KGM-45 is an important live load model because it consists of axle load of truck combined with a lane load. Axle loads of KGM-45 is lighter according to H30S24 load, but presence of lane load in KGM-45 makes this truck load arrangement can be more critical for long span bridges.

This study also aims to investigate the statistical parameters related to resistance of post tensioned box girder bridges. Concrete quality and outside factors are effective parameters for actual concrete class. To determine the uncertainties for resistance of the bridge superstructure, statistical parameters of materials are also investigated.

AASHTO LRFD aims to achieve the reliability index of 3.5 for the ultimate strength state. For Turkish Design Code which is prepared in the scope of TUBITAK 110G093, same reliability index is arranged as 4.5. Using different live load model and reliability index, there should be difference between the stress limits of AASHTO and Turkish Design Code. Another purpose of this study is to check the AASHTO tensile stress limits for Service 3 load combination and calibrate it if the corresponding reliability index for ultimate flexural capacities do not meet the target (4.5).

| Determining the bias factors and coefficient of variations for demand and resistance parameters. (CH3&4) | → | Calculating the Service 3 stresses and corresponding reliability indices for ultimate limit state. (CH5&6) |

| Service 3 stress values vs ultimate state reliability index graphs are constructed according to calculations (CH6). | ← | Stress values for Service 3 Load Combination are deviated through changing number of tendonds.(CH6) |

| AASHTO LRFD Tensile stress limit for Service 3 is verified at a target reliability index of 3.5 (CH7). | → | The tension limit stress is rearranged for Turkish Design Code with a target reliability of 4.5 (CH7). |

**Figure 1. Flowchart for Thesis Procedure and Obtaining Service 3 Tension Stress Limit**

## 1.2    SCOPE


The content of the thesis is explained below:


Second Chapter contains the review of the literature on reliability analysis and different live load models. Reliability studies for different variables and comparisons are documented according to different live load modals.


In the Third Chapter, live load models are presented; HL93, H30-S24 Truck and Lane Load, KGM-45 and the truck data are investigated. Moreover, the extreme value theory, presenting heavier group of trucks is used to obtain the increase of live load in 75 years. Statistical parameters of live load models are calculated and illustrated in tabular form according to Gumbel distribution.


Statistical parameters of resistance are illustrated to determine the uncertainties of parameters in the Chapter Four. Also these uncertainty values are used in reliability index calculations.


In the Chapter Five, flexural resistance capacity of segmental box girder-bridge is calculated for different four span lengths of bridges according to AASHTO LRFD. Modelling details, constructional stage results and structural analysis results are illustrated. Moreover, principal stresses at the webs are controlled.


Four different span length bridge models are constructed to investigate construction stages and service loads. Main span length of 90, 120, 150, 180 meters bridge models are constructed and necessary post tensioning determined. For time dependent analysis, 10000. day analysis results are used for steel relaxation and creep-shrinkage effects. Target reliability index is set as 4.5 for the negative moment of box section post-tensioned balanced cantilever for ultimate flexural strength.

Chapter Six includes the reliability analysis of the bridge superstructure for the ultimate capacity state at the closed position. For ultimate limit state H30-S24T and L used from Turkish Highway Design Code (1982), HL-93 from the AASHTO LRFD Bridge Design Specifications and AYK-45 live load model from Koç (2013). AYK-45 live load model is later called as KGM-45.

In the Chapter Seven, results from reliability analyses are compared and additional studies are explained which can be in the future.

# CHAPTER 2

# LITERATURE REVIEW

First printed version of AASHTO was released as Standard Specifications for Highway bridges and Incidental Structures in 1914. In early 1970's AASHTO released Load Factor Design Specification for bridge design. After 1986, AASHTO realized that LFD specification need to be revised related to developing technology and industry. As a result of this, AASHTO started to develop the Load Resistance Factor Design specification which based on uncertainty and reliability aspects. Considering the statistical parameters of resistance and demand, safety level of the LRFD specification is more consistent and reliable.

## 2.1 RELIABILITY INDEX IN LITERATURE

To understand the logic behind the Load Resistance and Factor Design, Nowak (1999) seek to illustrate the procedures used in the development of load and resistance factors. Different types of bridges were investigated for both ultimate strength limit state and service limit state. Moreover, HL93 was developed in LRFD Bridge Design Code as a new live load model and compared to the old one, HS20.

Argınhan (2010) studied a thesis named as "Reliability Based Safety Level of Turkish Type Precast Pre-Stressed Concrete Bridges Designed Accordance with LRFD". Load and resistance parameters were derived from corresponding local data and valid studies. Turkish live load, H30S24 and AASHTO LRFD live load, HL93 were used in

7

his thesis. Four different span lengths are investigated; 25, 30, 35 40 meters. Argınhan used different load and resistance factors to observe the changes in the reliability indices. As shown in figure below, he used 15 different sets of live load and resistance factors and calculate the corresponding reliability indices.
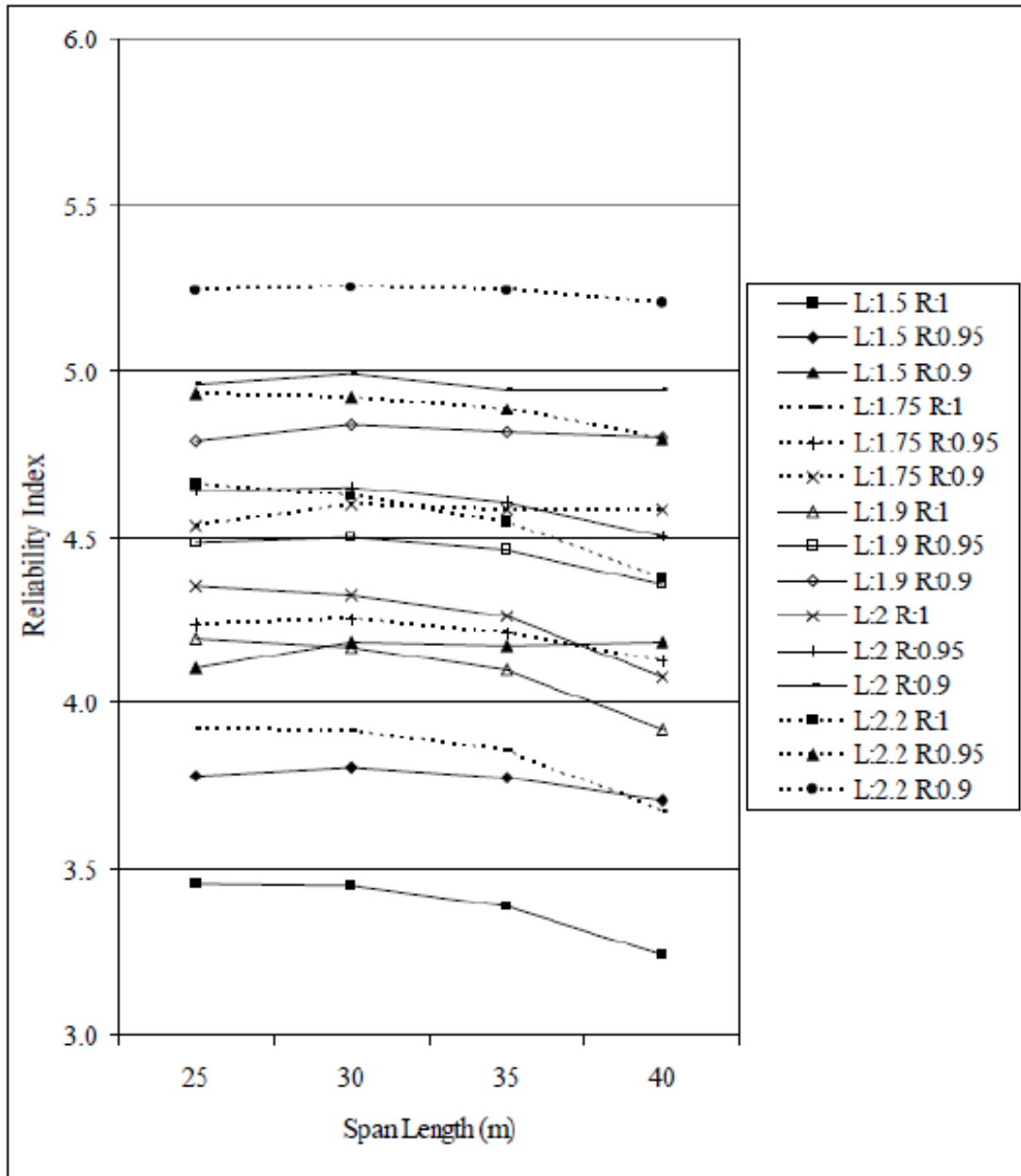


**Figure 2. Reliability Indices for Pretensioned Girders with Different Load and Resistance Factors (Argınhan, 2010)**

With a similar approach to Argınhan's study, Koç (2013) studied on steel bridges to obtain target reliability indices. AASHTO LRFD live load model, HL93 is used and a new suggested live load model AYK-45 were used in his study. Afterwards, AYK-45 is adopted by the Turkish General Directorate of Highways and named as KGM-45. Koç investigated four different span lengths of 50, 60, 70 and 80 meters and the corresponding reliability index values for different live load and resistance factors are shown below.

**Table 1. Reliability Indices for Steel Girder Composite Bridges with Different Load and Resistance Factors for KGM-45 Live Load Model (Koç, 2013)**

| Live Load (LL) and Resistance (R) Factors | Span Length (m) | | | | Average |
|---|---|---|---|---|---|
| | 50 | 60 | 70 | 80 | β |
| LL: 1.50; R: 0.90 | 4.53 | 4.41 | 4.40 | 4.29 | 4.41 |
| LL: 1.50; R: 0.95 | 4.31 | 4.14 | 4.11 | 3.99 | 4.14 |
| LL: 1.50; R: 1.00 | 4.02 | 3.86 | 3.83 | 3.69 | 3.85 |
| LL: 1.75; R: 0.90 | 4.89 | 4.74 | 4.74 | 4.60 | 4.74 |
| LL: 1.75; R: 0.95 | 4.63 | 4.49 | 4.46 | 4.32 | 4.48 |
| LL: 1.75; R: 1.00 | 4.39 | 4.23 | 4.19 | 4.03 | 4.21 |
| LL: 2.00; R: 0.90 | 5.20 | 5.20 | 5.03 | 4.89 | 5.08 |
| LL: 2.00; R: 0.95 | 4.97 | 4.80 | 4.77 | 4.62 | 4.79 |
| LL: 2.00; R: 1.00 | 4.73 | 4.56 | 4.51 | 4.34 | 4.54 |
| LL: 2.25; R: 0.90 | 5.47 | 5.48 | 5.30 | 5.14 | 5.35 |
| LL: 2.25; R: 0.95 | 5.26 | 5.24 | 5.05 | 4.88 | 5.11 |
| LL: 2.25; R: 1.00 | 5.03 | 4.84 | 4.80 | 4.62 | 4.82 |
| LL: 2.50; R: 0.90 | 5.71 | 5.73 | 5.54 | 5.37 | 5.59 |
| LL: 2.50; R: 0.95 | 5.51 | 5.50 | 5.30 | 5.12 | 5.36 |
| LL: 2.50; R: 1.00 | 5.30 | 5.27 | 5.06 | 4.88 | 5.13 |

Dönmez (2015) studied the reliability level of the cable stayed bridges with a main span of 420, 470, 520 and 550meters. He considered uncertainties of the design approach and the construction techniques in Turkey. Considering the data of the Cost Studies of the General Directorate of Highways of Turkey, he obtained the statistical parameters for live load models.

The specified target reliability index is arranged as 4.3 in his study for Strength 1 load combination. Moreover, he calibrated the resistance factor (Ø) to reach the target reliability index. Reliability index and the calibrated resistance factor values for KGM-45 live load model according to Dönmez (2015) is shown in table below.

**Table 2. Reliability Indices for Cable Stayed Composite Bridges with Different Load and Resistance Factors (Dönmez, 2015)**

| Live Load (LL) & Resistance (R) Factors | Span Length (m) | | | | Average β |
|---|---|---|---|---|---|
| | 420 | 470 | 500 | 550 | |
| LL: 1.75; R:0.60 | 4.76 | 4.7 | 4.77 | 4.73 | 4.74 |
| LL: 1.75; R:0.65 | 4.63 | 4.56 | 4.63 | 4.59 | 4.60 |
| LL: 1.75; R:0.70 | 4.49 | 4.42 | 4.5 | 4.45 | 4.47 |
| LL: 1.75; R:0.75 | 4.36 | 4.29 | 4.36 | 4.31 | 4.33 |
| LL: 1.75; R:0.80 | 4.22 | 4.15 | 4.22 | 4.18 | 4.19 |
| LL: 1.75; R:0.85 | 4.09 | 4.01 | 4.09 | 4.04 | 4.06 |
| LL: 1.75; R:0.90 | 3.95 | 3.87 | 3.96 | 3.9 | 3.92 |
| LL: 1.75; R:0.95 | 3.82 | 3.73 | 3.82 | 3.77 | 3.79 |

To reach the target reliability index, the average calibrated resistance factors are illustrated in Figure below.
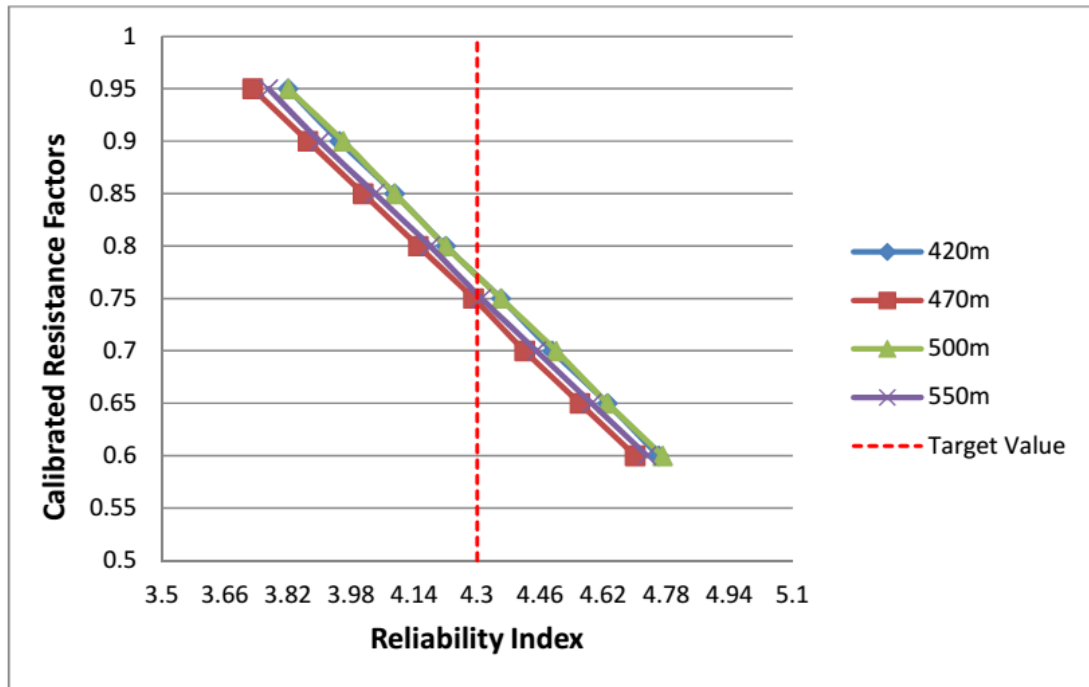


**Figure 3. Calibrated Resistance Factors According to Different Span Length for Cable Stayed Bridges (Dönmez, 2015)**

### 2.1.1 Reliability Index of Chinese Highway Bridges According to Different Variables

Argınhan (2010), Koç (2013) and Dönmez (2015) studies are considerably new and regional studies for Turkey. There are other studies performed around the world to better understand the effect of other parameters on survival probability.

According to Xie's studies, the most important parameters effecting reliability indices are girder spacing and the span length. The reliability index of larger girder spacing are higher based on the more conservative values of girder distribution factors of larger spacing bridges. Besides that, the amount of reinforcement, number of design lanes, concrete grade and load rating are the parameters which effects reliability indices (Xie, 2013).

Huibing Xie, Yuanfeng Wang and Ruofei Zou studied the effect of these parameters on reliability index analyses. In this study only the live load and dead load are considered. The dead load composed of self-weight of precast girders, the weight of deck and parapets and the wearing surface of the bridge. Two types of live load are used through this study, Highway level 1 and Highway level 2. Both live load models are studied according to Code for Design of Highway Bridges and Culverts (China) and also details of these load models will be given.
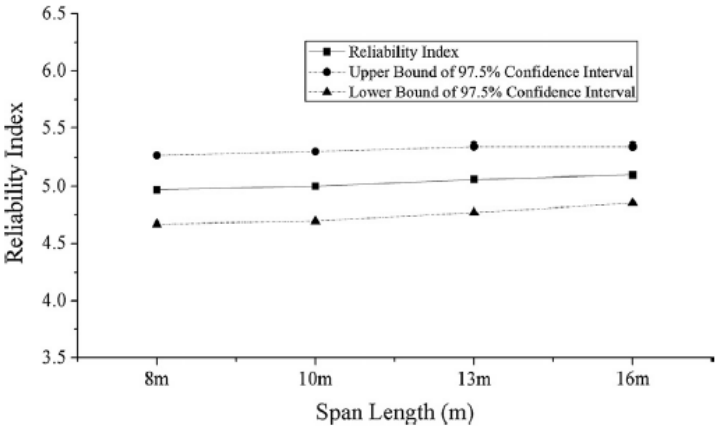


**Figure 4. Reliability Index vs Span Length (Xie, 2013)**
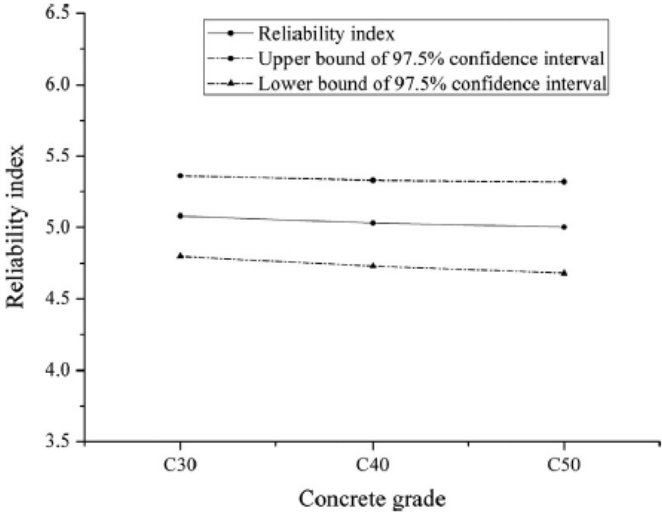


**Figure 5. Reliability Index vs Concrete Grade (Xie, 2013)**

12

### 2.1.2 Comparison of Reliability Index for Eurocode, Spanish Norma IAP and AASHTO LRFD

Another study about reliability index is performed by Nowak, Park and Casas to compare the Eurocode, Spanish Norma IAP and AASHTO LRFD. Since the live load is the most site-specific variable, the calculations were carried out for the live load models based on the Spanish data and Ontario truck surveys. Through this study, reliability indices according to different codes are determined and compared (Nowak, Park and Casas, 2001).
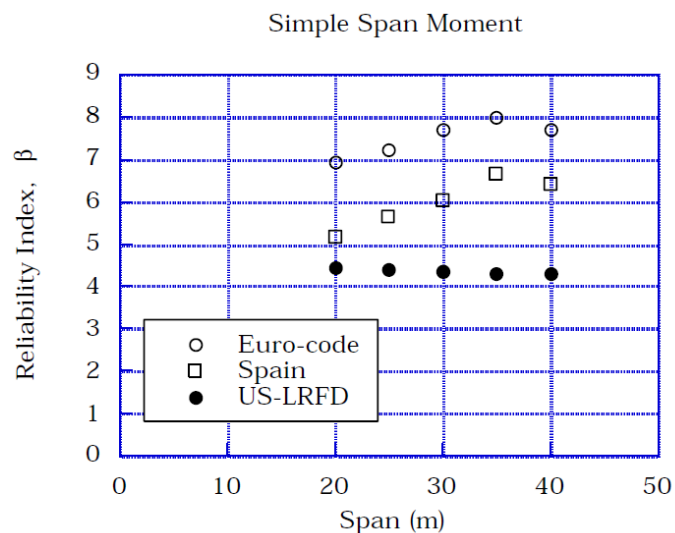


**Figure 6. Reliability Index According to Different Highway Design Codes (Nowak, Park and Casas, 2001)**

## 2.2 LIVE LOAD MODELS OF DIFFERENT HIGHWAY DESIGN CODES

There are different live load models for highway bridges around the world. Among others Eurocode and AASHTO live load models are the most internationally recognized ones. HL-93 is one of the important live load models of AASHTO LRFD. AASHTO Live Load Models will be explained in Chapter 3 because they are

13

considered as main live loads in this study, but to have an idea, other live load models are explained in this chapter. AASHTO and the Eurocode are the most popular two bridge design specification across the world. According to the Eurocode design specification there are 4 different load model type for highway bridges.

### 2.2.1 Eurocode Load Model 1

Load model 1 consists of double point load and uniformly distributed load. Double point load weights specified as $\alpha_Q Q_k$ where, $\alpha_Q$ is adjustment factor and $Q_k$ is the axle weight.

- One tandem system is taken into account per notional lane
- To obtain the maximum effects, each truck load is assumed as moving along the lane
- Each axle load of the tandem system should be taken as equal and 0.5 $\alpha_Q Q_k$
- Wheel contact area is 0.4 x 0.4 meter square

Uniformly distributed loads is defined as $\alpha_q q_k$ per square meter for notional lane where $\alpha_q$ is adjustment factor. The UDL loads are applied to unfavourable parts or the influence surface, both longitudinally and transversally.

Load Model 1 should be applied to each notional lanes and on the remaining areas. For each notional lane, the load magnitudes ($\alpha_{Qi} Q_{ik}$, $\alpha_{qi} q_{ik}$) are specified in Table 3. Beyond this specified lane loads, the load is designated as $\alpha_{qr} q_{rk}$ for the remaining areas. $\alpha_{Qi}$, $\alpha_{qi}$, $\alpha_{qr}$ adjustment factors should be selected based on the expected traffic volume. On the other hand, if there is an absence of this information the load factors are taken as 1.0. Dynamic amplification factor must be applied to the characteristics values of $Q_{ik}$, $q_{ik}$ shown in Table 3.

**Table 3. Characteristic Values for Eurocode Load Model 1 (Eurocode 1991-2:2003)**

| Location | Tandem System TS | UDL system |
|---|---|---|
| | Axle loads $Q_{ik}$ (kN) | $q_{ik}$ (or $q_{rk}$) (kN/m2) |
| Lane Number 1 | 300 | 9 |
| Lane Number 2 | 200 | 2.5 |
| Lane Number 3 | 100 | 2.5 |
| Other Lanes | 0 | 2.5 |
| Remaining area($q_{rk}$) | 0 | 2.5 |
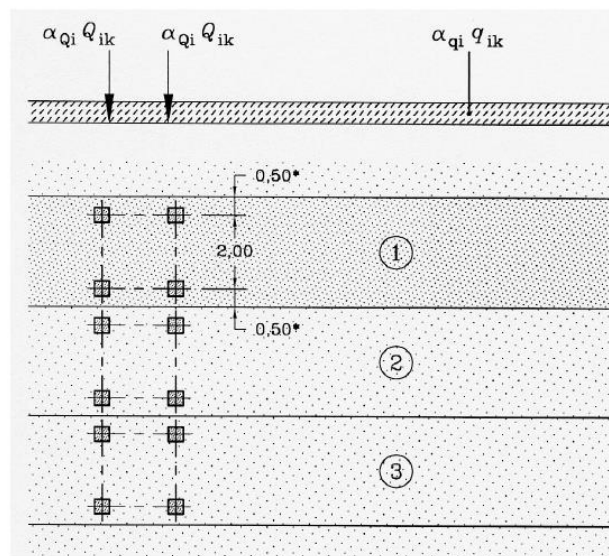


**Figure 7. Axle Configuration and Live Load Details of Load Model 1 (Eurocode 1991-2:2003)**

To obtain the maximum results for truck loads, the tandem system must be located for the most critical results. In case of occurrence for the two tandem systems on one lane there should be a minimum distance of 0.5 meters as shown in Figure 8.
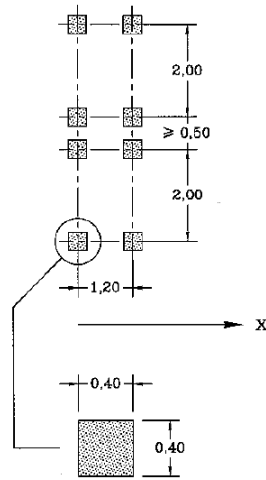
**Figure 8. Tandem Application System for Local Verifications (Eurocode 1991-2:2003)**

To obtain the general and local effects separately, the general effects may be calculated with simplified general rules given below;

a) An alternative second tandem system is used as substitute for the second and third tandem systems displayed as :

(200 kN $\alpha_{Q2}$ + 100 kN $\alpha_{Q3}$) kN or,

b) Spans lengths which is greater than 10 meters, tandem systems are modified to single axle load that weighs two axle loads.

- 600 $\alpha_{Q1}$ kN on Lane Number 1
- 400 $\alpha_{Q2}$ kN on Lane Number 2
- 200 $\alpha_{Q3}$ kN on Lane Number 3

### 2.2.2 Eurocode Load Model 2

There is a single tandem system load in Load Model 2 which is specified as $\beta_Q Q_{ak}$ with $Q_{ak}$ equal to 400 kN. On the other hand, 200 $\beta_Q$ kN load can be used alone when it is suitable. According to Eurocode specified $\beta_Q$ value is taken as equal to $\alpha_{Q1}$. The dynamic amplification is included to axle load, however it is also recommended that there should be an additional amplification factor for expansion joints.

16
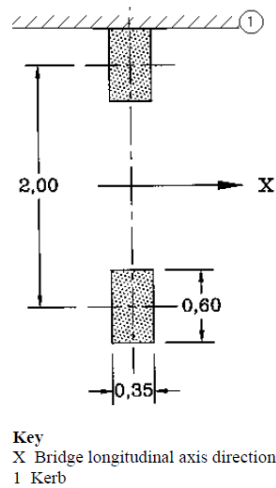
**Figure 9. Tandem Application System for Local Verifications (Eurocode 1991-2:2003)**

Dynamic load amplification is included to Load Models 1 to 4 for pavements of good quality. Moreover, an additional amplification factor should be considered for near expansion joints and should be applied to all loads:

$$\Delta\varphi_{fat} = 1.30\left(1 - \frac{D}{26}\right) \quad ; \quad \Delta\varphi_{fat} \geq 1 \qquad [1]$$

D(m) is the distance of the cross section under consideration from expansion joint.
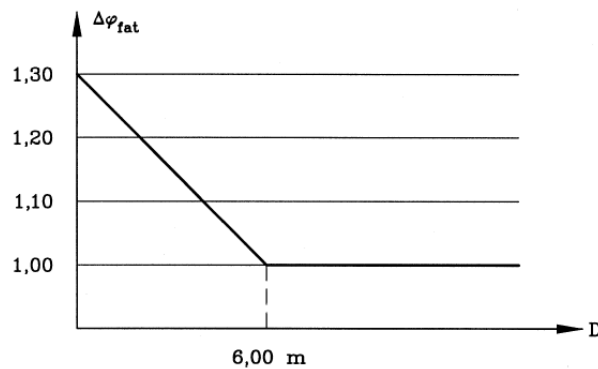


**Figure 10. Additional Amplification Factor (Eurocode 1991-2:2003)**

## 2.2.3 Eurocode Load Model 3

Load model 3 specifies the basic special vehicles as shown in Table 4 and 5 according to EN 1991-2:2003 Annex A Model of Special Vehicles for Road Bridges.

**Table 4. Classes of Special Vehicles (Eurocode 1991-2:2003)**

| Total Weight | Composition | Notation |
|---|---|---|
| 600 kN | 4 axle-lines of 150 kN | 600/150 |
| 900 kN | 6 axle-lines of 150 kN | 900/150 |
| 1200 kN | 8 axle-lines of 150 kN | 1200/150 |
| | or 6 axle-lines of 200 kN | 1200/200 |
| 1500 kN | 10 axle lines of 150 kN or | 1500/150 |
| | 7 axle-lines of 200 kN + 1 axle line of 100 kN | 1500/200 |
| 1800kN | 12 axle lines of 150 kN | 1800/150 |
| | or 9 axle-lines of 200 kN | 1800/200 |
| 2400 kN | 12 axle-lines of 200 kN | 2400/200 |
| | or 10 axle-lines of 240 kN or 6 axle-lines of 200 kN + | 2400/240 |
| | 6 axle-lines of 200 kN | 2400/200/200 |
| 3000 kN | 15 axle-lines of 200 kN | 3000/200 |
| | or 12 axle-lines of 240 kN + 1 axle-line of 120 kN or 8 | 3000/240 |
| | axle-lines of 200 kN + 7 axle-lines of 200 kN | 3000/200/200 |
| 3600 kN | 18 axle-lines of 200 kN | 3600/200 |
| | or 15 axle-lines of 240 kN | 3600/240 |
| | or 9 axle-lines of 200 kN + 9 axle-lines of 200 kN | 3600/200/200 |

**Table 5. Description of Special Vehicles (Eurocode 1991-2:2003)**

| Total Weight | Axle Lines of 150 kN | Axle Lines of 200 kN | Axle Lines of 240 kN |
|---|---|---|---|
| 600 kN | n = 4 x 150<br>e = 1.50 m | | |
| 900 kN | n = 6 x 150<br>e = 1.50 m | | |
| 1200 kN | n = 8 x 150<br>e = 1.50 m | n = 6 x 200<br>e = 1.50 m | |
| 1500 kN | n = 10 x 150<br>e = 1.50 m | n = 1 x 100 + 7 x 200<br>e = 1.50 m | |
| 1800kN | n = 12 x 150<br>e = 1.50 m | n = 9 x 200<br>e = 1.50 m | |
| 2400 kN | | n = 15 x 200<br>e = 1.50 m<br>n = 6 x 200 + 6 x 200<br>e = 5 x 1.5 + 12 + 5 x 1.5 | N = 10 x 240<br>e = 1.50 m |
| 3000 kN | | n = 15 x 200<br>e = 1.50 m<br>n = 8 x 200 + 7 x 200<br>e = 7 x 1.5 + 12 + 6 x 1.5 | N = 1 x 120 + 12 x 240<br>e = 1.50 m |
| 3600 kN | | n = 18 x 200<br>e = 1.50 m | N = 15 x 240<br>e = 1.50 m<br>n = 8 x 240 + 7 x 240<br>e = 7 x 1.5 + 12 + 6 x 1.5 |
| NOTE | | | |
| n   number of axles multiplied by the weight (kN) of each axle in each group | | | |
| e   axle spacing (m) within and between each group | | | |

### 2.2.4 Eurocode Lode Model 4

Load Model composed of 5 kN/m$^2$ uniformly distributed load including dynamic effects. Load Model 4 should be applied on the relevant parts of the bridge in longitudinal or transverse ways, if necessary.

### 2.2.5 Spanish Highway Truck Load According to Spanish Norma IAP-98

According to the Spanish Norma IAP-98 Actions in Highway bridges, the live load model for Spain Highway bridges consists of six axle load with lane loading. Axle loads are 100 kN each and tire contact areas are 0.2m x 0.6m. Six axle loads represents the effect of two trucks with three axle loads. Lane load is 4 kN/m$^2$ over the entire bridge surface. The corresponding illustration of the Spanish Highway Truck Load is given in Figure 11. Additional dynamic load is specified as equal to 15% of the static live load.
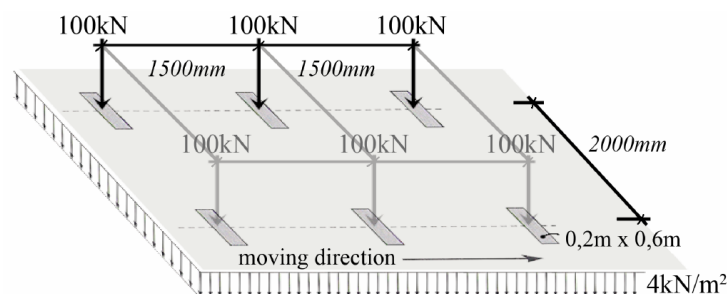


**Figure 11. Spanish Live Load Model for Highway Bridges (J.J.Orr, 2008)**

## 2.2.6 The Highway Live Load Model of Chinese Bridge Specifications

There are two highway load types for Technical Standard of Highway Engineering (JTG B01-2003, China). Design live loads are composed of both concentrated load and uniform load. Highway load types for China Bridge Design Specifications is given in tabular and schematic form correlatively.
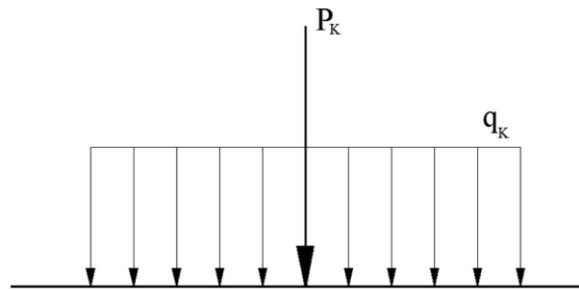


**Figure 12. Simple Sketch of Chinese Highway Load Types (Xie, 2013)**

**Table 6. Description of Design Lane Loading (Xie, 2013)**

| Design Lane Load | Concentrated Load(kN)** | Uniform Load(kN/m) |
|---|---|---|
| Highway level 1 | 4I + 160* | 10.5 |
| Highway level 2 | 3I + 120 | 7.9 |
| *l is the span length | **Range of span length is 5m < L < 50m | |

# CHAPTER 3

# STATISTICS OF LOADS

In the design process of the highway bridges, the most common loads used in design are dead load (concrete, wearing surface, miscellaneous), temperature load (uniform or gradient temperature), live load (vehicular live load; highway or railway). The combinations of these loads may be effective for bridge service life. To complete the reliability analysis, the statistical parameters of these loads must be computed. Moreover, loads are effecting the reliability analysis through related load combinations and to begin with, these load combinations should be explained.

AASHTO LRFD include the necessary load combinations for both service limit state and strength limit state to be used in the design. For concrete bridges, post tensioning tendons are determined at Service 3 limit state, the strength limit state is just used as a design check of selection. Moreover, for segmentally constructed post tensioned bridges, constructional stage analyses must be investigated to have a better crack control and excessive deformations that may develop at different phases of construction. The load combinations according to AASHTO LRFD design specification are explained below;

- Service 1: Wind load plus normal operational use of the bridge and all load factors are 1. Service 1 load combination is used in transverse analysis relating to tension in concrete and to control crack width in reinforced concrete members.

- Service 2: This combination is used to control yielding of steel structures and slip of slip critical steel connections due to vehicular live load.

- Service 3: To determine the flexural tension stresses by longitudinal analysis, Service 3 combination is used. Moreover, the requirements for crack control in pre-tensioned beams is satisfied.

- Service 4: Tension in pre-stressed concrete columns is investigated through this combination.

- Strength 1: Simple load combination consists of operational bridge load without wind.

- Strength 2: Load combination for special vehicular live load which is specified before.

- Strength 3: Load combination according to the bridge exposed to wind force.

- Strength 4: Load combination relating to very high dead load to live load force effect ratios.

- Extreme Event 1: Load combination including earthquake. The load factor for live load shall be specific for different projects.

- Extreme Event 2: Load combinations according to collision by vehicle or vessels, ice load, floods and possible hydraulic events.

- Fatigue: Load combination related to the repetitive loads and dynamic effects for bridges.

For post tensioned bridges constructed with balanced cantilever method, Service 3 load combinations should be used to determine the amount of post tensioning. Stresses and deflections during different stages of construction investigated. Strength 1 load combination is used to estimate the ultimate strength of the superstructure. The new live load KGM-45 and the other live load models can only be checked at closed position of the bridge at Service 3 and Strength 1 limit states.

$$\text{Service } 3 = DC + DW + 0.8*LL*(1+IM) \tag{2}$$

$$\text{Strength } 1 = 1.25*DC + 1.5*DW + 1.75*LL*(1+IM) \tag{3}$$

DC = Weight of structural and non-structural parameters

DW = Weight of wearing surface

LL = Vehicular live load

IM = Impact factor

## 3.1  DEAD LOAD

In this study, dead load components are investigated as three different load case.

$D_1$ = Weight of cast in place concrete

$D_2$ = Weight of wearing surface (15.9 kN/m)

$D_3$ = Weight of miscellaneous (10.34 kN/m)

Statistical parameters for dead load components are taken from Nowak's study (Nowak, 1999). Uncertainties of specified dead load parameters are assumed to be normally distributed and corresponding parameters are given in Table 7 below.

**Table 7. Dead Load Statistical Parameters According to Nowak's Calibration Report**

| Dead Load Component | Bias Factor | Coefficient of Variation |
|---|---|---|
| Cast-in-place Concrete, $D_1$ | 1.05 | 0.1 |
| Wearing Surface, $D_2$ | 1 | 0.25 |
| Miscellaneous, $D_3$ | 1.03 - 1.05 | 0.08 - 0.10 |

## 3.2    LIVE LOADS

Four different types of live load model are used in this study. HL-93 is taken from AASHTO LRFD, KGM-45, H30-S24 Truck and Lane load from Turkish Highway Design Specifications. Moreover, the data collected from the government agencies responsible for recording truck weights and over 28.000 truck data are used to determine the statistical parameters of live load models.

### 3.2.1    HL-93 Live Load Model

HL-93 Live load model is obtained from AASHTO LRFD Bridge Design Specifications. This load model has 3 axle loads and a lane load. First two axle spacing is 4.3 meters, but the distance between second axle and the third is varies from 4.3 to 9 meters to develop more critical results. First axle load is 35 kN, the other axle loads are 145 kN and the lane load is 9.3 kN/m as uniformly distributed live load. Corresponding load schema for HL-93 live load is shown in Figure 13 and Figure 14.
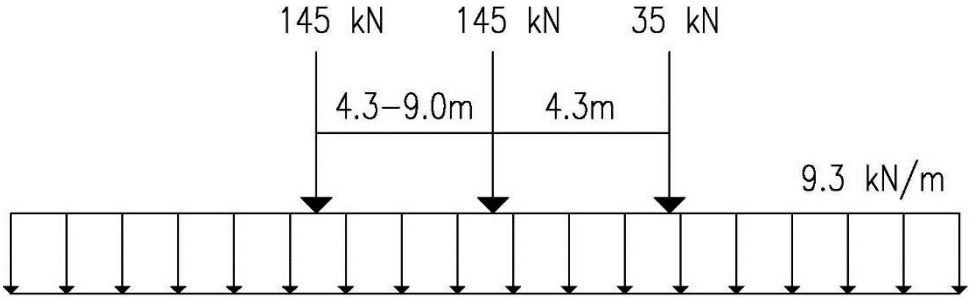


**Figure 13. HL-93 Live Load and Truck Load (AASHTO LRFD)**

26
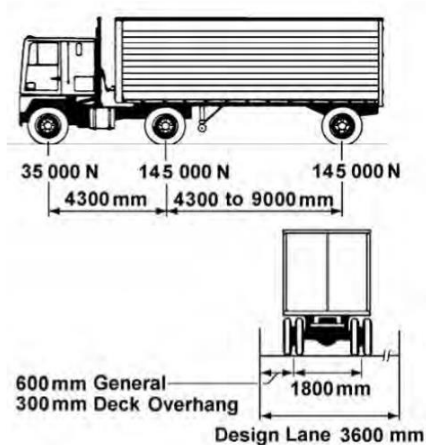
**Figure 14. HL-93 Live Load Truck Details (AASHTO LRFD)**

### 3.2.2 H30-S24 Truck Load Model

Turkish Highway Design Specification (1982) proposed a live load model named H30-S24. Basically this load is 1.5 times escalation of HS20-44 live load model from AASHTO specifications. H30-S24 live load model has two different types; first one is a 3 axle truck load with axle loads as 60 kN, 240 kN, 240 kN. First two axle spacing is 4.25 meters and the distance between second and third axle varies from 4.25 to 9 meters. Second type of H30-S24 load model is lane loading with one axle load to create the maximum moment or shear effect. H30-S24 truck load details are given below.
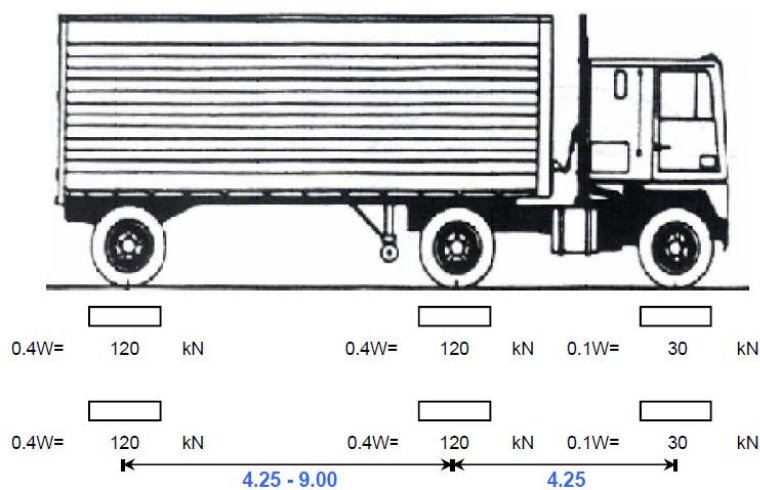


**Figure 15. H30-S24 Truck Load Details (KGM, 1982)**

27
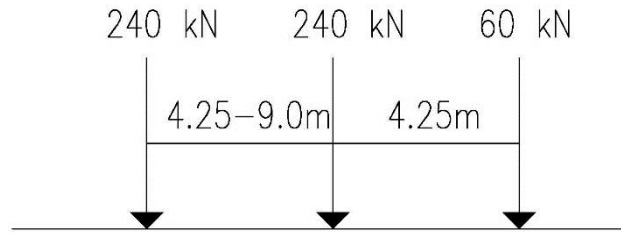
**Figure 16. H30-S24 Truck Load Details (KGM, 1982)**

### 3.2.3  H30-S24 Lane Load Model

H30-S24 lane load is another live load model of Turkish Highway Design Specification (1982) which is composed of lane load and single axle load. There are two types of H30-S24 lane load the first one is to obtain maximum moment and axle load is 135 kN which is applied to mid-span. The second one is to obtain maximum shear force and axle load is 195 kN and it should be located near supports. In addition, there is 15 kN/m lane load with both axle loads. The detailed live load models are given in Figure 17 and 18 for H30-S24 lane loads.
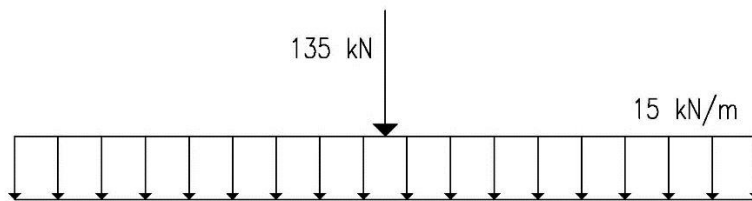


**Figure 17. H30-S24M Lane Load Details (KGM, 1982)**
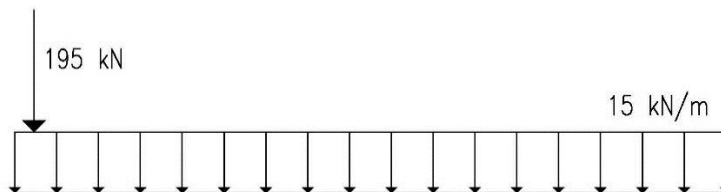


**Figure 18. H30-S24V Lane Load Details (KGM, 1982)**

28

### 3.2.4 KGM-45 Truck Load Model

*"In the calibration of AASHTO LRFD for Turkey, a new live load model is going to be implemented. The new model is called AYK45, in which AYK stands for "Ağır Yük Kamyonu" meaning "Heavy Load Truck" in Turkish and "45" is total weight of truck in units of ton. Similar to HL-93 truck model philosophy, AYK45 needs to be used with a uniform lane load of 10 kN/m* (Koç, 2013)."

After the relevant studies and researches, Turkish General Directorate of Highways adopted the new load model as KGM-45. KGM-45 consists of a truck and lane loading. Truck load of KGM-45 has 3 axle loads as 50 kN, 200 kN and 200 kN respectively. The distance is 4.25 meters between the first axle load and the second one. On the other hand, the distance between 200 kN's is varying from 4.25 up to 9.3 meters.
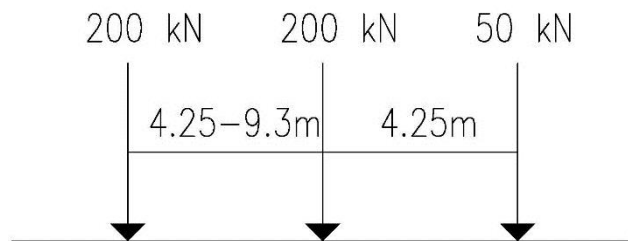


**Figure 19. KGM-45 Truck Load Details (Koç, 2013)**
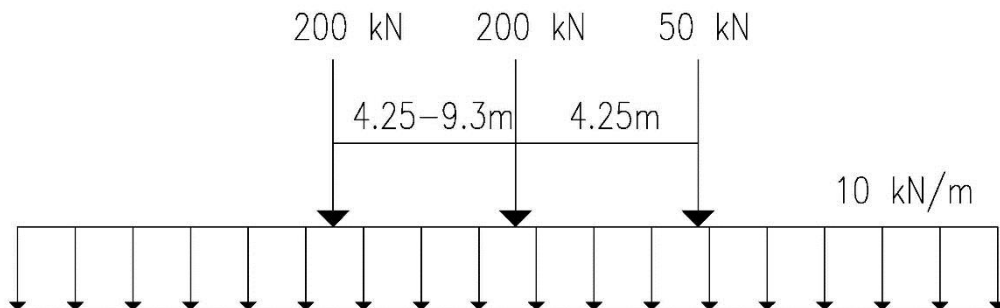


**Figure 20. KGM-45 Live Load Model (Koç, 2013)**

29

### 3.2.5   Actual Truck Loading for Turkey

Over 28.000 truck data collected from the government agencies responsible for recording truck weights at different zones of Turkey is used in this study. The number of axle loads of trucks ranged from 2 to 5 for the years 2005, 2006 and 2013. The selected truck loads are compared to the design loads through a probabilistic study.

**Table 8. Truck Survey Data**

| Axle Count | Number of Data | Percentage (%) |
|---|---|---|
| 2 Axle | 2904 | 10.35 |
| 3 Axle | 15084 | 53.77 |
| 4 Axle | 7351 | 26.20 |
| 5 Axle | 2715 | 9.68 |
| Total | 28054 | 100 |

2 axle and 5 axle trucks are not common types in Turkey as shown in Table 8. The most popular trucks have either 3 axle, or 4 axles. Moments due to pass of each truck is investigated for post tensioned bridges. To obtain the most critical negative moment, two trucks following each other by 15 meters of back to front spacing are used at the same time. As a result of this process, for every bridge there are 28054 maximum moment results to perform a statistical analysis and obtain the uncertainties of live loads.
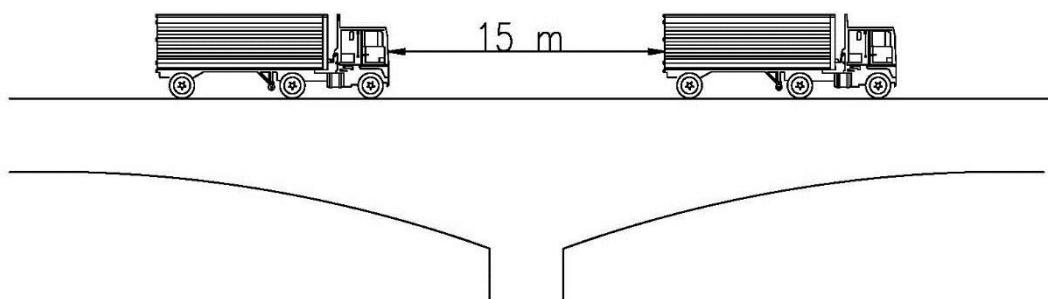


**Figure 21. Live Load Arrangement for Maximum Negative Moment**

### 3.2.6 Moments resulting from live loads models

Moment results for vehicular loads are calculated for 90, 120, 150 and 180 meters of span length using design live load models and actual truck loading. To obtain the maximum moments for truck loads, moving load analysis are performed. The governing truck load model is KGM-45 due to the long span variations except the span length of 180 meters when there is no dynamic factor. The live loads are arranged for three lane bridges. For comparison of the results, Table 9 and Figure 22 are shown below.

**Table 9. Maximum Truck Load Results for 3 Lanes (Without Dynamic Amplification Factor)**

| Span Length (m) | Maximum Moment (kN.m) | | |
|---|---|---|---|
| | HL-93 | H30-S24 | AYK-45 |
| 90 | 31751.1 | 29460.9 | 38261.8 |
| 120 | 60768.8 | 44715.6 | 66180.9 |
| 150 | 82734.3 | 58012.6 | 97080.7 |
| 180 | 113994.5 | 70864.8 | 132492.8 |
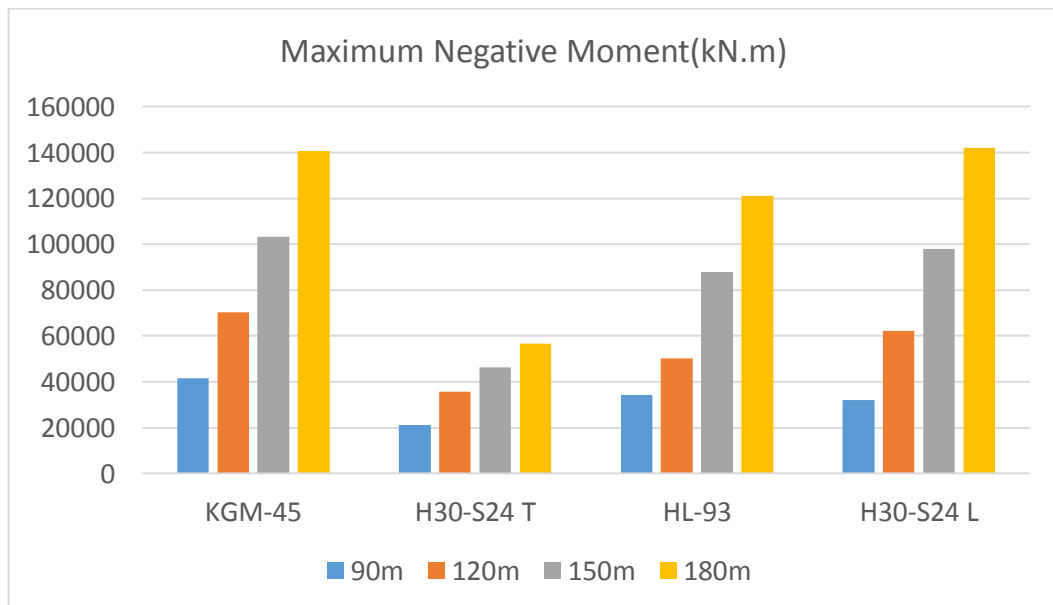


**Figure 22. Negative Moment Comparison for Different Live Load Models and Span Length**

31

### 3.2.7 Statistical Evaluation of Truck Survey Data

In calibration of AASHTO LRFD, the extreme value theory was used to determine the statistical parameters for current live loads (Nowak, 1999). The idea of evaluating this method for truck loads is to determine the changes through years for truck live loads. The moment ratios for surveyed trucks and truck live loads, KGM-45, H30-S24 and HL-93 are plotted with normal and Gumbel probability approach for three different cases named as overall, upper-tail and extreme. Also there is an additional 10 kN/m for each truck survey finding the statistical parameters of H30-S24 Lane, HL-93 and KGM-45 Load Models. On the other hand, H30-S24 statistical parameters are obtained by using the truck data without lane loading.

Overall surveyed truck moments are determined through using 28054 truck data. To determine the statistical parameters for the live load cumulative distribution functions of overall data are plotted. In upper-tail case, cumulative distribution function is calculated according to the highest %10 of the surveyed truck moments. The last approach for surveyed trucks is isolated case for top %10 of the truck moments. By fitting straight lines to the evaluated truck moment data, the maximum moments of future are determined for the time periods of; 1 day, 2 weeks, 1 month, 2 months, 6 months, 1 year, 5 years, 50 years and 75 years.
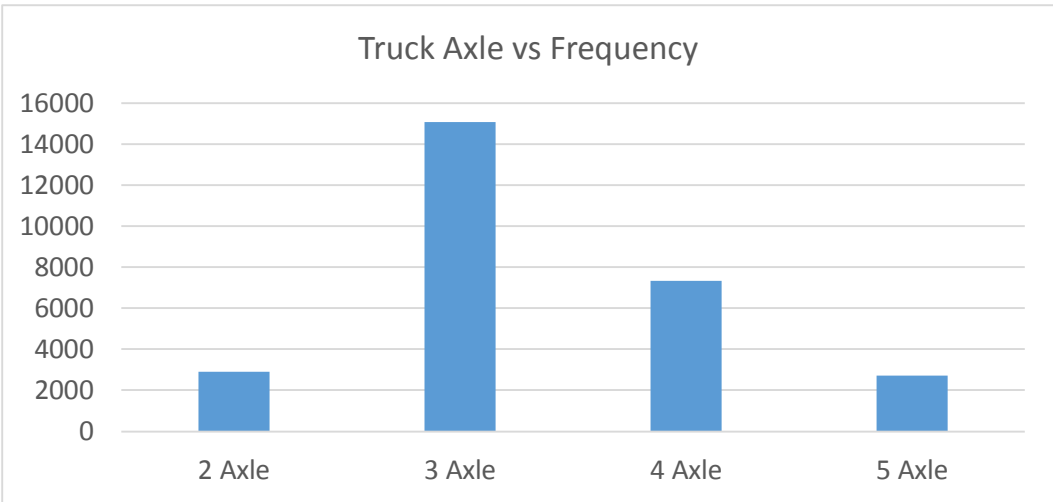


**Figure 23. Surveyed Truck Axle Configuration Frequency**
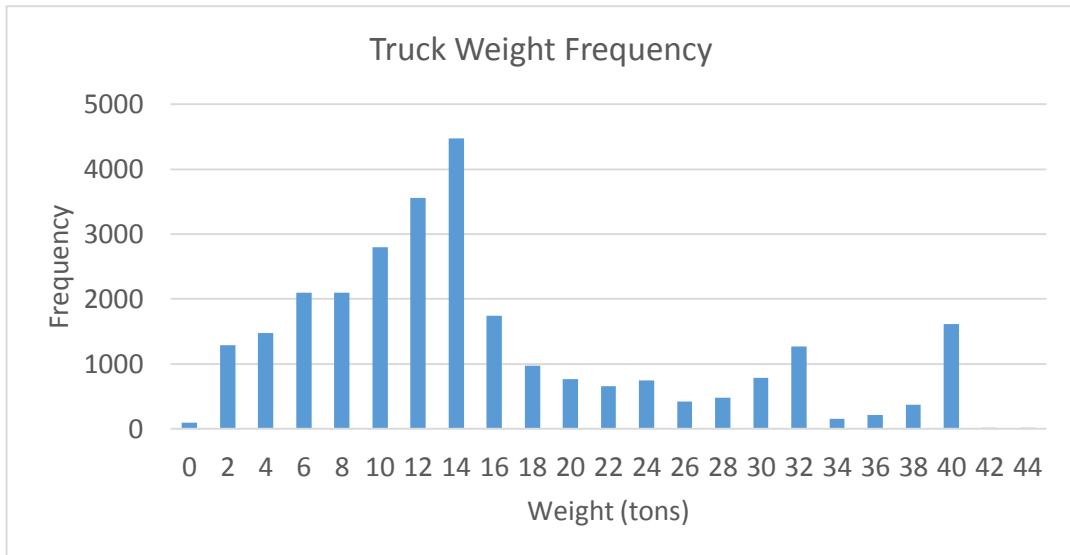
**Figure 24. Surveyed Truck Weight Histogram**

The maximum pier moments are calculated according to 28054 truck survey data for the bridge span lengths of 90, 120, 150 and 180 meters. Related histograms constructed according to the resultant moments and illustrated between Figure 25 and Figure 28 below.
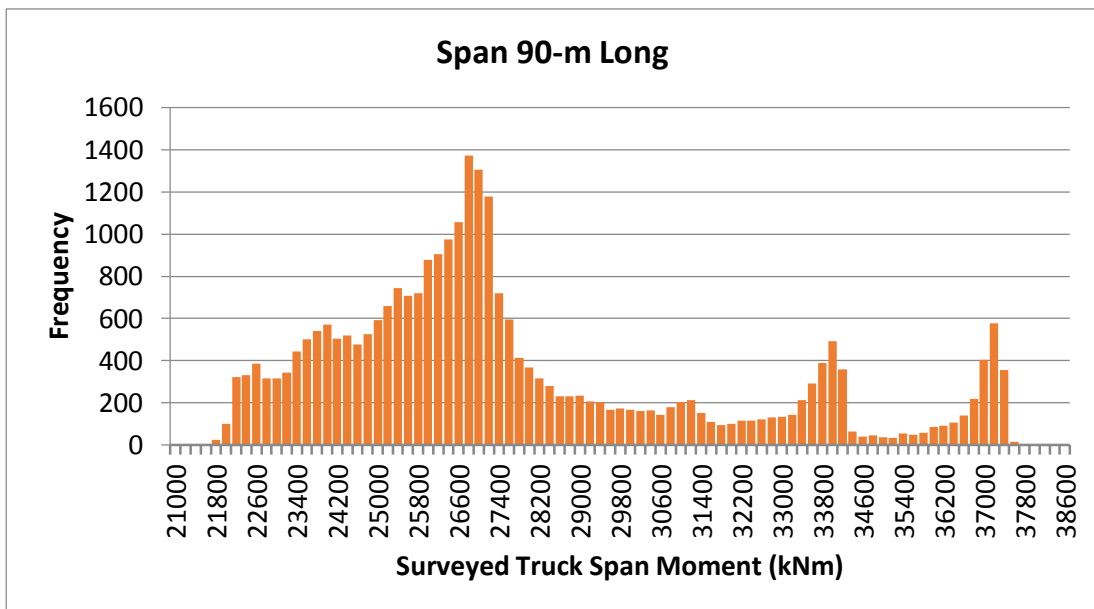


**Figure 25. Negative Moment Histograms of Surveyed Trucks for 90 meter Span Length**
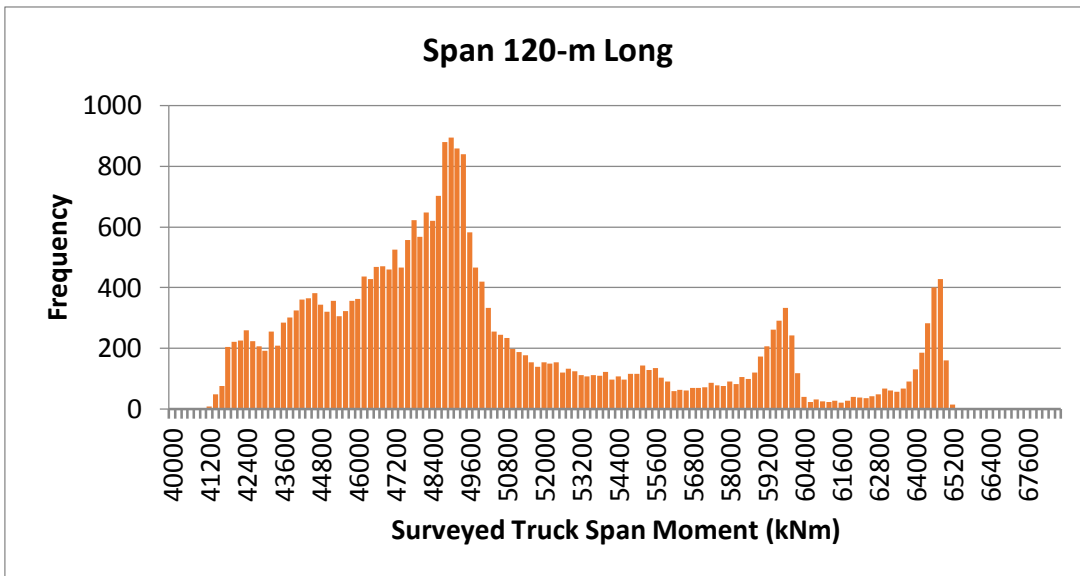
**Figure 26. Negative Moment Histograms of Surveyed Trucks for 120 meter Span Length**
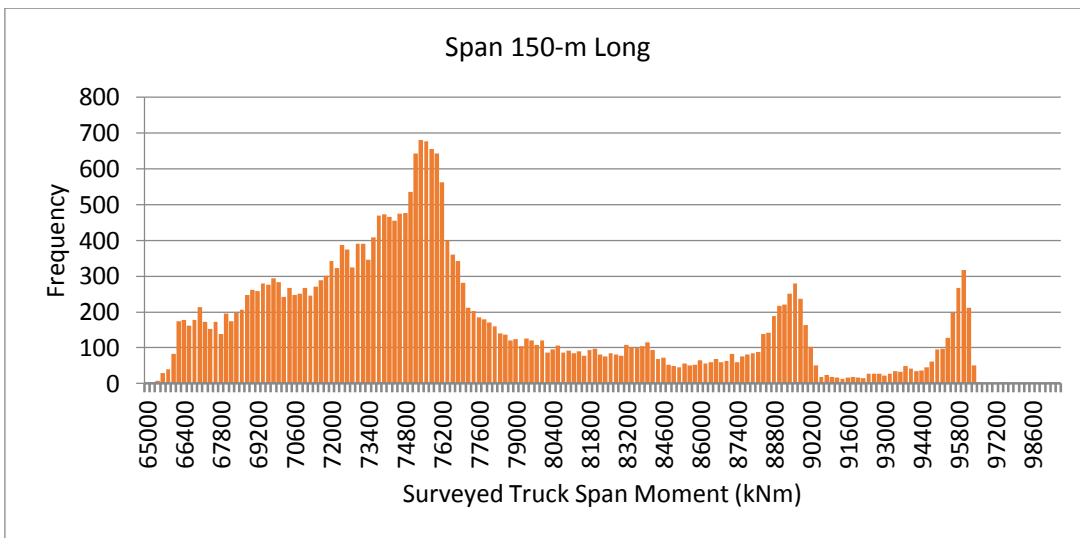


**Figure 27. Negative Moment Histograms of Surveyed Trucks for 150 meter Span Length**
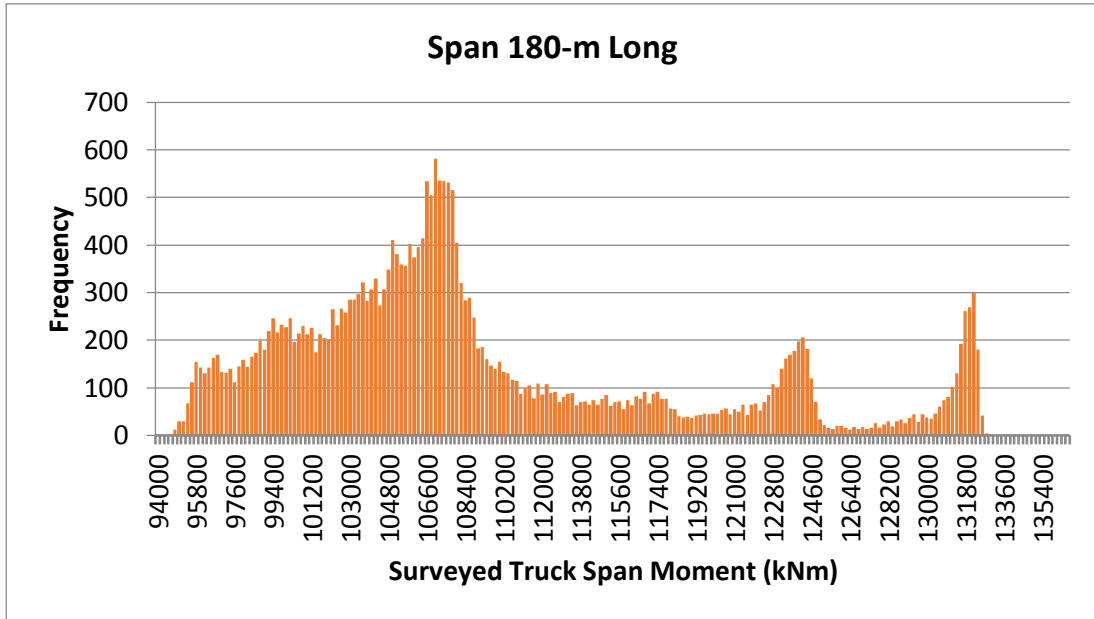
**Figure 28. Negative Moment Histograms of Surveyed Trucks for 180 meter Span Length**

## 3.2.8 Fitting Straight Lines to the Cumulative Distribution Functions of Surveyed Trucks

To determine the cumulative distribution functions of the surveyed truck moments, normal and Gumbel probability approaches are evaluated and according to the level of fitting, distribution type is determined. KGM-45, HL-93 and H30-S24 Truck and Lane live load moment ratios according to overall surveyed truck data are presented in Figures 29 to 32. The vertical axis in these graphs stands for the inverse of the standard normal distribution, expressed according to z,

$$z = \Phi^{-1}\left[F(M)\right] \qquad [4]$$

M is the superstructure moment at the piers and F(M) is the cumulative distribution function of pier top moment. Moreover, the horizontal axis values are illustrating the pier top moment ratios for truck live loads.

35

For each live load models and span lengths for normal probability approach are illustrated between Figures 49 to 64. As seen in the figures normal distribution is not fit the data. As a result of this, normal distribution is not the appropriate distribution for survey truck data. So, Gumbel probability method is used to determine the statistical parameters for survey truck data. Gumbel probability method is valid when the limit distribution of data is not known.

Different from normal distribution, in Gumbel probability method η is defined as in the following equation (Castillo, 1988);

$$\eta = -ln[-ln[F(M)]] \qquad [5]$$

The vertical axis stands for the inverse of the standard normal distribution and the horizontal axis. Where M is the superstructure moment at piers, F(M) is the cumulative distribution function.

Between the Figures 33 to 40, overall truck survey data moment ratios to live load models for each spans were plotted according to Gumbel Probability papers. As a result of comparison of the two probability methods, results shows that Gumbel probability approach is more suitable for truck survey data. Moreover, the statistical parameters calculated according to Gumbel probability and used to obtain the reliability indices.

Upper-tail and extreme approaches for Gumbel probability papers are illustrated in Figure 41 to 64 respectively. These equations obtained by using Gumbel distribution will be used to extrapolate the moment results up to 75 year time period for the expected truck moments in future. Moreover, the constants of equations are used to determine the statistical parameters of truck live loads.
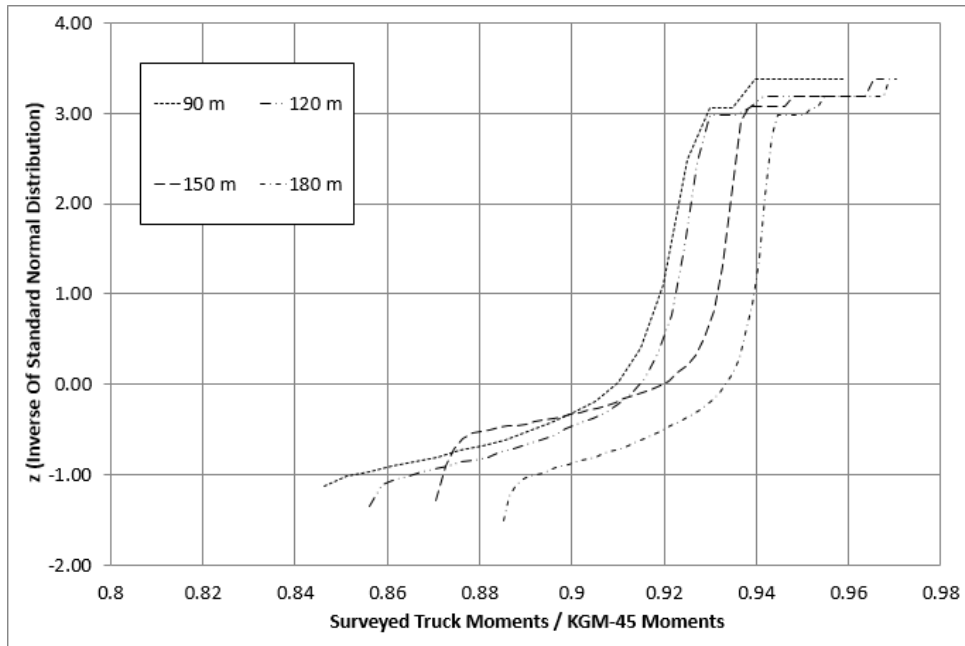
**Figure 29. Normal Probability Paper of Extreme Truck Survey Data for the Live Load Model KGM-45**
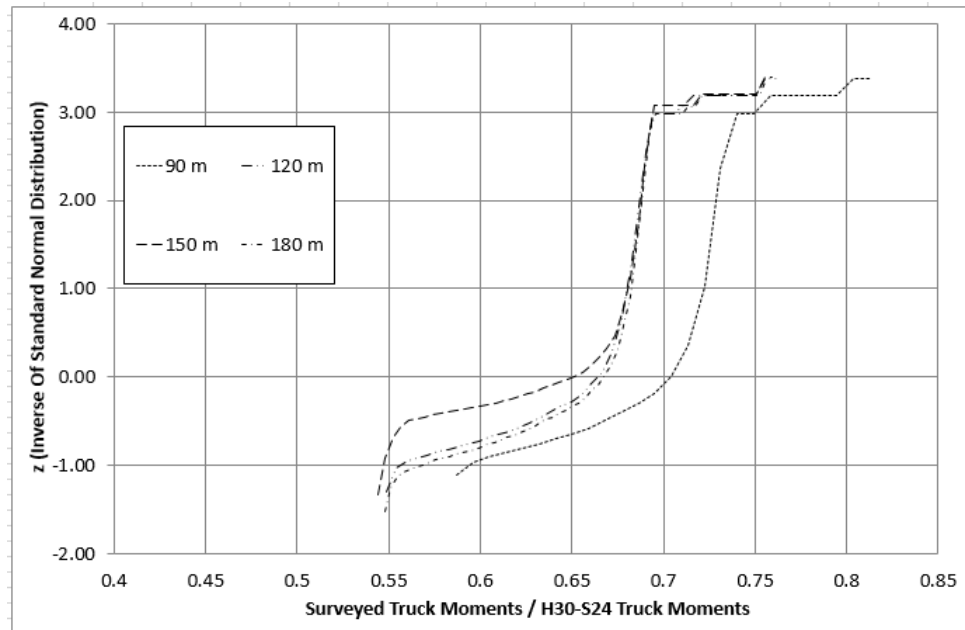


**Figure 30. Normal Probability Paper of Extreme Truck Survey Data for the Live Load Model H30-S24**

37
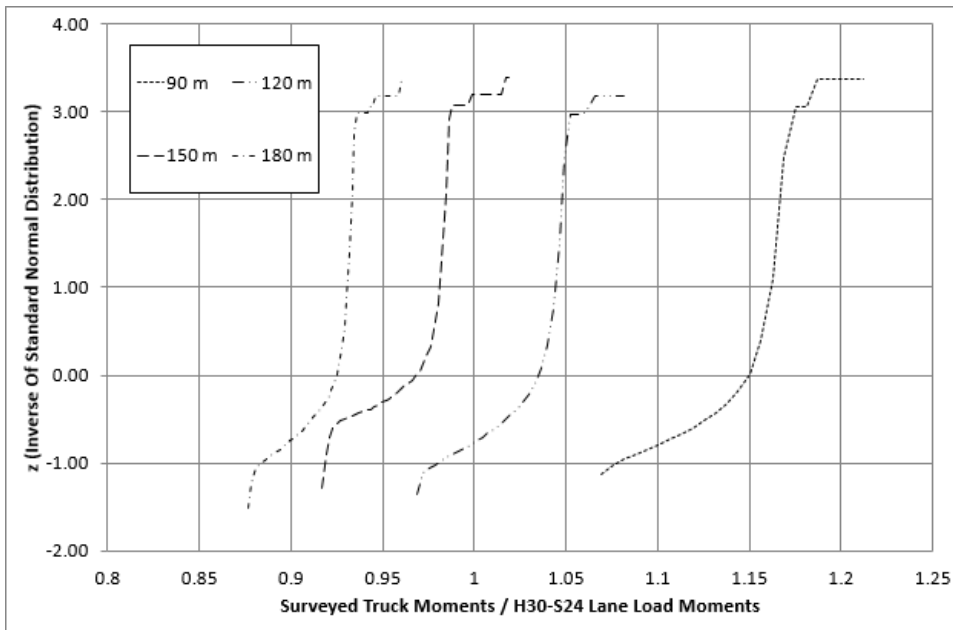
**Figure 31. Normal Probability Paper of Extreme Truck Survey Data for the Live Load Model H30-S24 Lane**
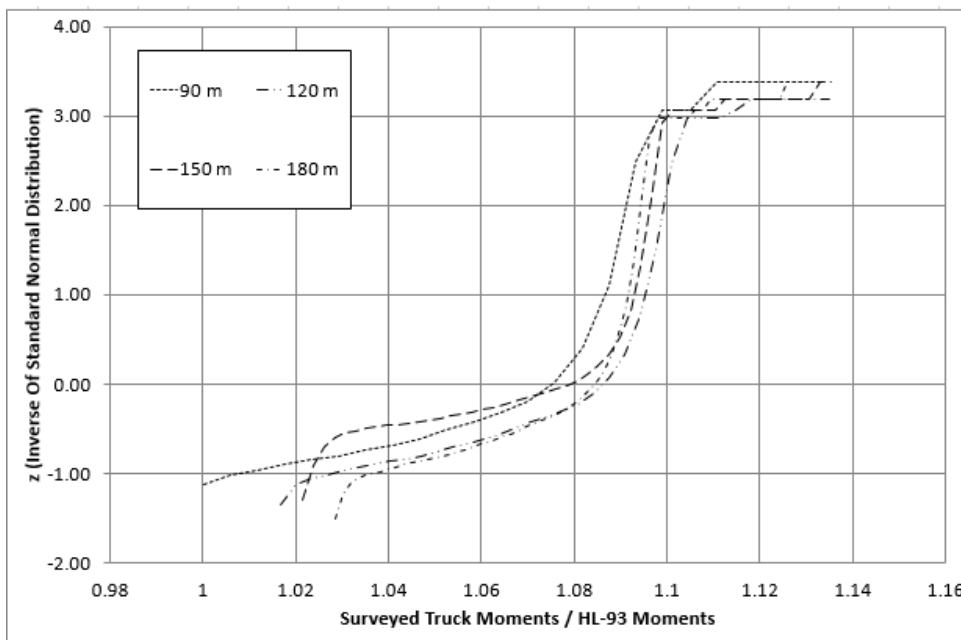


**Figure 32. Normal Probability Paper of Extreme Truck Survey Data for the Live Load Model HL-93 Load Model**
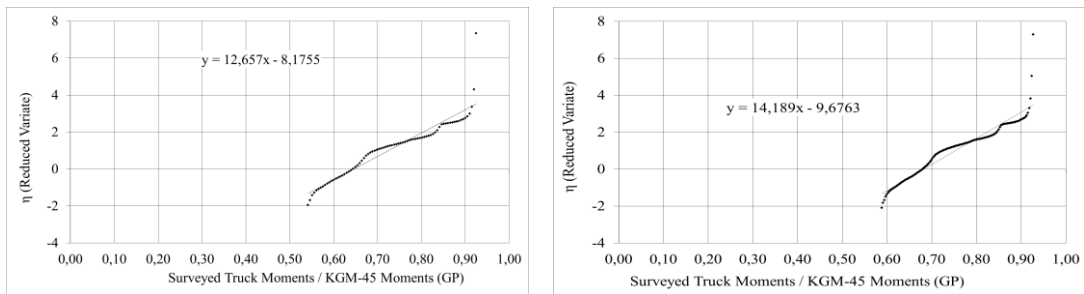
**Figure 33. The Straight Lines and Equations for Gumbel Probability of 90 and 120 meters KGM-45(overall)**
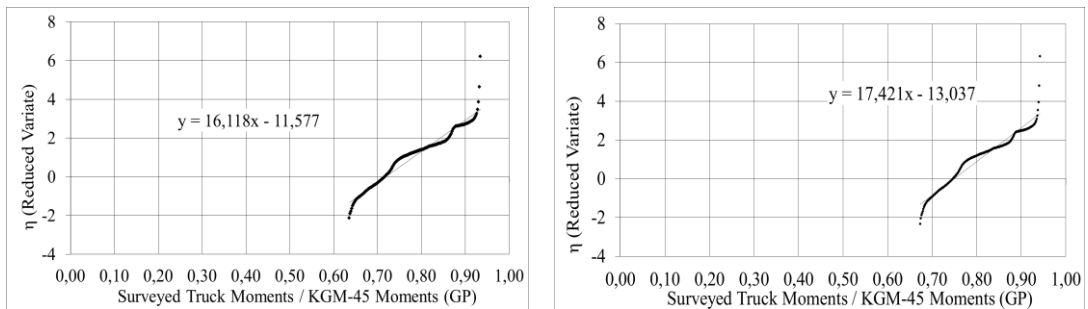


**Figure 34. The Straight Lines and Equations for Gumbel Probability of 150 and 180 meters KGM-45(overall)**
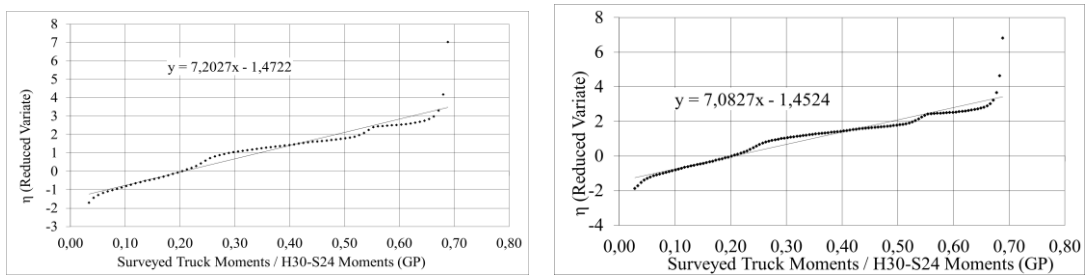


**Figure 35. The Straight Lines and Equations for Gumbel Probability of 90 and 120 meters H30-S24 (overall)**
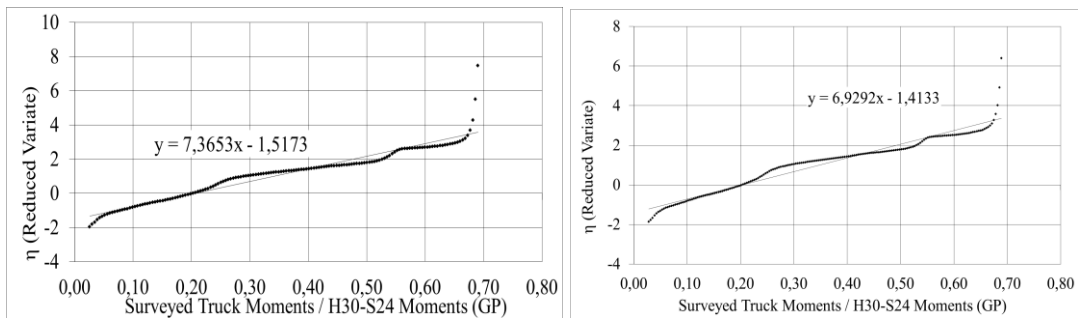
**Figure 36. The Straight Lines and Equations for Gumbel Probability of 150 and 180 meters H30-S24 (overall)**
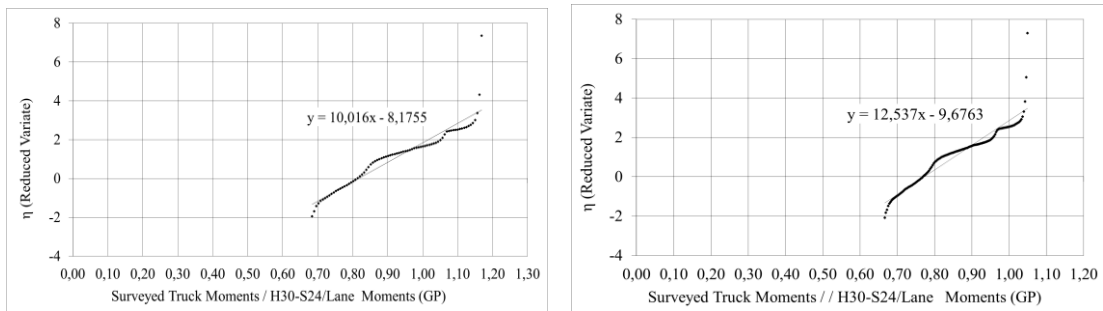


**Figure 37. The Straight Lines and Equations for Gumbel Probability of 90 and 120 meters H30-S24/Lane (overall)**
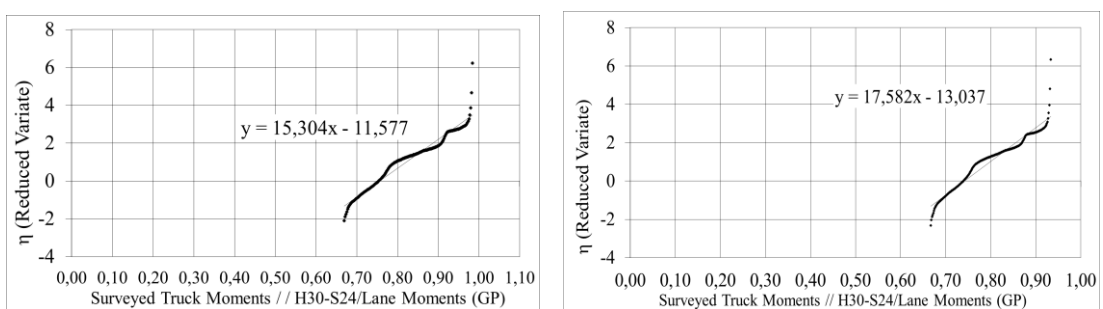


**Figure 38. The Straight Lines and Equations for Gumbel Probability of 150 and 180 meters H30-S24/Lane (overall)**
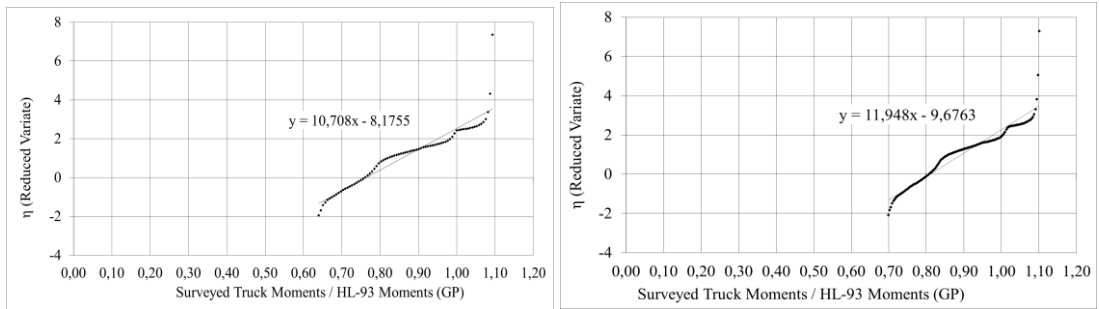
**Figure 39. The Straight Lines and Equations for Gumbel Probability of 90 and 120 meters HL-93 (overall)**
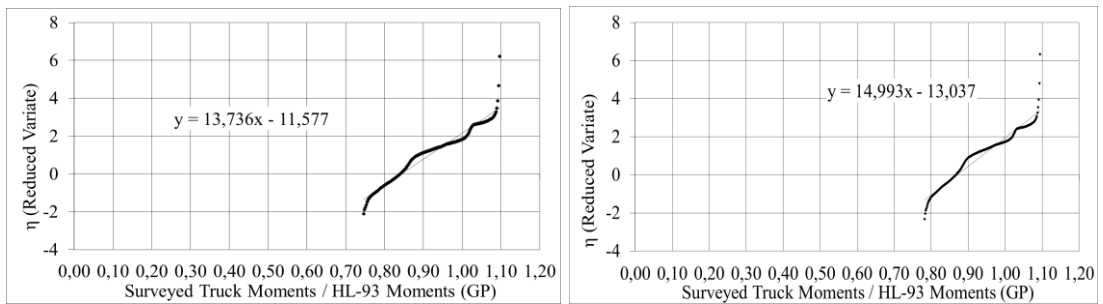


**Figure 40. The Straight Lines and Equations for Gumbel Probability of 150 and 180 meters HL-93 (overall)**
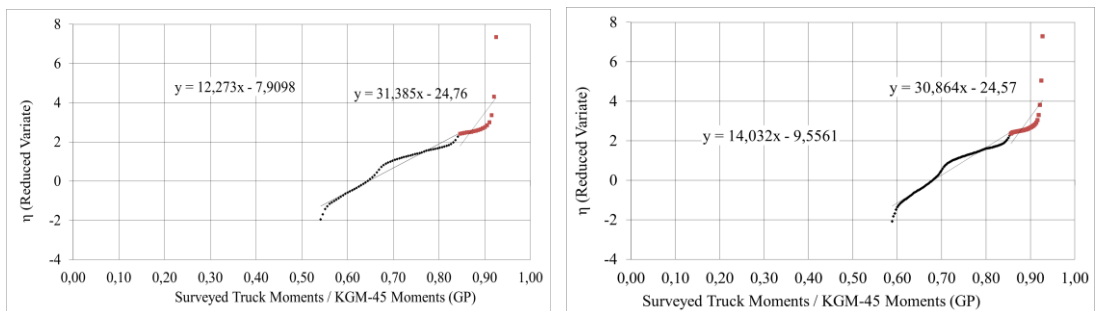


**Figure 41. The Straight Lines and Equations for Gumbel Probability of 90 and 120 meters KGM-45 (upper-tail)**
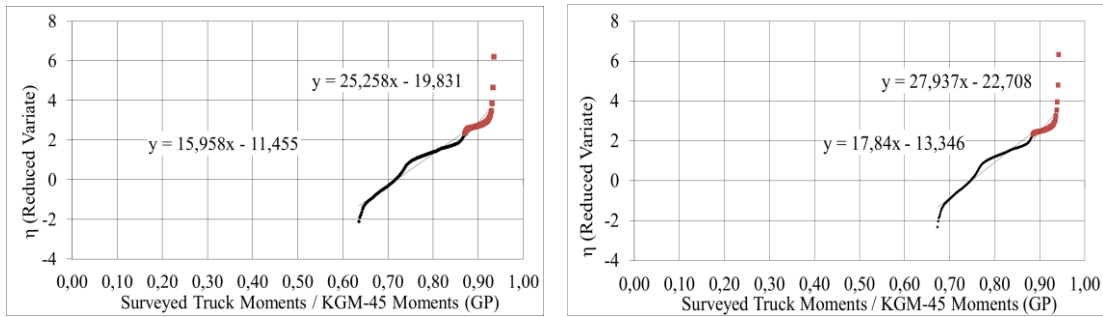
**Figure 42. The Straight Lines and Equations for Gumbel Probability of 150 and 180 meters KGM-45 (upper-tail)**
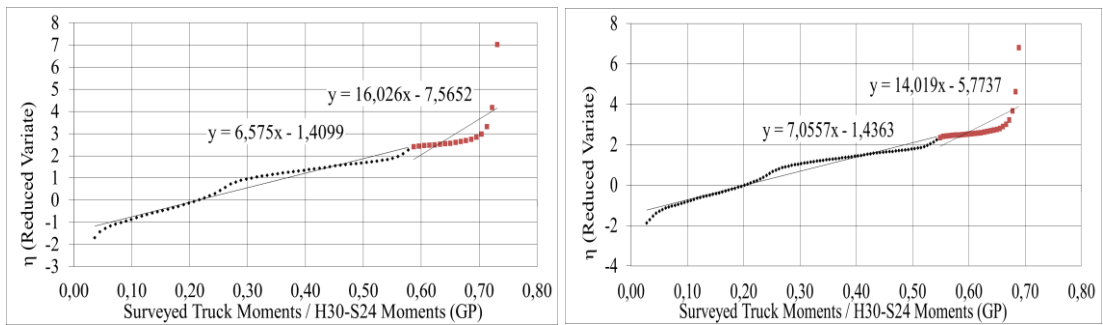


**Figure 43. The Straight Lines and Equations for Gumbel Probability of 90 and 120 meters H30-S24 (upper-tail)**
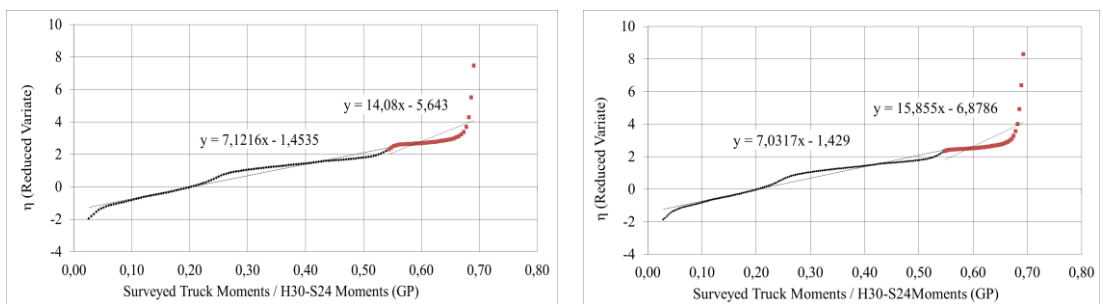


**Figure 44. The Straight Lines and Equations for Gumbel Probability of 150 and 180 meters H30-S24 (upper-tail)**
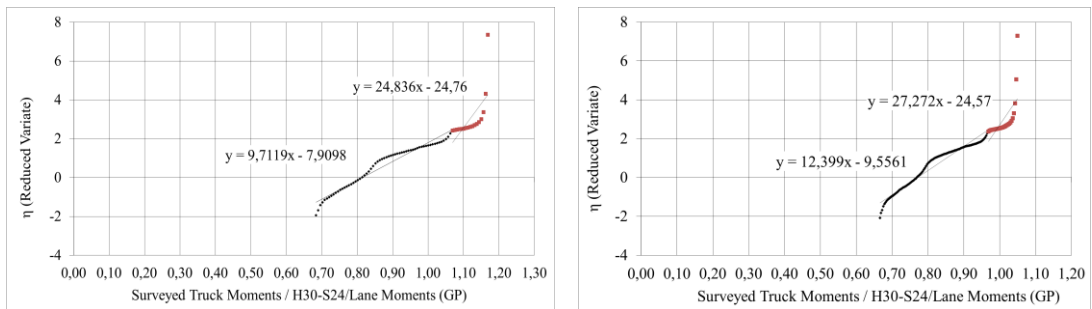
**Figure 45. The Straight Lines and Equations for Gumbel Probability of 90 and 120 meters H30-S24/Lane (upper-tail)**
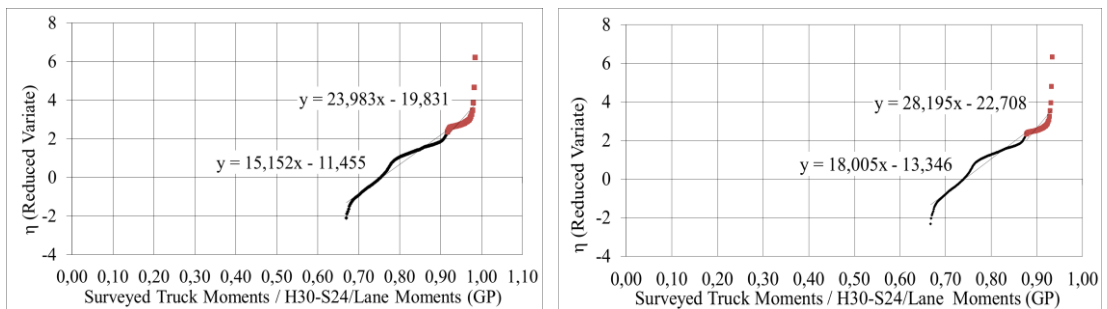


**Figure 46. The Straight Lines and Equations for Gumbel Probability of 150 and 180 meters H30-S24/Lane (upper-tail)**
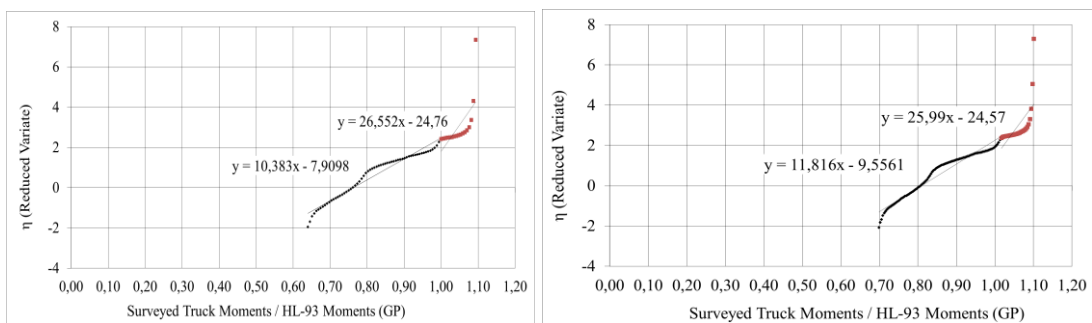


**Figure 47. The Straight Lines and Equations for Gumbel Probability of 90 and 120 meters HL-93 (upper-tail)**

43
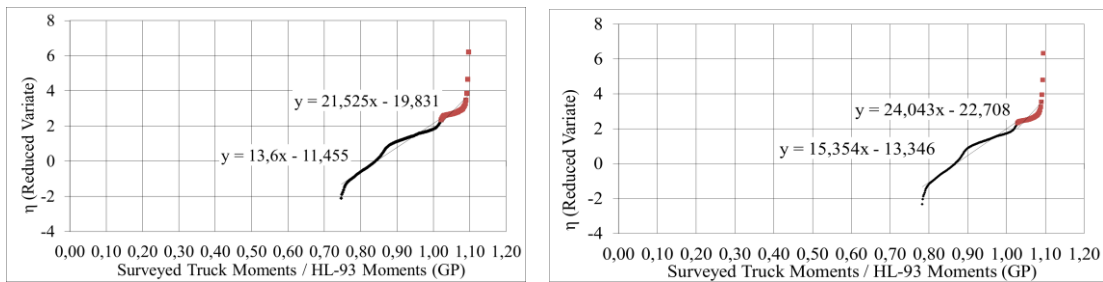
**Figure 48. The Straight Lines and Equations for Gumbel Probability of 150 and 180 meters HL-93 (upper-tail)**
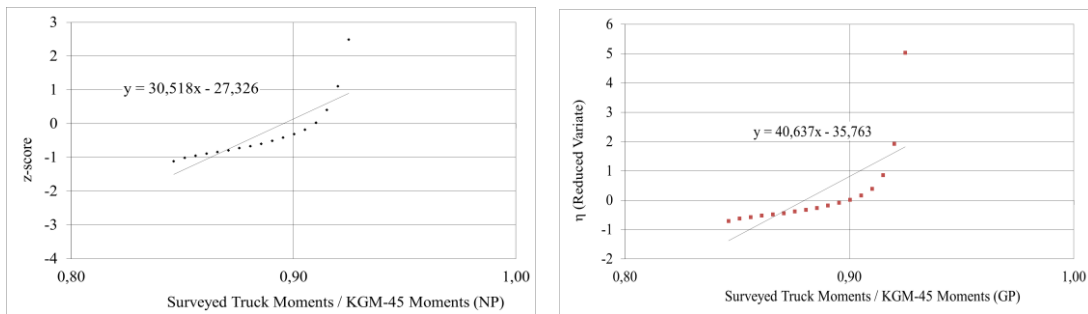


**Figure 49. The Straight Lines and Equations for Normal and Gumbel Probability of 90 meters KGM-45 (extreme)**
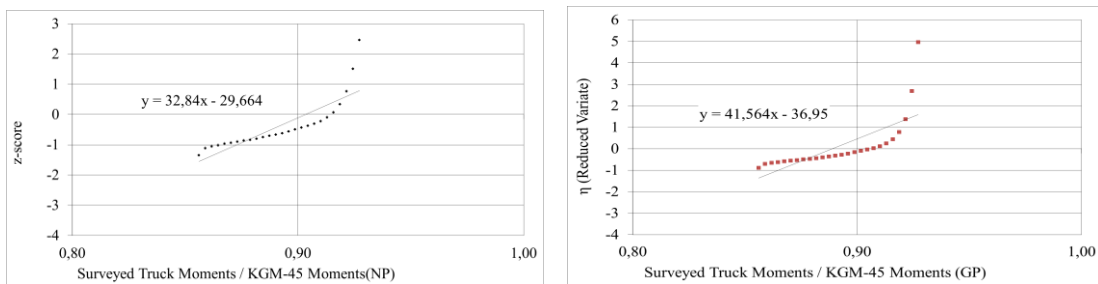


**Figure 50. The Straight Lines and Equations for Normal and Gumbel Probability of 120 meters KGM-45 (extreme)**
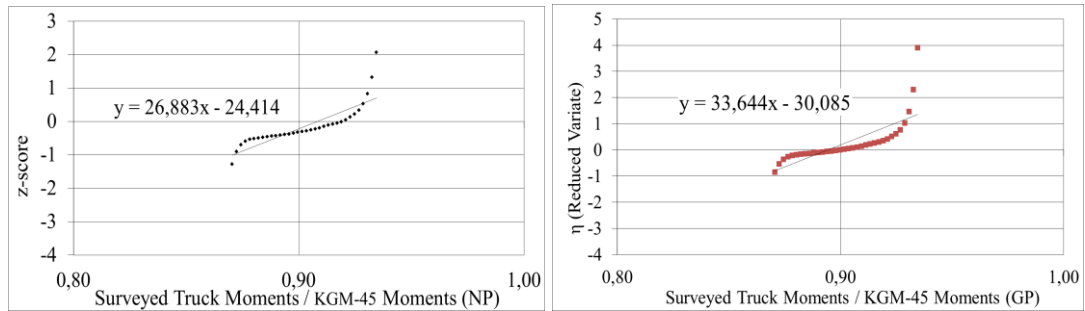
**Figure 51. The Straight Lines and Equations for Normal and Gumbel Probability of 150 meters KGM-45 (extreme)**
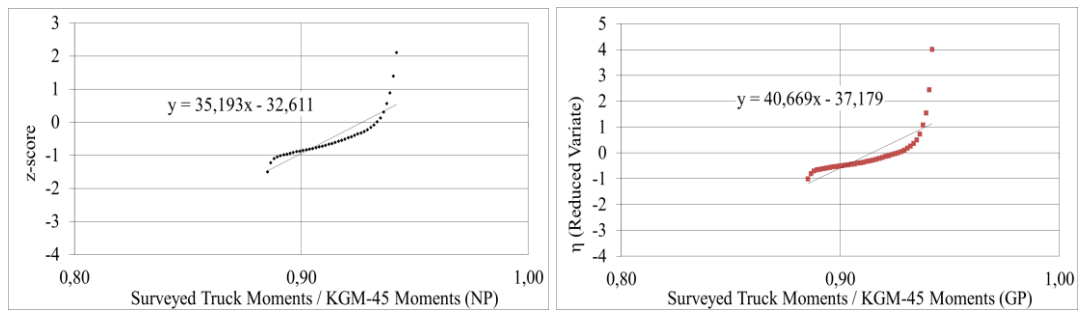


**Figure 52. The Straight Lines and Equations for Normal and Gumbel Probability of 180 meters KGM-45 (extreme)**
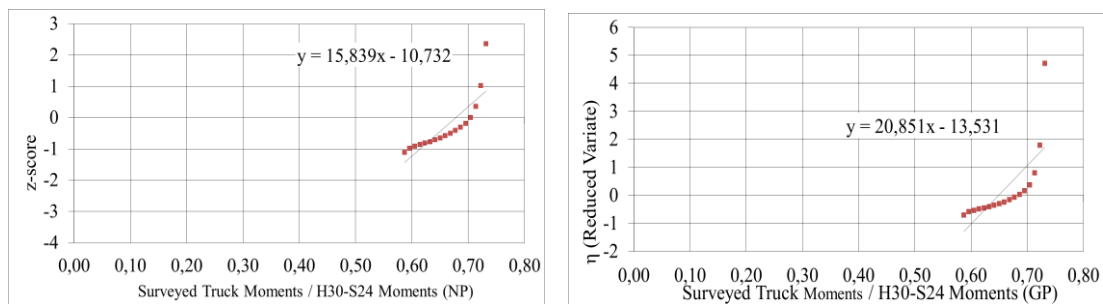


**Figure 53. The Straight Lines and Equations for Normal and Gumbel Probability of 90 meters H30-S24 (extreme)**

45
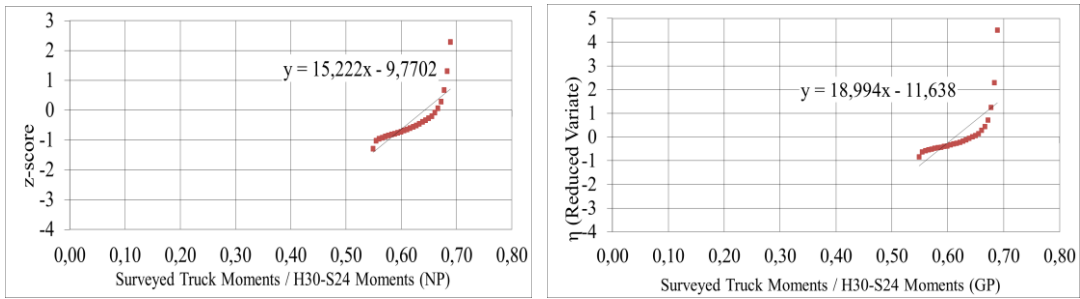
**Figure 54. The Straight Lines and Equations for Normal and Gumbel Probability of 120 meters H30-S24 (extreme)**
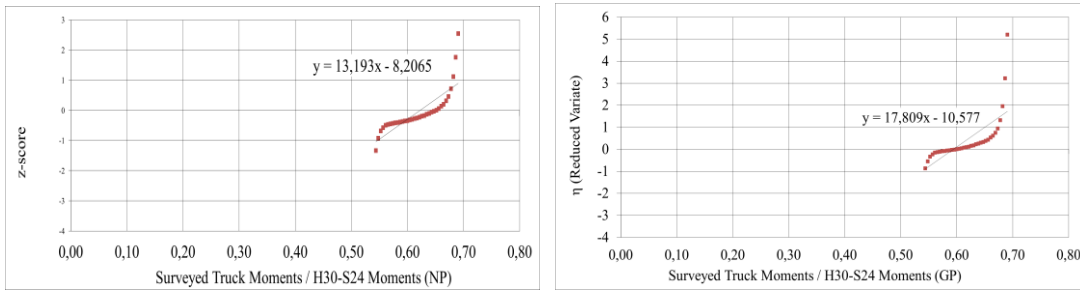


**Figure 55. The Straight Lines and Equations for Normal and Gumbel Probability of 150 meters H30-S24 (extreme)**
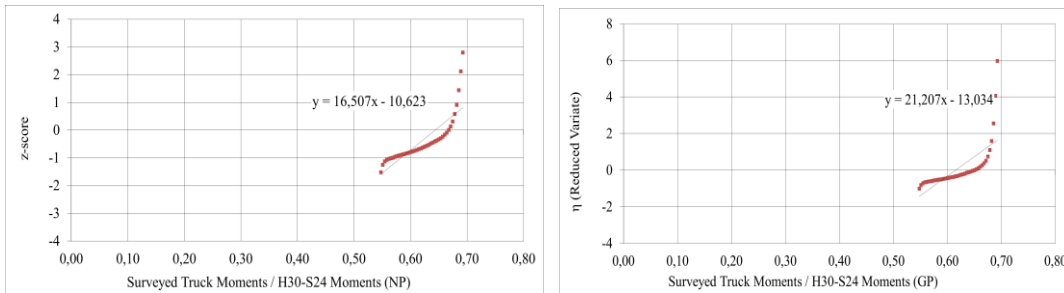


**Figure 56. The Straight Lines and Equations for Normal and Gumbel Probability of 180 meters H30-S24 (extreme)**
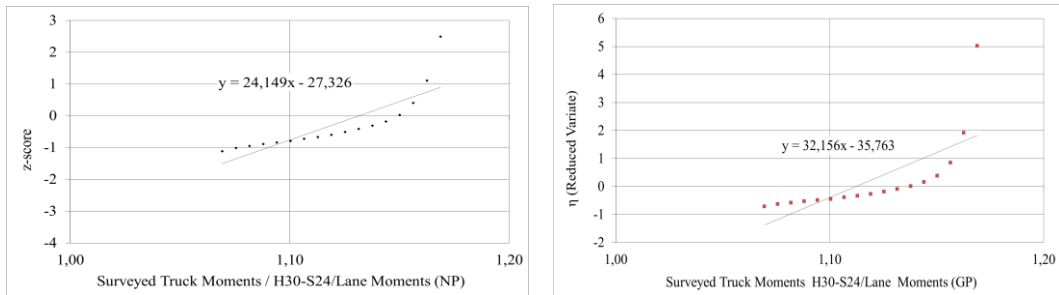
**Figure 57. The Straight Lines and Equations for Normal and Gumbel Probability of 90 meters H30-S24/Lane (extreme)**
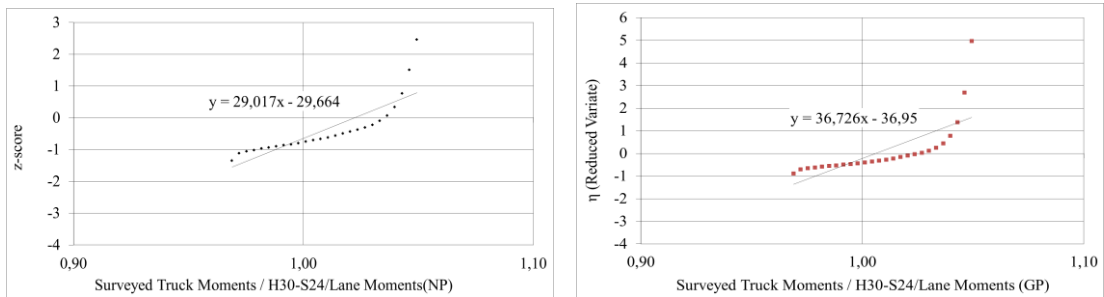


**Figure 58. The Straight Lines and Equations for Normal and Gumbel Probability of 120 meters H30-S24/Lane (extreme)**
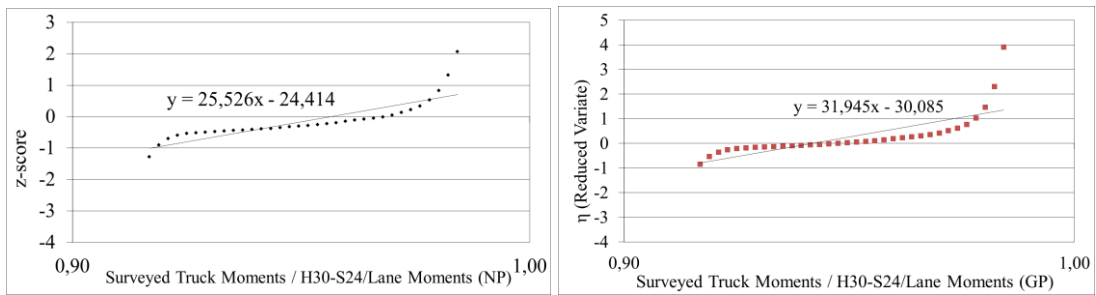


**Figure 59. The Straight Lines and Equations for Normal and Gumbel Probability of 150 meters H30-S24/Lane (extreme)**
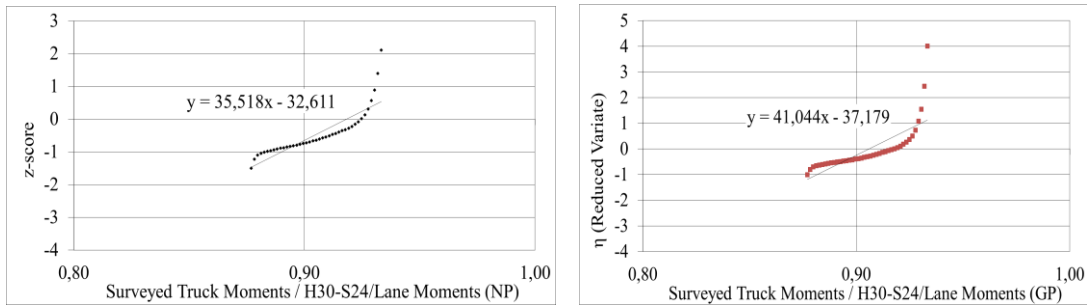
**Figure 60. The Straight Lines and Equations for Normal and Gumbel Probability of 180 meters H30-S24/Lane (extreme)**
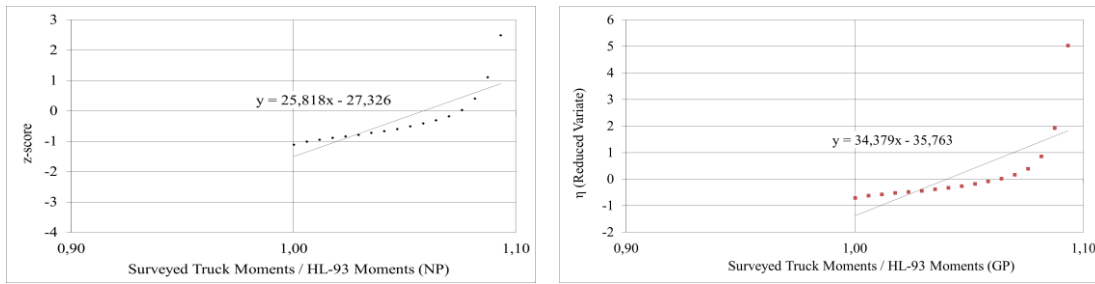


**Figure 61. The Straight Lines and Equations for Normal and Gumbel Probability of 90 meters HL-93 (extreme)**
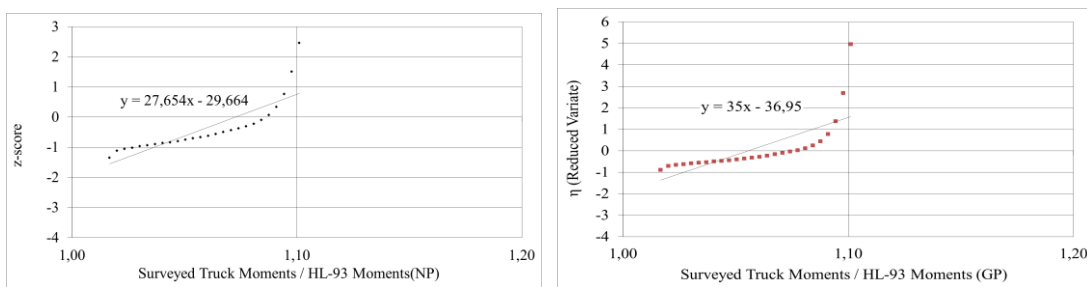


**Figure 62. The Straight Lines and Equations for Normal and Gumbel Probability of 120 meters HL-93 (extreme)**

48
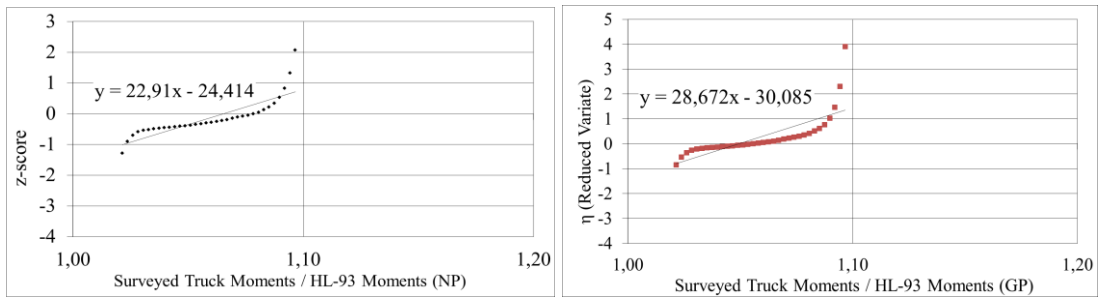
**Figure 63. The Straight Lines and Equations for Normal and Gumbel Probability of 150 meters HL-93 (extreme)**
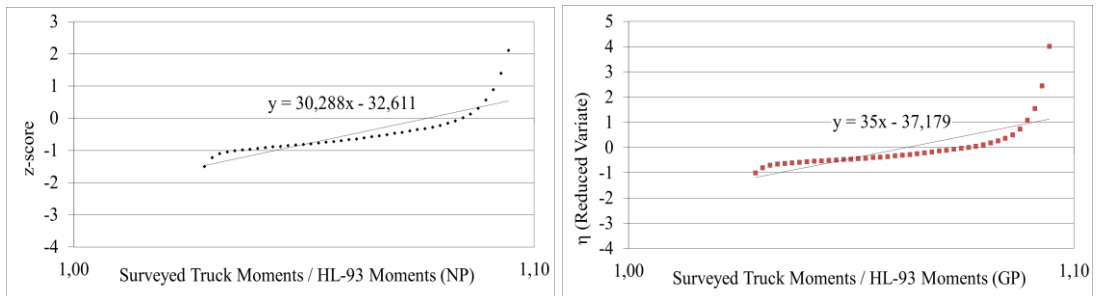


**Figure 64. The Straight Lines and Equations for Normal and Gumbel Probability of 180 meters HL-93 (extreme)**

### 3.2.9  Enhanced Maximum Mean Moments by Prediction

According to AASHTO LRFD bridge design specification, the service life for bridges is 75 years. It is impossible to gather future truck load data for 75 years later. On the other hand, it is possible to estimate the extrapolated truck moments by using the obtained truck data. Cumulative distribution functions are extrapolated for 75 years to expect the maximum truck moments for 1 day, 2 weeks, 1 month, 2 months, 6 months, 1 year, 5 years, 50 years and 75 years.

Based on the Nowak's calibration report of AASHTO LRFD, average daily traffic is assumed as 1000 trucks for two weeks of heavy traffic. Maximum moments of truck

49

loads are extrapolated by extending the cumulative distribution functions of moment ratios. For instance, in the time period of 75 years there are 1950 two weeks-time periods. Considering the fact that two weeks-time period consists of 10000 trucks, 1950 times 10000 = 20 million truck. As a result of this, the occurrence probability of the heaviest truck is 1/20000000 = 5 x $10^{-8}$. This probability corresponds to z = 5.33 for normal distribution and for Gumbel distribution (Nowak, 1999);

$$-\ln[-\ln(5x10^{-8})] = 16.81$$

In this approach, it is also observed that the changes in the traffic volume assumption does not effect the results significantly. For example, if there the traffic volume is divided in half, the occurrence probability of the heaviest truck is calculated as 10 x $10^{-8}$ and the corresponding normal distribution z = $\varnothing^{-1}(10*10^{-8})$ = 5.199. The total difference in percentage is calculated as (5.33/5.19-1)*100 = %2.7 is considerably small for big difference in traffic volume.

Various time periods are evaluated as mentioned above and the Table 10 constructed. Time periods, number of trucks, inverse standard normal distribution values and reduced variates are calculated and listed in Table 10. The assumption is made for number of trucks per year is taken from the calibration report of the AASHTO LRFD (Nowak, 1999).

By evaluating the equations of straight lines for Gumbel Distributions and using the statistical parameters for longer time periods, mean moment ratio factors for extrapolation are determined. These factors calculated with truck survey data for overall, upper-tail and extreme cases and results are given in graphical form in Figures 65 to 76.

**Table 10. Time Period vs Number of Trucks and Probability**

| Time Period | Number of Trucks | Probability | ISND | Reduced Variate |
|---|---|---|---|---|
| T | N | 1/N | z | η |
| 75 years | 20000000 | 0.00000005 | 5.3267239 | 16.8112428 |
| 50 years | 15000000 | 6.67E-08 | 5.2742043 | 16.5235607 |
| 5 years | 1500000 | 6.67E-07 | 4.8347198 | 14.2209753 |
| 1 year | 300000 | 3.33E-06 | 4.5040622 | 12.6115361 |
| 6 months | 150000 | 6.67E-06 | 4.3545618 | 11.9183872 |
| 2 months | 50000 | 0.00002 | 4.1074797 | 10.8197683 |
| 1 month | 30000 | 3.33E-05 | 3.9878789 | 10.3089360 |
| 2 weeks | 10000 | 0.0001 | 3.7190165 | 9.21029037 |
| 1 day | 1000 | 0.001 | 3.0902323 | 6.90725507 |

**Table 11. Moment Ratios for Extrapolation for Overall Case (KGM-45)**

| Span (m) | Surveyed Truck Moment / KGM-45 Moment | | | | | | | | |
|---|---|---|---|---|---|---|---|---|---|
| | 1 day | 2 weeks | 1 month | 2 months | 6 months | 1 year | 5 years | 50 years | 75 years |
| 90 | 1.19 | 1.37 | 1.46 | 1.50 | 1.59 | 1.64 | 1.77 | 1.95 | 1.97 |
| 120 | 1.17 | 1.33 | 1.41 | 1.44 | 1.52 | 1.57 | 1.68 | 1.85 | 1.87 |
| 150 | 1.15 | 1.29 | 1.36 | 1.39 | 1.46 | 1.50 | 1.60 | 1.74 | 1.76 |
| 180 | 1.14 | 1.28 | 1.34 | 1.37 | 1.43 | 1.47 | 1.56 | 1.70 | 1.71 |

**Table 12. Moment Ratios for Extrapolation for Upper-tail Case (KGM-45)**

| Span (m) | Surveyed Truck Moment / KGM-45 Moment | | | | | | | | |
|---|---|---|---|---|---|---|---|---|---|
| | 1 day | 2 weeks | 1 month | 2 months | 6 months | 1 year | 5 years | 50 years | 75 years |
| 90 | 1.02 | 1.09 | 1.12 | 1.14 | 1.18 | 1.2 | 1.25 | 1.32 | 1.33 |
| 120 | 1.02 | 1.09 | 1.13 | 1.15 | 1.18 | 1.2 | 1.26 | 1.33 | 1.34 |
| 150 | 1.06 | 1.15 | 1.19 | 1.21 | 1.26 | 1.28 | 1.35 | 1.44 | 1.45 |
| 180 | 1.06 | 1.14 | 1.18 | 1.2 | 1.24 | 1.26 | 1.32 | 1.4 | 1.41 |

**Table 13. Moment Ratios for Extrapolation for Extreme Case (KGM-45)**

| Span (m) | Surveyed Truck Moment / KGM-45 Moment | | | | | | | | |
|---|---|---|---|---|---|---|---|---|---|
| | 1 day | 2 weeks | 1 month | 2 months | 6 months | 1 year | 5 years | 50 years | 75 years |
| 90 | 1.05 | 1.11 | 1.13 | 1.15 | 1.17 | 1.19 | 1.23 | 1.29 | 1.29 |
| 120 | 1.06 | 1.11 | 1.14 | 1.15 | 1.18 | 1.19 | 1.23 | 1.29 | 1.29 |
| 150 | 1.1 | 1.17 | 1.2 | 1.22 | 1.25 | 1.27 | 1.32 | 1.39 | 1.39 |
| 180 | 1.08 | 1.14 | 1.17 | 1.18 | 1.21 | 1.22 | 1.26 | 1.32 | 1.33 |

**Table 14. Moment Ratios for Extrapolation for Overall Case (H30-S24)**

| Span (m) | Surveyed Truck Moment / H30-S24 Moment | | | | | | | | |
|---|---|---|---|---|---|---|---|---|---|
| | 1 day | 2 weeks | 1 month | 2 months | 6 months | 1 year | 5 years | 50 years | 75 years |
| 90 | 1.24 | 1.58 | 1.74 | 1.81 | 1.98 | 2.08 | 2.31 | 2.65 | 2.7 |
| 120 | 1.18 | 1.51 | 1.66 | 1.73 | 1.89 | 1.99 | 2.21 | 2.54 | 2.58 |
| 150 | 1.14 | 1.46 | 1.61 | 1.68 | 1.82 | 1.92 | 2.14 | 2.45 | 2.49 |
| 180 | 1.2 | 1.53 | 1.69 | 1.77 | 1.92 | 2.02 | 2.26 | 2.59 | 2.63 |

**Table 15. Moment Ratios for Extrapolation for Upper-tail Case (H30-S24)**

| Span (m) | Surveyed Truck Moment / H30-S24 Moment | | | | | | | | |
|---|---|---|---|---|---|---|---|---|---|
| | 1 day | 2 weeks | 1 month | 2 months | 6 months | 1 year | 5 years | 50 years | 75 years |
| 90 | 0.9 | 1.05 | 1.12 | 1.15 | 1.22 | 1.26 | 1.36 | 1.5 | 1.52 |
| 120 | 0.9 | 1.07 | 1.15 | 1.18 | 1.26 | 1.31 | 1.43 | 1.59 | 1.61 |
| 150 | 0.89 | 1.05 | 1.13 | 1.17 | 1.25 | 1.3 | 1.41 | 1.57 | 1.59 |
| 180 | 0.87 | 1.01 | 1.08 | 1.12 | 1.19 | 1.23 | 1.33 | 1.48 | 1.49 |

**Table 16. Moment Ratios for Extrapolation for Extreme Case (H30-S24)**

| Span (m) | Surveyed Truck Moment / H30-S24 Moment | | | | | | | | |
|---|---|---|---|---|---|---|---|---|---|
| | 1 day | 2 weeks | 1 month | 2 months | 6 months | 1 year | 5 years | 50 years | 75 years |
| 90 | 0.98 | 1.09 | 1.14 | 1.17 | 1.22 | 1.25 | 1.33 | 1.44 | 1.46 |
| 120 | 0.98 | 1.1 | 1.16 | 1.18 | 1.24 | 1.28 | 1.36 | 1.48 | 1.5 |
| 150 | 0.98 | 1.11 | 1.17 | 1.2 | 1.26 | 1.3 | 1.39 | 1.52 | 1.54 |
| 180 | 0.94 | 1.05 | 1.1 | 1.12 | 1.18 | 1.21 | 1.29 | 1.39 | 1.41 |

**Table 17. Moment Ratios for Extrapolation for Overall Case (H30-S24 Lane)**

| Span (m) | Surveyed Truck Moment / H30-S24 Lane Moment | | | | | | | | |
|---|---|---|---|---|---|---|---|---|---|
| | 1 day | 2 weeks | 1 month | 2 months | 6 months | 1 year | 5 years | 50 years | 75 years |
| 90 | 1.51 | 1.74 | 1.85 | 1.9 | 2.01 | 2.08 | 2.24 | 2.47 | 2.49 |
| 120 | 1.32 | 1.51 | 1.59 | 1.63 | 1.72 | 1.78 | 1.91 | 2.09 | 2.11 |
| 150 | 1.21 | 1.36 | 1.43 | 1.46 | 1.54 | 1.58 | 1.69 | 1.84 | 1.85 |
| 180 | 1.13 | 1.27 | 1.33 | 1.36 | 1.42 | 1.46 | 1.55 | 1.68 | 1.7 |

**Table 18. Moment Ratios for Extrapolation for Upper-tail Case (H30-S24 Lane)**

| Span (m) | Surveyed Truck Moment / H30-S24 Lane Moment | | | | | | | | |
|---|---|---|---|---|---|---|---|---|---|
| | 1 day | 2 weeks | 1 month | 2 months | 6 months | 1 year | 5 years | 50 years | 75 years |
| 90 | 1.28 | 1.37 | 1.41 | 1.43 | 1.48 | 1.5 | 1.57 | 1.66 | 1.67 |
| 120 | 1.15 | 1.24 | 1.28 | 1.3 | 1.34 | 1.36 | 1.42 | 1.51 | 1.52 |
| 150 | 1.11 | 1.21 | 1.26 | 1.28 | 1.32 | 1.35 | 1.42 | 1.52 | 1.53 |
| 180 | 1.05 | 1.13 | 1.17 | 1.19 | 1.23 | 1.25 | 1.31 | 1.39 | 1.4 |

**Table 19. Moment Ratios for Extrapolation for Extreme Case (H30-S24 Lane)**

| Span (m) | Surveyed Truck Moment / H30-S24 Lane Moment | | | | | | | | |
|---|---|---|---|---|---|---|---|---|---|
| | 1 day | 2 weeks | 1 month | 2 months | 6 months | 1 year | 5 years | 50 years | 75 years |
| 90 | 1.33 | 1.4 | 1.43 | 1.45 | 1.48 | 1.5 | 1.55 | 1.63 | 1.63 |
| 120 | 1.19 | 1.26 | 1.29 | 1.3 | 1.33 | 1.35 | 1.39 | 1.46 | 1.46 |
| 150 | 1.17 | 1.25 | 1.28 | 1.3 | 1.33 | 1.36 | 1.41 | 1.48 | 1.49 |
| 180 | 1.07 | 1.13 | 1.16 | 1.17 | 1.2 | 1.21 | 1.25 | 1.31 | 1.32 |

**Table 20. Moment Ratios for Extrapolation for Overall Case (HL-93)**

| Span (m) | Surveyed Truck Moment / HL-93 Moment | | | | | | | | |
|---|---|---|---|---|---|---|---|---|---|
| | 1 day | 2 weeks | 1 month | 2 months | 6 months | 1 year | 5 years | 50 years | 75 years |
| 90 | 1.41 | 1.62 | 1.73 | 1.77 | 1.88 | 1.94 | 2.09 | 2.31 | 2.33 |
| 120 | 1.39 | 1.58 | 1.67 | 1.72 | 1.81 | 1.87 | 2 | 2.19 | 2.22 |
| 150 | 1.35 | 1.51 | 1.59 | 1.63 | 1.71 | 1.76 | 1.88 | 2.05 | 2.07 |
| 180 | 1.33 | 1.48 | 1.56 | 1.59 | 1.66 | 1.71 | 1.82 | 1.97 | 1.99 |

**Table 21. Moment Ratios for Extrapolation for Upper-tail Case (HL-93)**

| Span (m) | Surveyed Truck Moment / HL-93 Moment | | | | | | | | |
|---|---|---|---|---|---|---|---|---|---|
| | 1 day | 2 weeks | 1 month | 2 months | 6 months | 1 year | 5 years | 50 years | 75 years |
| 90 | 1.19 | 1.28 | 1.32 | 1.34 | 1.38 | 1.41 | 1.47 | 1.55 | 1.57 |
| 120 | 1.21 | 1.3 | 1.34 | 1.36 | 1.4 | 1.43 | 1.49 | 1.58 | 1.59 |
| 150 | 1.24 | 1.35 | 1.4 | 1.42 | 1.48 | 1.51 | 1.58 | 1.69 | 1.7 |
| 180 | 1.23 | 1.33 | 1.37 | 1.39 | 1.44 | 1.47 | 1.54 | 1.63 | 1.64 |

**Table 22. Moment Ratios for Extrapolation for Extreme Case (HL-93)**

| Span (m) | Surveyed Truck Moment / HL-93 Moment | | | | | | | | |
|---|---|---|---|---|---|---|---|---|---|
| | 1 day | 2 weeks | 1 month | 2 months | 6 months | 1 year | 5 years | 50 years | 75 years |
| 90 | 1.24 | 1.31 | 1.34 | 1.35 | 1.39 | 1.41 | 1.45 | 1.52 | 1.53 |
| 120 | 1.25 | 1.32 | 1.35 | 1.36 | 1.4 | 1.42 | 1.46 | 1.53 | 1.54 |
| 150 | 1.29 | 1.37 | 1.41 | 1.43 | 1.46 | 1.49 | 1.55 | 1.63 | 1.64 |
| 180 | 1.26 | 1.33 | 1.36 | 1.37 | 1.4 | 1.42 | 1.47 | 1.53 | 1.54 |
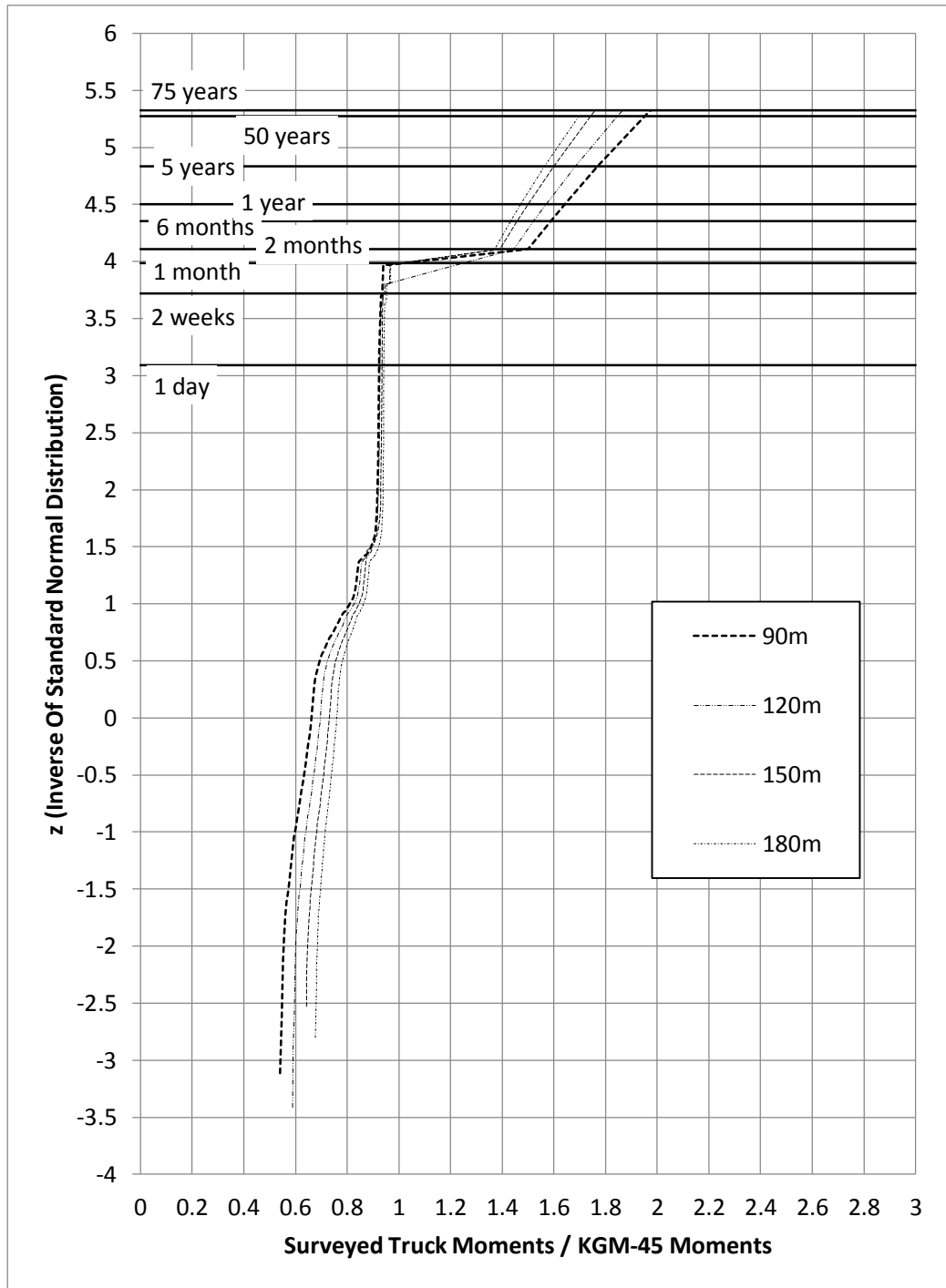
**Figure 65. Extrapolation Moment Ratios for KGM-45 (Overall)**
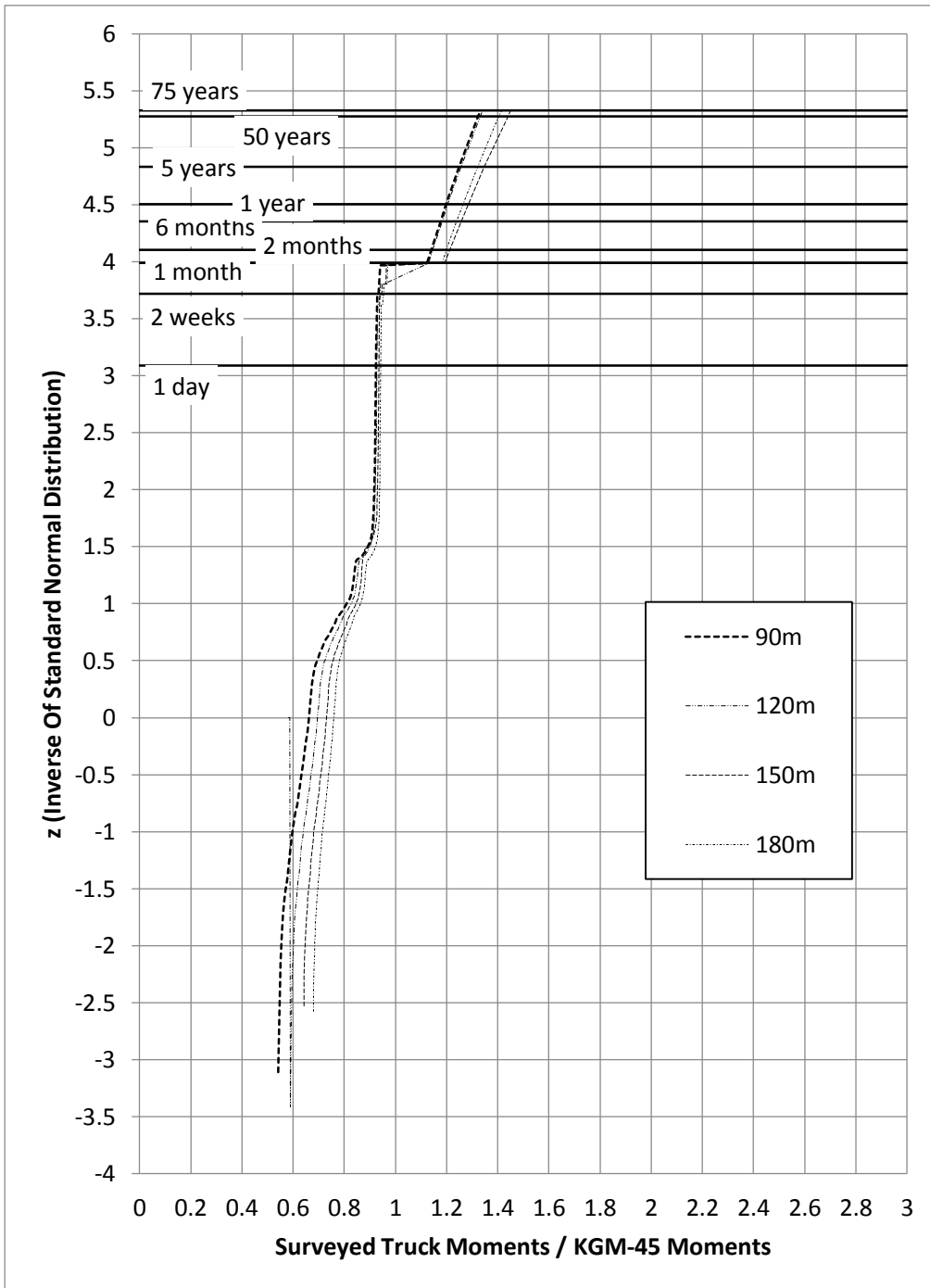
**Figure 66. Extrapolation Moment Ratios for KGM-45 (Upper-tail)**
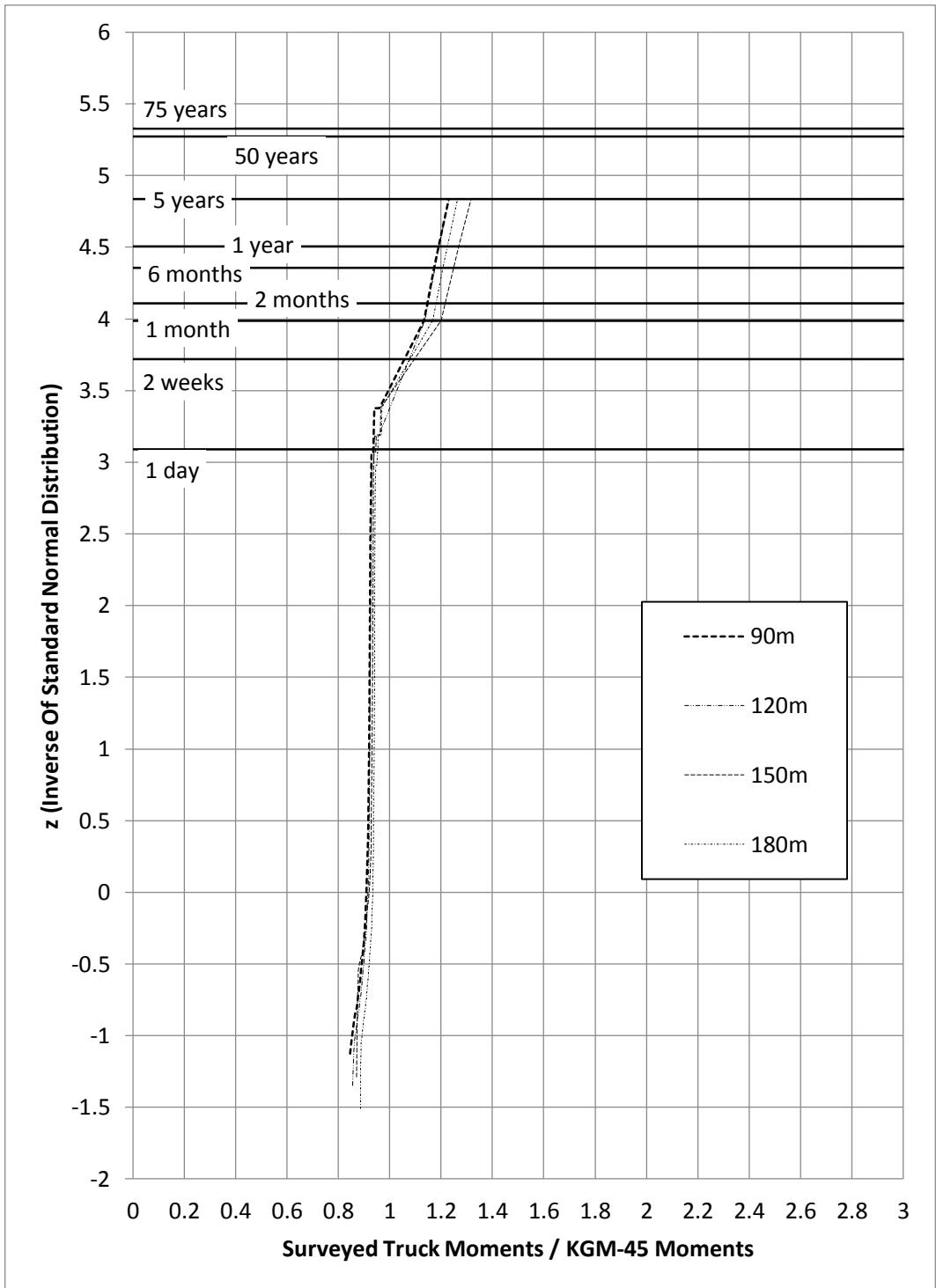
**Figure 67. Extrapolation Moment Ratios for KGM-45 (Extreme)**
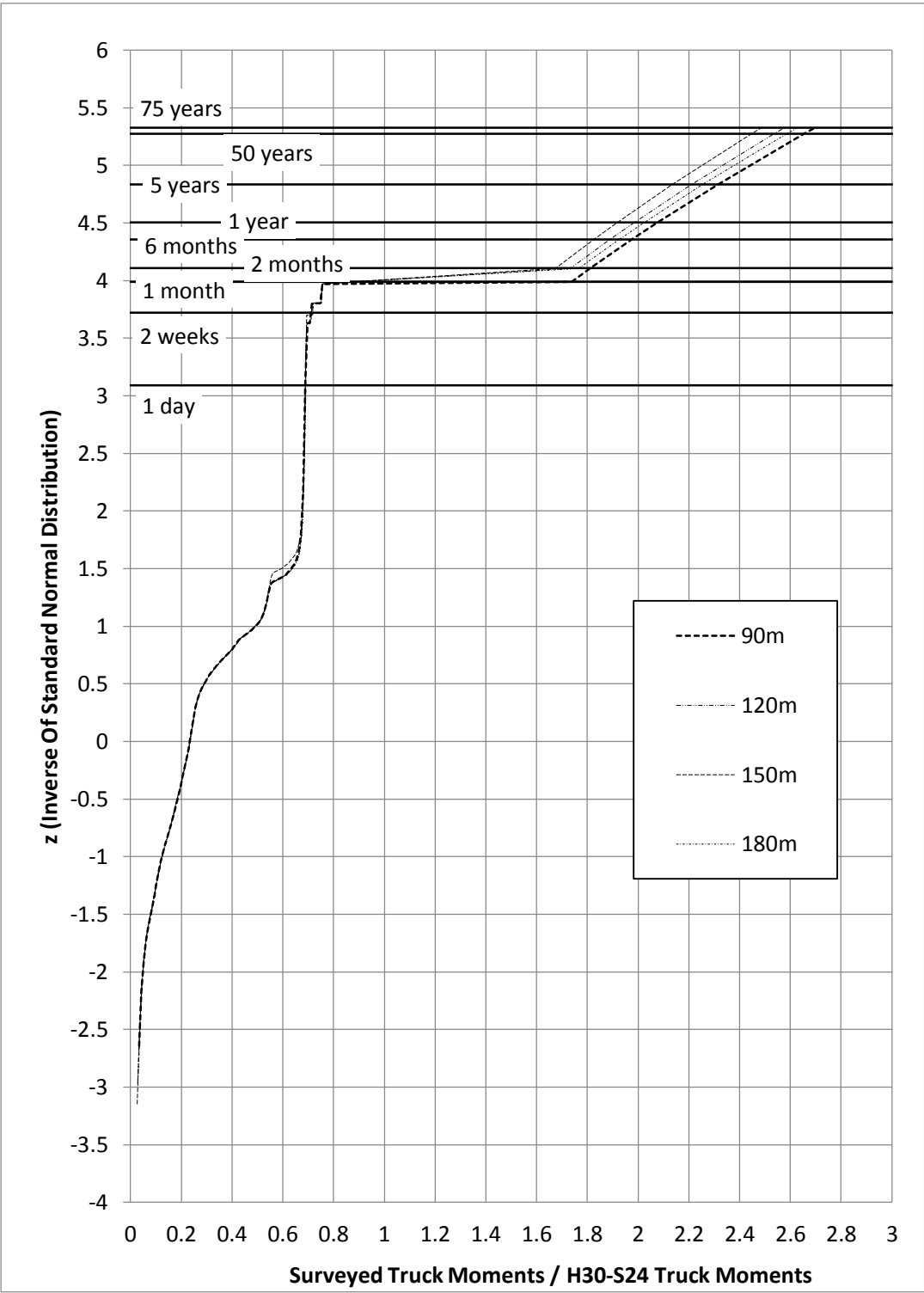
**Figure 68. Extrapolation Moment Ratios for H30-S24 Truck (Overall)**
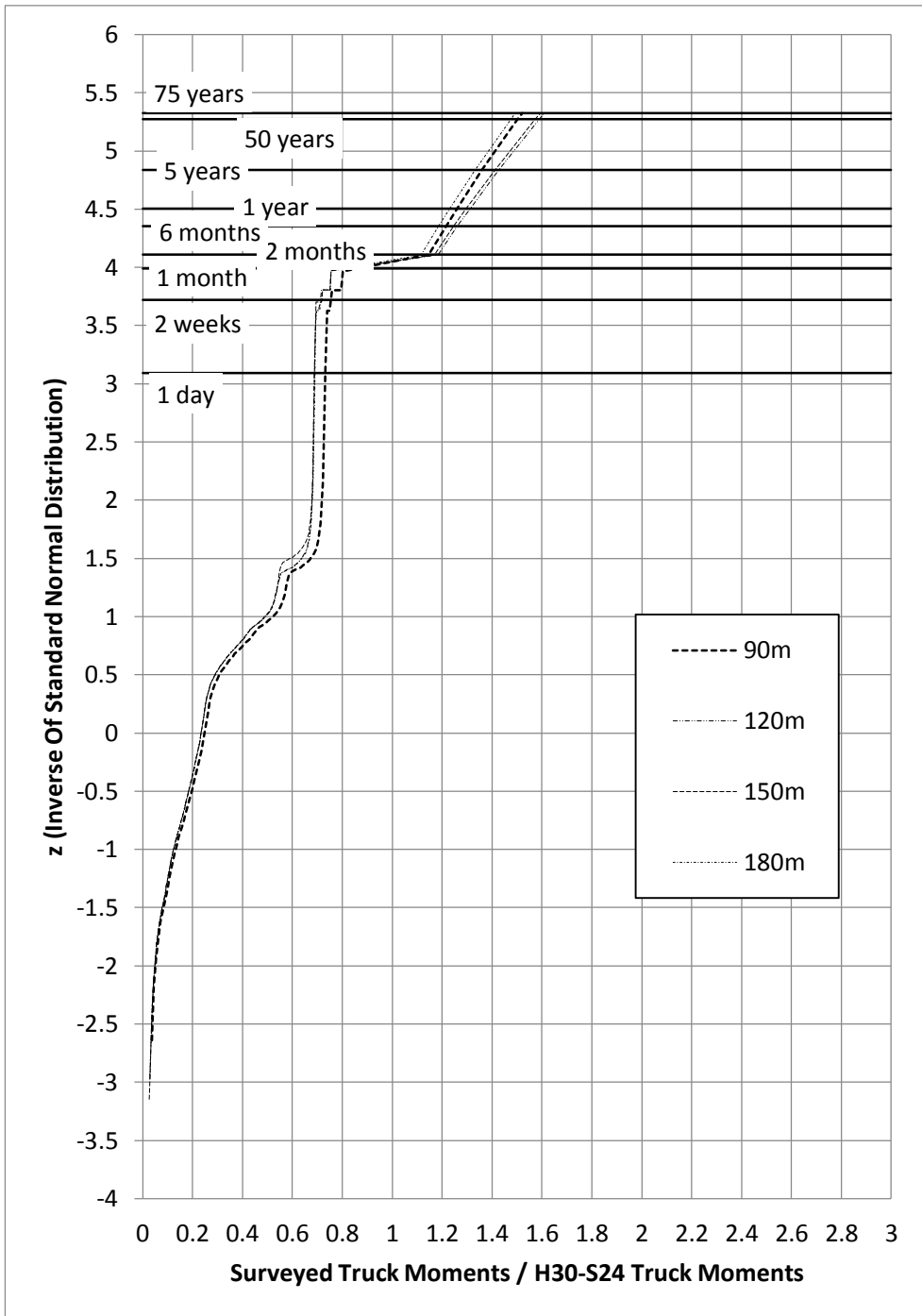
**Figure 69. Extrapolation Moment Ratios for H30-S24 Truck (Upper-tail)**
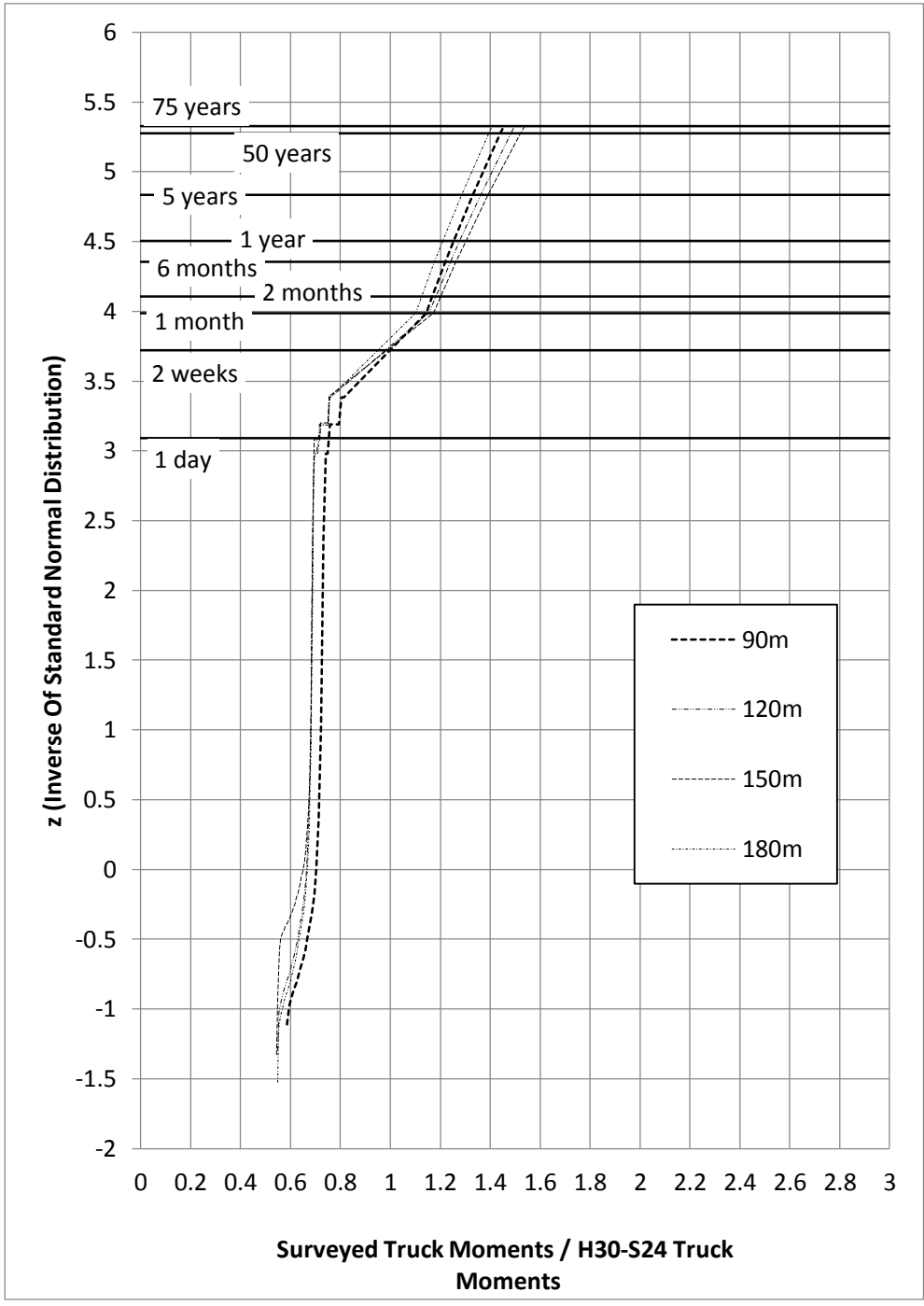
**Figure 70. Extrapolation Moment Ratios for H30-S24 Truck (Extreme)**
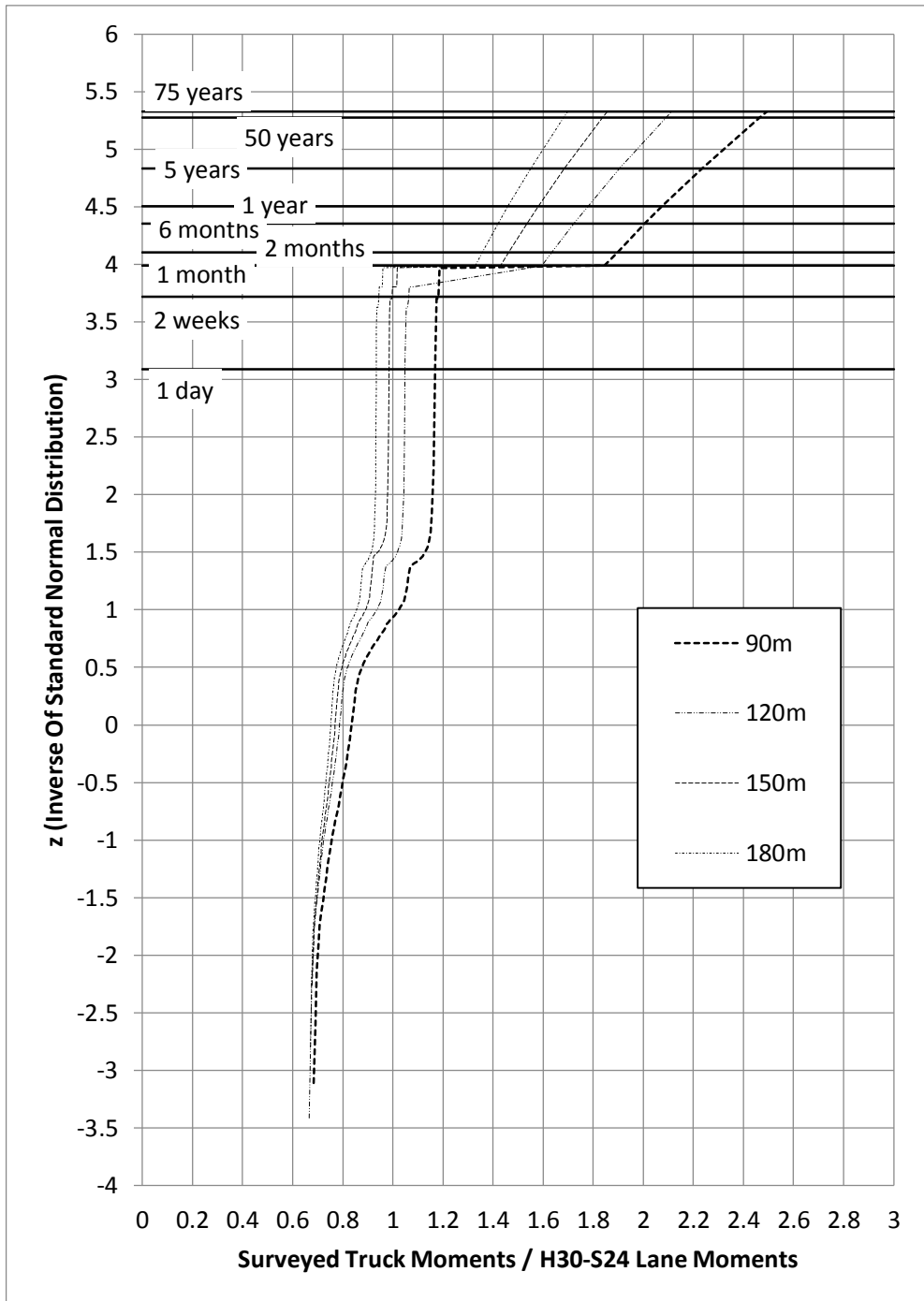
**Figure 71. Extrapolation Moment Ratios for H30-S24 Lane (Overall)**

61
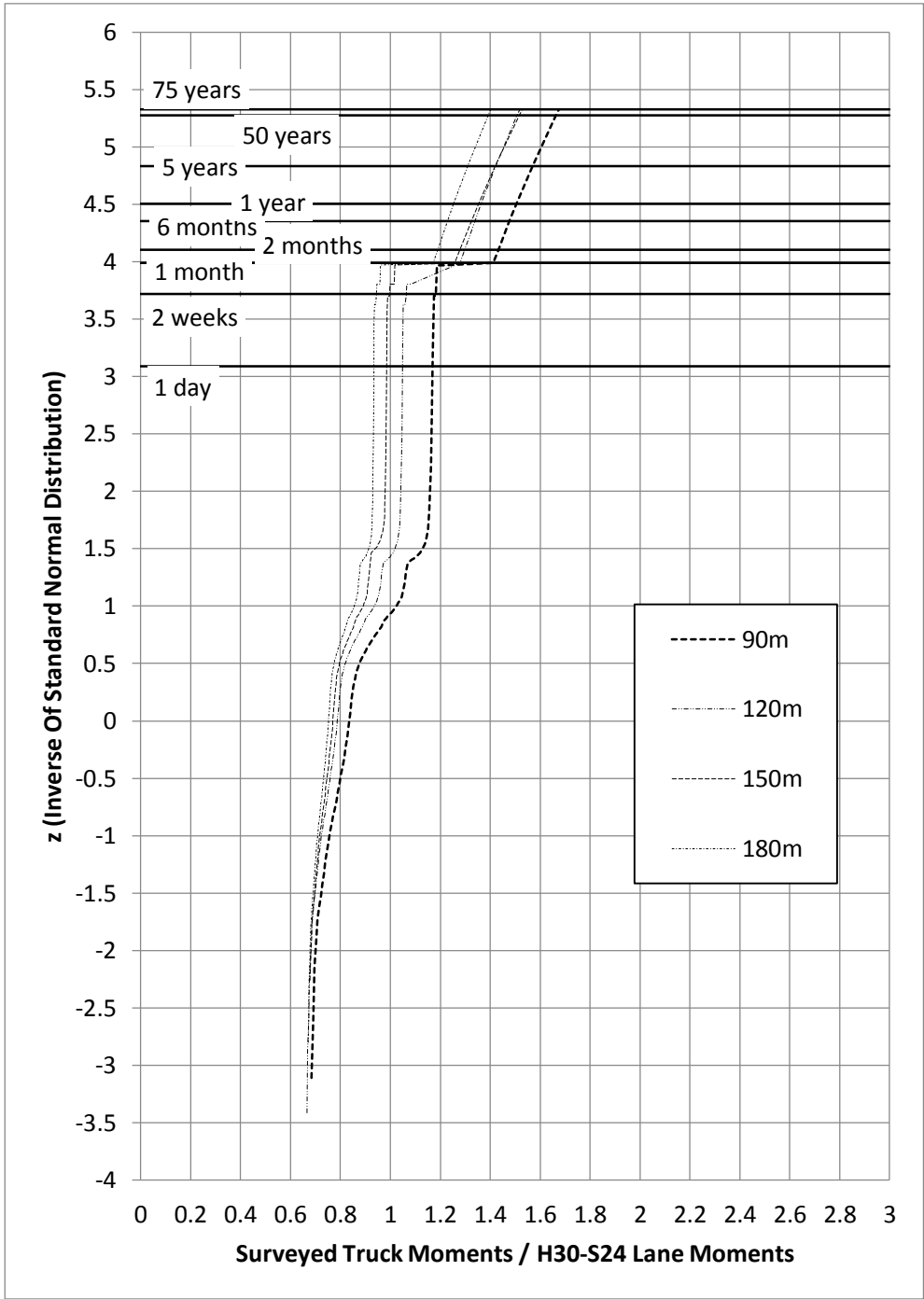
**Figure 72. Extrapolation Moment Ratios for H30-S24 Lane (Upper-tail)**
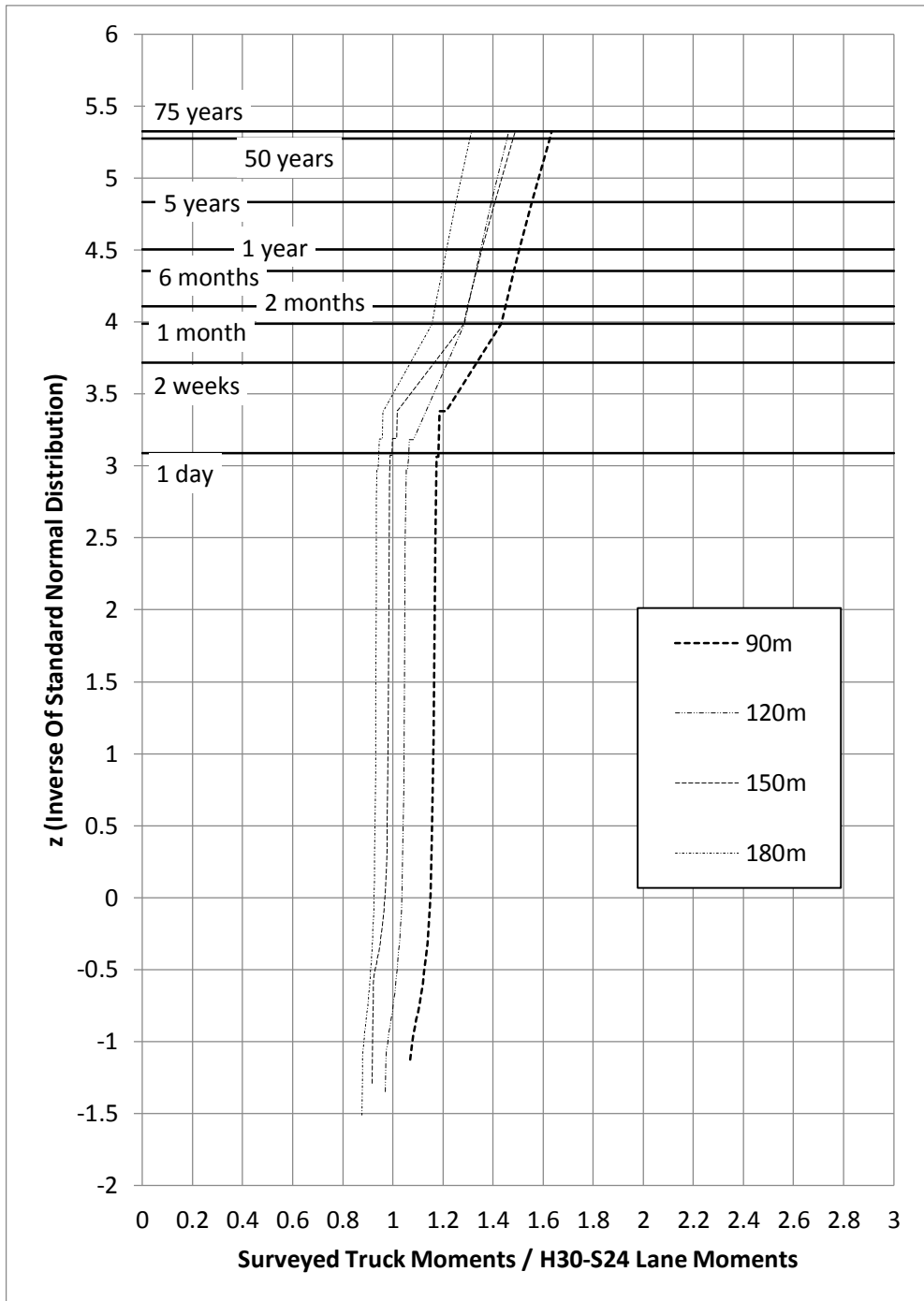
**Figure 73. Extrapolation Moment Ratios for H30-S24 Lane (Extreme)**

63
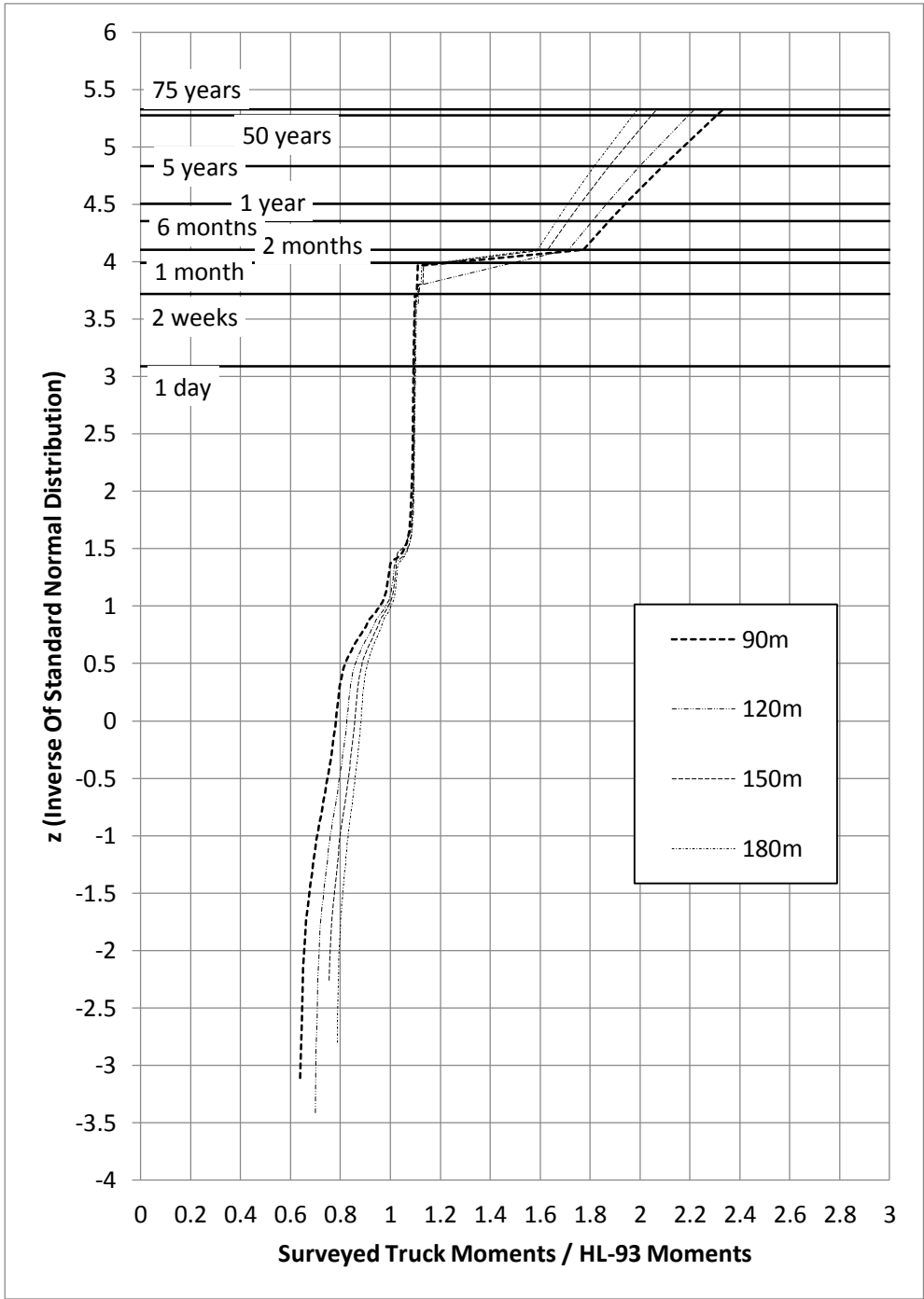
**Figure 74. Extrapolation Moment Ratios for HL-93 (Overall)**
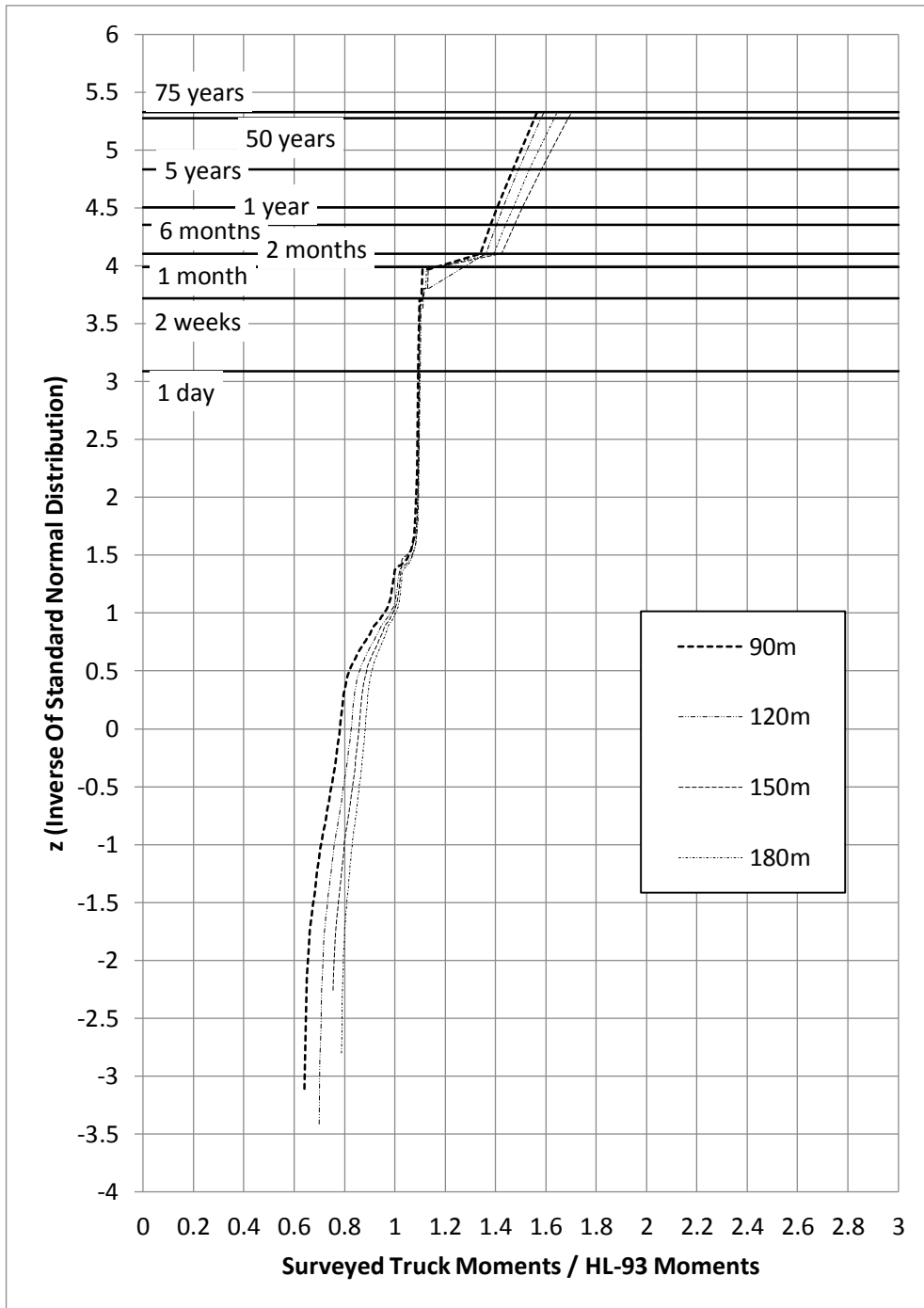
**Figure 75. Extrapolation Moment Ratios for HL-93 (Upper-tail)**
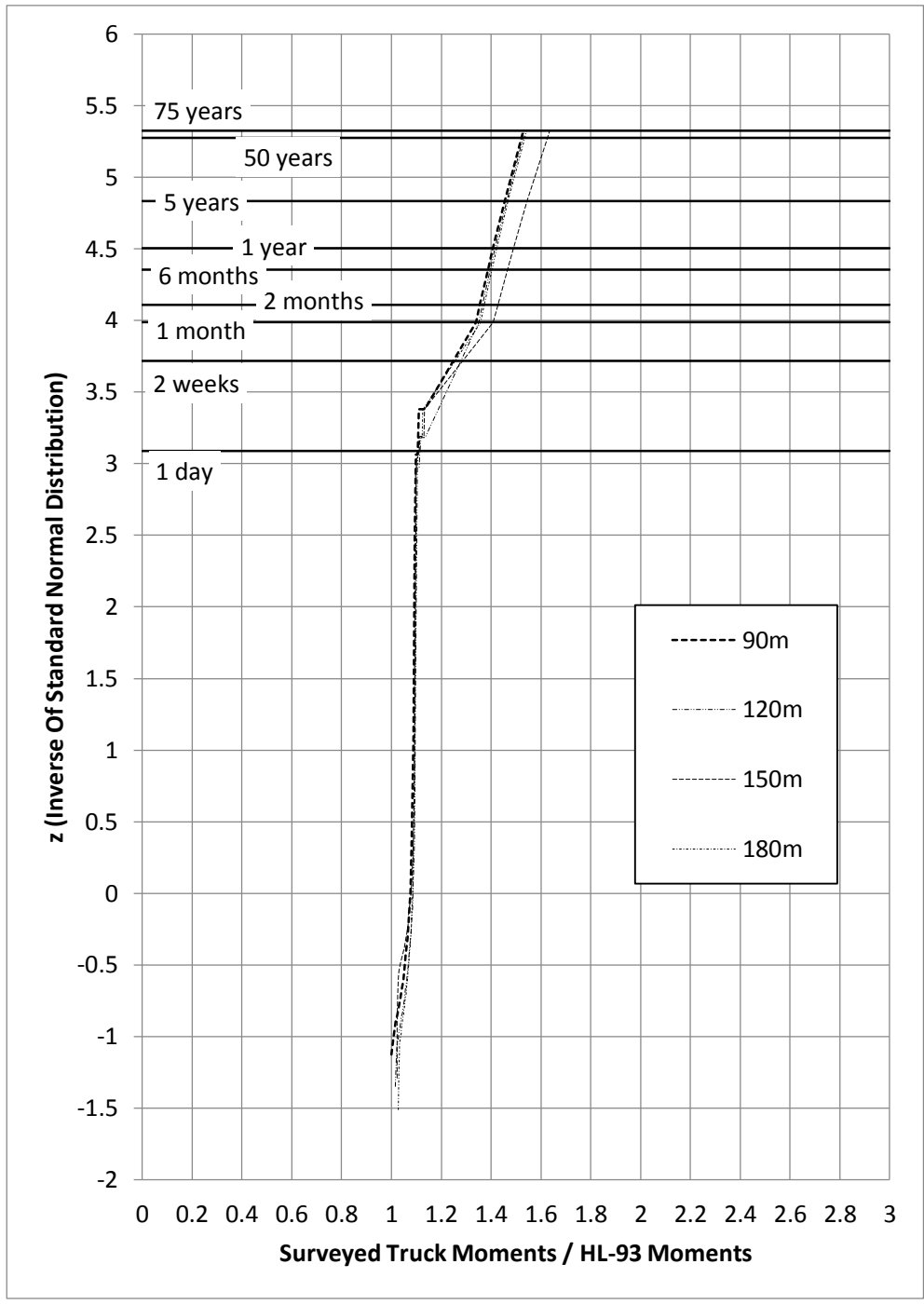
**Figure 76. Extrapolation Moment Ratios for HL-93 (Extreme)**

### 3.2.10 The Uncertainties of Live Load Models

Uncertainties for Overall, Upper-tail and Extreme Cases are calculated according to the track survey data and a straight line fitted to these data points according to Gumbel Probability Method. The coefficient of variation and the mean factor are calculated according to formulas below.

$$\mu = \frac{\sum Mi}{N} \qquad \sigma^2 = \frac{\sum (Mi - \mu)^2}{N-1} \quad \Longrightarrow \quad COV = \frac{\sigma}{\mu} \qquad \qquad [6]$$

$\mu$ = Mean Value

$\sigma$ = Standard Deviation

COV = Coefficient of Variation

Mi = i$^{th}$ Moment Ratio

N = Total Number of Data

From the straight lines fitted to the surveyed truck moments, Gumbel distribution method obtains the uncertainties for live loads. The cumulative distribution functions of the Gumbel distribution for maxima is given by (Castillo, 1988);

$$y = F(x; \lambda, \delta) = exp\left[-exp\left[-\frac{x - \lambda}{\delta}\right]\right] ; \quad -\infty < x < \infty \qquad \qquad [7]$$

where, $\lambda$ and $\delta$ are the Gumbel distribution parameters. Otherwise, equations based on the data for Gumbel probability paper written as in (Castillo, 1988);

$$\eta = h(y) = -\log\left[\log\left(\frac{1}{y}\right)\right] \rightarrow \eta = \frac{x - \lambda}{\delta} \qquad \qquad [8]$$

The parameters λ and δ can be obtained by setting η = 0 and η = 1 (Castillo, 1988);

$$0 = x - \lambda \rightarrow x = \lambda \quad \text{and} \quad 1 = \frac{x - \lambda}{\delta} \rightarrow x = \lambda + \delta \qquad [9]$$

*After fitting the straight line on Gumbel probability paper, the abscissas associated with ordinate values 0 and λ of the reduced variate, η, give the values of λ and 1+ δ, respectively. After obtaining the values of λ and, mean and variance of the Gumbel distribution can be calculated by the following expressions* (Argınhan, 2010);

$$\mu = \lambda + 0.5772\delta \quad \text{and} \quad \sigma^2 = \frac{\pi^2 \delta^2}{6} \qquad [10]$$

μ = Mean

σ = Standard Deviation

Table 23. Gumbel Distribution Parameters for Overall Case

| Span(m) | AYK-45 | | H30-S24 | | H30-S24 Lane | | HL-93 | |
|---|---|---|---|---|---|---|---|---|
| | λ | δ | λ | δ | λ | δ | λ | δ |
| 90 | 0.646 | 0.079 | 0.217 | 0.148 | 0.816 | 0.100 | 0.763 | 0.093 |
| 120 | 0.682 | 0.070 | 0.205 | 0.141 | 0.772 | 0.080 | 0.810 | 0.084 |
| 150 | 0.718 | 0.062 | 0.206 | 0.136 | 0.756 | 0.065 | 0.843 | 0.073 |
| 180 | 0.748 | 0.057 | 0.204 | 0.144 | 0.741 | 0.057 | 0.870 | 0.067 |

Table 24. Statistical Parameters for Overall Case

| Span (m) | AYK-45 | | | H30-S24 | | | H30-S24 Lane | | | HL-93 | | |
|---|---|---|---|---|---|---|---|---|---|---|---|---|
| | μ | σ | cov | μ | σ | cov | μ | σ | cov | μ | σ | cov |
| 90 | 0.69 | 0.10 | 0.15 | 0.30 | 0.19 | 0.63 | 0.87 | 0.13 | 0.15 | 0.82 | 0.12 | 0.15 |
| 120 | 0.72 | 0.09 | 0.13 | 0.29 | 0.18 | 0.63 | 0.82 | 0.10 | 0.13 | 0.86 | 0.11 | 0.13 |
| 150 | 0.75 | 0.08 | 0.11 | 0.28 | 0.17 | 0.61 | 0.79 | 0.08 | 0.11 | 0.88 | 0.09 | 0.11 |
| 180 | 0.78 | 0.07 | 0.09 | 0.29 | 0.19 | 0.64 | 0.77 | 0.07 | 0.09 | 0.91 | 0.09 | 0.09 |

**Table 25. Gumbel Distribution Parameters for Upper-tail Case**

| Span(m) | AYK-45 | | H30-S24 | | H30-S24 Lane | | HL-93 | |
|---|---|---|---|---|---|---|---|---|
| | λ | δ | λ | δ | λ | δ | λ | δ |
| 90 | 0.794 | 0.032 | 0.472 | 0.062 | 0.997 | 0.040 | 0.933 | 0.038 |
| 120 | 0.796 | 0.032 | 0.412 | 0.071 | 0.901 | 0.037 | 0.945 | 0.038 |
| 150 | 0.785 | 0.040 | 0.401 | 0.071 | 0.827 | 0.042 | 0.921 | 0.046 |
| 180 | 0.813 | 0.036 | 0.434 | 0.063 | 0.805 | 0.035 | 0.944 | 0.042 |

**Table 26. Statistical Parameters for Upper-tail Case**

| Span (m) | AYK-45 | | | H30-S24 | | | H30-S24 Lane | | | HL-93 | | |
|---|---|---|---|---|---|---|---|---|---|---|---|---|
| | μ | σ | cov | μ | σ | cov | μ | σ | cov | μ | σ | cov |
| 90 | 0.81 | 0.04 | 0.05 | 0.51 | 0.08 | 0.16 | 1.02 | 0.05 | 0.05 | 0.95 | 0.05 | 0.05 |
| 120 | 0.81 | 0.04 | 0.05 | 0.45 | 0.09 | 0.20 | 0.92 | 0.05 | 0.05 | 0.97 | 0.05 | 0.05 |
| 150 | 0.81 | 0.05 | 0.06 | 0.44 | 0.09 | 0.21 | 0.85 | 0.05 | 0.06 | 0.95 | 0.06 | 0.06 |
| 180 | 0.83 | 0.05 | 0.06 | 0.47 | 0.08 | 0.17 | 0.83 | 0.05 | 0.06 | 0.97 | 0.05 | 0.06 |

**Table 27. Gumbel Distribution Parameters for Extreme Case**

| Span(m) | AYK-45 | | H30-S24 | | H30-S24 Lane | | HL-93 | |
|---|---|---|---|---|---|---|---|---|
| | λ | δ | λ | δ | λ | δ | λ | δ |
| 90 | 0.8801 | 0.0246 | 0.6489 | 0.048 | 1.1122 | 0.0311 | 1.040 | 0.029 |
| 120 | 0.889 | 0.0241 | 0.6127 | 0.0526 | 1.0061 | 0.0272 | 1.056 | 0.029 |
| 150 | 0.8942 | 0.0297 | 0.5939 | 0.0562 | 0.9552 | 0.0318 | 1.049 | 0.035 |
| 180 | 0.9142 | 0.0246 | 0.6146 | 0.0472 | 0.9058 | 0.0244 | 1.062 | 0.029 |

**Table 28. Statistical Parameters for Upper-tail Case**

| Span (m) | AYK-45 | | | H30-S24 | | | H30-S24 Lane | | | HL-93 | | |
|---|---|---|---|---|---|---|---|---|---|---|---|---|
| | μ | σ | cov | μ | σ | cov | μ | σ | cov | μ | σ | cov |
| 90 | 0.89 | 0.03 | 0.04 | 0.68 | 0.06 | 0.09 | 1.13 | 0.04 | 0.04 | 1.06 | 0.04 | 0.04 |
| 120 | 0.90 | 0.03 | 0.03 | 0.64 | 0.07 | 0.10 | 1.02 | 0.03 | 0.03 | 1.07 | 0.04 | 0.03 |
| 150 | 0.91 | 0.04 | 0.04 | 0.63 | 0.07 | 0.11 | 0.97 | 0.04 | 0.04 | 1.07 | 0.04 | 0.04 |
| 180 | 0.93 | 0.03 | 0.03 | 0.64 | 0.06 | 0.09 | 0.92 | 0.03 | 0.03 | 1.08 | 0.04 | 0.03 |

### 3.2.11 Comparison of Different Extrapolation Cases

Using the surveyed truck data gathered from the Turkish General Directorate of Highways, statistical parameters are determined and Gumbel parameters are calculated. Moreover, the extrapolation moment factors are calculated according to the Overall, Upper-tail and Extreme Cases for the live load models. As the calculations illustrates, the bias factors are higher and the coefficient of variations are lower for Extreme Cases comparing other methods. Extreme Case stands for the top ten percent of surveyed truck data, as a result of this the statistical parameters of Extreme Case is used to reflect the most critical situation. Moreover, extrapolated moment factors given better results when Extreme Case is considered.
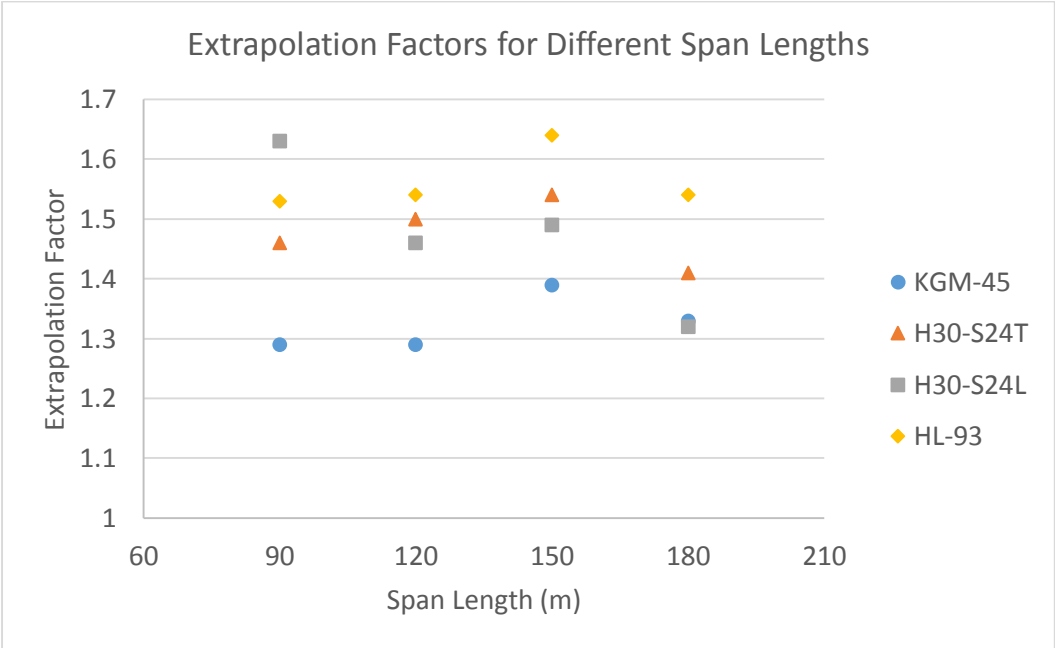


**Figure 77. Extrapolation Moment Ratios for Three Types of Live Load Models with the Span Lengths of 90, 120, 150 and 180m (Extreme)**

## 3.3   DYNAMIC LOAD FACTOR

The vehicular live load models should be increased by the dynamic load factors. Dynamic load factor is determined according to bridge span length, weight of the truck, axle configuration, road roughness. Basically, dynamic load factor is the ratio of dynamic response to static response. Moreover, dynamic response means the absolute maximum dynamic results at any point by means of deflection, stress or strain. Static response stands for the maximum static response from the filtered dynamic response. The comparison of the dynamic and static behaviour of a bridge for the truck load composed of 5 axle, is given below for the speed of 104 km/hr (Nassif and Nowak, 1995).
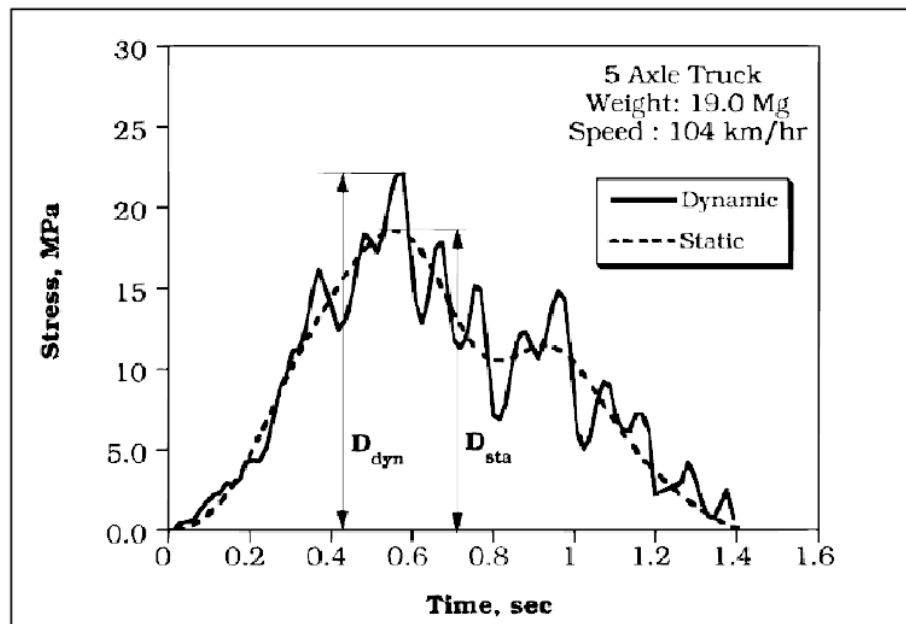


**Figure 78. The Comparison of Dynamic and Static Behaviour for Bridges (Nassif and Nowak, 1995)**

According to the Nowak's calibration report on AASHTO LRFD Bridge Design Specification, the bias factor for dynamic factor is 0.15 and the coefficient of variation is 0.8 respectively. Moreover, the truck moments are increased by 1.33 to take into account the dynamic effects in compliance with AASHTO LRFD.

## 3.4   MULTIPLE PRESENCE FACTOR

In this study, bridge models are constructed to have three lanes. In accordance with the AASHTO LRFD bridge design specification, the following table should be used to increase or decrease the truck live load to take into account the occurrence of having multiple trucks at the same time. Bridges are modeled to have three lanes, so 0.85 is used as multiple presence factor in this study.

**Table 29. Multiple Presence Factor for Different Number of Design Lanes**

| Number of Design Lanes | Multiple Presence Factor |
|---|---|
| 1 | 1.2 |
| 2 | 1 |
| 3 | 0.85 |
| More Than 3 | 0.65 |

## 3.5   SUMMARY OF STATISTICAL PARAMETERS OF LOADS

The uncertainties of statistical parameters are given below in tabular form. The bias factor and the coefficient of variation values are used in reliability analysis to determine the safety level of truck loads.

**Table 30. Summary of Statistical Parameters for Different Load Types**

| Load | Description | Distribution Type | Bias Factor | Coefficient of Variation |
|---|---|---|---|---|
| D1 | Cast in Place - Dead Load | Normal | 1.05 | 0.1 |
| D2 | Wearing Surface - Dead Load | Normal | 1 | 0.25 |
| D3 | Dead Load - Miscellaneous | Normal | 1.05 | 0.1 |
| LL | KGM-45 | Gumbel | 0.909 | 0.036 |
| | H30-S24T | Gumbel | 0.647 | 0.101 |
| | H30-S24L | Gumbel | 1.011 | 0.036 |
| | HL-93 | Gumbel | 1.069 | 0.036 |
| DF | Dynamic Factor | Normal | 0.15 | 0.8 |

# CHAPTER 4

# STATISTICS OF SUPERSTRUCTURE RESISTANCE PARAMETERS

This chapter introduces the uncertainties involved with flexural resistance of segmental box girder post tensioned bridges. To complete the reliability approach for post tensioned bridges, it is necessary to gather information about the uncertainties of resistance parameters for flexural capacity. Data are chosen from Turkey databases to stimulate the uncertainties of Turkish engineering practice. In case of lack or limited amount of Turkish data for a certain case, statistical values are obtained from foreign sources.

## 4.1 MATERIAL PROPERTIES

In the process of designing a segmental box girder post tensioned bridge, three construction materials are usually required; pre-stressing strands, mild reinforcement and concrete. Typically mild reinforcement is placed for constructive reasons and can be ignored in structural resistance computations.

### 4.1.1 Concrete

When compared to the other countries Turkey is a fairly new in concrete industry. The table below illustrates the time of several countries when they started concrete production (Karakule and Akakın, 2005).

**Table 31. Concrete production years of countries (Akakın, T.-Kılınç, C.-Işık, A.-Zengin, H., 2013)**

| Germany | 1903 |
|---|---|
| England | 1930 |
| French | 1933 |
| Spain | 1942 |
| Netherlands | 1948 |
| Belgium | 1956 |
| Austria | 1961 |
| Italy | 1962 |
| Israel | 1963 |
| Turkey | 1976 |

**Table 32. Concrete Production in Turkey between the years 1988 and 2011 (Akakın, T.-Kılınç, C.-Işık, A.-Zengin, H., 2013)**

| Year | # of Companies | # of Facilities | Production$*10^6$ (m$^3$) |
|---|---|---|---|
| 1988 | 25 | 30 | 1.5 |
| 1993 | 70 | 110 | 10 |
| 1998 | 166 | 341 | 26.5 |
| 2003 | 238 | 439 | 25.8 |
| 2004 | 247 | 482 | 31.6 |
| 2005 | 277 | 568 | 46.3 |
| 2006 | 409 | 718 | 70.73 |
| 2007 | 477 | 845 | 74.3 |
| 2008 | 462 | 825 | 69.6 |
| 2009 | 467 | 845 | 66 |
| 2010 | 500 | 900 | 79.7 |
| 2011 | 520 | 945 | 90.5 |

In Table 32 the number of companies, the facilities involved in concrete production and the concrete amount produced in years between 1988 and 2011 (Akakın, T.-Kılınç, C.-Işık, A.-Zengin, H., 2013). Based on this table there is a great increase in concrete production especially after 2005. Concrete become a more popular construction material within years, as a result of this it has a vital effect on the quality of structures.

As the technology and the industrialization improving the necessity of taller buildings, longer bridges, durable structures was increased. On the other hand, considering economy, it is not feasible to use higher amounts of steel to improve the durability of structures. In consequence of this, concrete quality has been improved by years to build high rise buildings, post tensioned bridges with extreme span lengths. In Table 33 below, the increase in higher concrete classes can be observed between 1996 and 2011 (Akakın, T.-Kılınç, C.-Işık, A.-Zengin, H., 2013).

**Table 33. Concrete Production for different concrete class in Turkey within years (Akakın, T.-Kılınç, C.-Işık, A.-Zengin, H., 2013)**

| Year | C14 | C18 | C20 | C25 | C30+ | C20 and lower % | C25 and higher % |
|---|---|---|---|---|---|---|---|
| **1996** | 37.5 | 52.3 | 6.4 | 3.4 | 0.6 | 96.2 | 4 |
| **1997** | 27 | 51.1 | 12 | 7.6 | 2.3 | 90.1 | 9.9 |
| **1998** | 24.4 | 45.4 | 18 | 8.1 | 4.1 | 87.8 | 12.2 |
| **1999** | 22.7 | 35.9 | 27.6 | 10.3 | 3.3 | 86.2 | 13.6 |
| **2000** | 11.5 | 25.1 | 41.3 | 13.2 | 4.9 | 77.9 | 18.1 |
| **2001** | 7 | 21.3 | 47.9 | 18 | 5.8 | 76.2 | 23.8 |
| **2002** | 5.9 | 21.1 | 46.9 | 19.2 | 6.9 | 73.9 | 26.1 |
| **2003** | 4.6 | 14.7 | 39.6 | 25.4 | 15.7 | 58.9 | 41.1 |
| **2004** | 3.3 | 10.3 | 40.6 | 30.7 | 15.1 | 54.2 | 45.8 |
| **2005** | 3.2 | 8.4 | 31.2 | 42.1 | 15.1 | 42.8 | 57.2 |
| **2006** | 2.92 | 7.66 | 35.09 | 36.56 | 17.77 | 45.67 | 54.33 |
| **2007** | 2.85 | 5.58 | 26.95 | 35.25 | 29.37 | 35.38 | 64.62 |
| **2008** | 2.76 | 5.51 | 22.13 | 38.76 | 30.84 | 30.4 | 69.6 |
| **2009** | 2.44 | 3.44 | 23.9 | 36.1 | 34.12 | 29.78 | 70.22 |
| **2010** | 1.99 | 2.39 | 14.62 | 38.45 | 39.33 | 19 | 77.78 |
| **2011** | 2.2 | 2 | 14.6 | 43.7 | 37.1 | 18.8 | 80.8 |
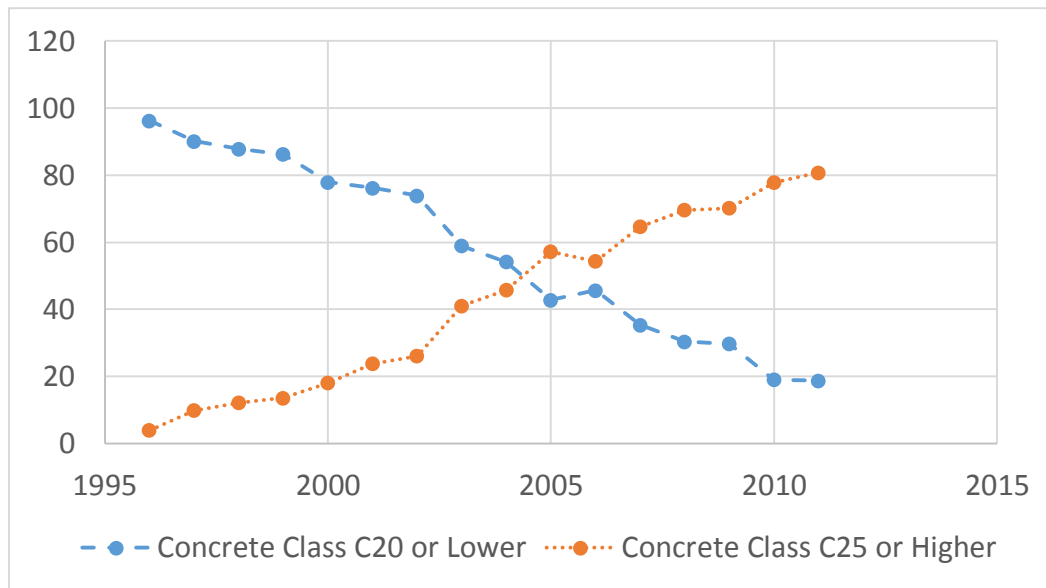
**Figure 79. Concrete Production for different concrete class in Turkey within years in graphic form (Akakın, T.-Kılınç, C.-Işık, A.-Zengin, H., 2013)**

## 4.1.2   Statistical Parameters of Concrete Used in Superstructure (C40)

C40 and C45 is most common concrete class for post tension bridge construction in Turkey. C40 concrete is used for designing of post tensioned superstructure in this study. Laboratory test results are gathered from concrete facilities to obtain the statistical parameters for C40 class concrete. Moreover, according to AASHTO LRFD 5.4.2.1 specified concrete strength cannot be used above 70 MPa and below 16 MPa.

Argınhan (2010) reveals the statistical parameters of the concrete production for Turkey. Documented the uncertainty of C30 and C40 concrete class upon the the collected laboratory results can be found at Argınhan's (2010) work. In this study, for the statistical parameters of C40 class concrete, such as coefficient of variation and bias factor are taken from Argınhan (2010).

Two types of statistical analyses has been performed in the work of Argınhan. In the first one, all data were included in computations to evaluate the statistical parameters

of concrete strength class. In the second method the mean and coefficient of variation were determined for the concrete specimen groups of three. It has been reported that the second method leads to lower values for coefficient of variation (Argınhan, 2010).

**Table 34. C40 Concrete Parameters According to the First Firm for 7 and 28 Day Strength (Argınhan, 2010)**

| Statistical Parameters | 7-Day | | 28-Day | |
|---|---|---|---|---|
| | Overall | In-Batch | Overall | In-Batch |
| Max Value (MPa) | 43.3 | 42.62 | 50.15 | 49.17 |
| Min Value (MPa) | 35.96 | 37.59 | 44.44 | 45.59 |
| μ, Mean (MPa) | 39.58 | | 47.57 | |
| σ, Standard Deviation (MPa) | 1.86 | 1.7 | 1.39 | 1.26 |
| COV, Coefficient of Variation | 0.047 | 0.043 | 0.029 | 0.026 |
| Bias Factor(mean/nominal) | - | | 1.189 | |

**Table 35. C40 Concrete Parameters According to the Second Firm for 7 and 28 Day Strength (Argınhan, 2010)**

| Statistical Parameters | 7-Day | | 28-Day | |
|---|---|---|---|---|
| | Overall | In-Batch | Overall | In-Batch |
| Max Value (MPa) | 47.52 | 44.68 | 60.2 | 57.78 |
| Min Value (MPa) | 30.85 | 31.9 | 40.87 | 42.72 |
| μ, Mean (MPa) | 37.24 | | 47.84 | |
| σ, Standard Deviation (MPa) | 3.37 | 3.13 | 3.66 | 3.16 |
| COV, Coefficient of Variation | 0.09 | 0.084 | 0.077 | 0.066 |
| Bias Factor(mean/nominal) | - | | 1.196 | |

**Table 36. C40 Concrete Parameters According to the First and Second Firm for 7 and 28 Day Strength (Argınhan, 2010)**

| Statistical Parameters | 7-Day | | 28-Day | |
|---|---|---|---|---|
| | Overall | In-Batch | Overall | In-Batch |
| Max Value (MPa) | 47.52 | 44.68 | 60.2 | 57.78 |
| Min Value (MPa) | 30.85 | 31.9 | 40.87 | 42.72 |
| μ, Mean (MPa) | 37.37 | | 47.82 | |
| σ, Standard Deviation (MPa) | 3.34 | 3.11 | 3.57 | 3.08 |
| COV, Coefficient of Variation | 0.089 | 0.083 | 0.075 | 0.066 |
| Bias Factor(mean/nominal) | - | | 1.2 | |

### 4.1.3 Evaluation of Statistical Parameters for C40 Concrete Class

Until this point, statistical uncertainties about C40 class concrete are illustrated. Beyond these aleatory uncertainties of concrete compressive strength, there are additional factors that effects the concrete strength.

To begin with, site measurement to determine the compressive strength of concrete can have large deviations compared to the ones obtained at laboratory conditions. As a result of the different concrete mix, segregation process, variable shape and size, different loads and variational temperature, the laboratory results cannot match with the in situ results. Mirza indicated that ratio of core strength to real strength varies between 0.74 and 0.96 and the corresponding coefficient of variation is 0.1(Mirza, 1979).

The mean of statistical parameters can be expressed according to the upper and lower boundaries. The average value of an uncertainty according to two limits and corresponding coefficient of variation can be determined. When it is compared to standard building construction, bridge constructions are usually well controlled. As a result of this, the difference between laboratory tests and in situ results can be expressed as upper triangular distribution as below (Ang-Tang, 1984).
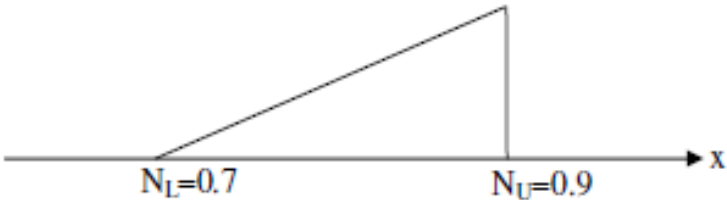


**Figure 80. Upper Triangle Probability Density Function for $N_L$ to $N_U$ (Ang-Tang, 1984)**

The mean value and coefficient of variation can be calculated by using the equations below

$$\overline{N} = \frac{1}{3}\left(N_L + 2N_U\right) \qquad \text{[11]}$$

$$\Delta = \frac{1}{\sqrt{2}}\left(\frac{N_U - N_L}{2N_U + N_L}\right) \qquad \text{[12]}$$

$N_U$: Upper limit

$N_L$: Lower limit

N: Mean correction factor

Δ: Coefficient of variation

$N_1$ is calculated as 0.89 and $\Delta_1$ is obtained 0.06, but to get more conservative results $\Delta_1$ is taken as 0.1. These calculations are fulfilled according to upper triangular distribution (Fırat, 2007).

Rate of loading is another parameter which effects the compressive strength of concrete. Laboratory conditions can not reflect the in situ characteristics, as the rate loading increases compressive strength of concrete increases. The mean correction factor is 0.89 and coefficient of variation is ignored (Mirza, 1979).

Another uncertainty effects the compressive strength of concrete is human errors. To determine the statistical parameters of compression strength of concrete, the specimens are selected randomly. As a result of this, variability concept exists for the compressive strength of randomly selected specimens. The mean correction factor is 1.0 and the corresponding coefficient of variation is 0.05 (Kömürcü, 1995).

Therefore, C40 concrete class uncertainty based on these three parameters calculated as, 0.89*0.89*1.00 = 0.8 and coefficient variation of C40 concrete is determined as

$\sqrt{(0.1^2 + 0.05^2)} = 0.11$. Combining with the original coefficient of variation resulting from specimens $\sqrt{(0.11^2 + 0.064^2)} = 0.127$.

**Table 37. Statistical Parameters for C40**

| Statistical Parameters | C40 |
|---|---|
| Laboratory Measured Mean (MPa) | 47.8 |
| In-situ Mean (MPa) | 38.3 |
| σ, Standard Deviation (MPa) | 4.9 |
| COV, Coefficient of Variation | 0.127 |
| Nominal Strength (MPa) | 40 |
| Bias Factor(mean/nominal) | 0.96 |

## 4.3.2 Prestressing Strands

Seven wire strand is basically composed of seven strands, twisting six strands around the other one which is at the center. It is the most popular stressing method in pre-stressed and post tensioned girders. There are two types of manufacturing seven wire strands. In the first manufacturing process, the residual stress which occurs by the twisting and the cooling of the strands is eliminated by heating the strands up to 350°C. The strands are allowed to cool slowly in order to cancel the extra stress resulting from the manufacturing process. As a result of this, the residual stresses are eliminated and the yield stress of the pre-stressing strand increases. This manufacturing process is called as stress relieving. Other process of production contains tensioning of the strands while cooling process to reduce the relaxation of the strands. The seven wire strand produced by this method is called low-relaxation strand.

The stress-strain relationship for different manufacturing process of seven wire strands is illustrated in According to the Figure 81 the most efficient method of manufacturing of seven wire strand low relaxation process.
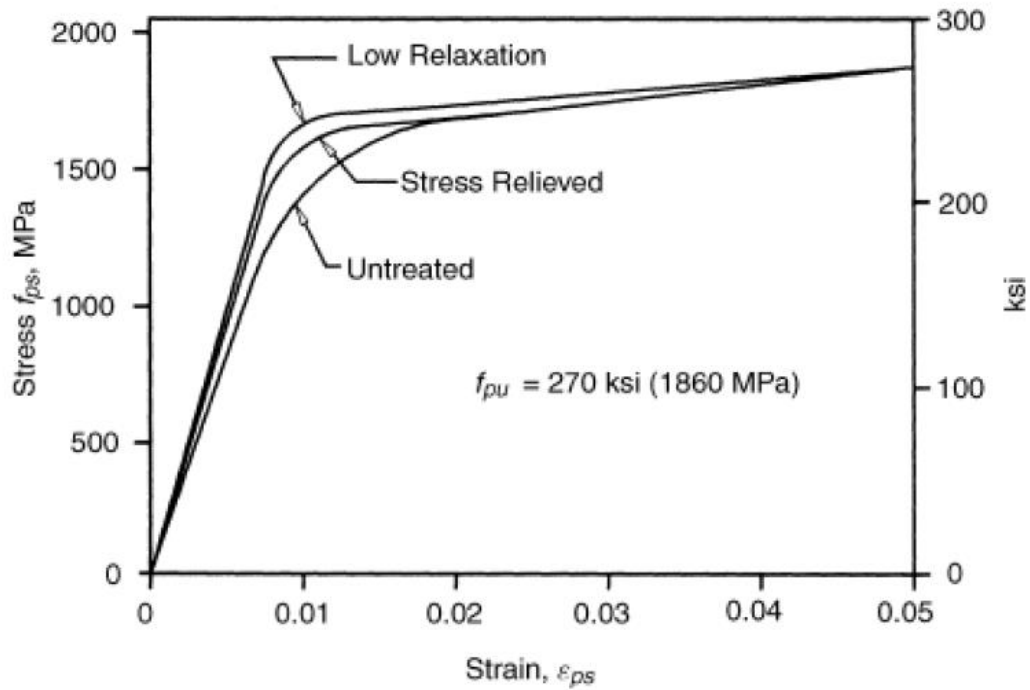
**Figure 81. The Results of Different Types of Manufacturing Process for Seven Wire Strands (Barker and Puckedd, 2007)**

### 4.1.4  Statistical Parameters of Prestressing Strands

Number of 146 tensile strength test results gathered and investigated for prestressing strands. Yield strength statistical parameters are listed in Table 38 (Argınhan, 2010).

**Table 38. Statistical Parameters for Ultimate Strength of Prestressing Strands**

| Statistical Parameters | Values |
|---|---|
| Max Value (MPa) | 1781 |
| Min Value (MPa) | 1599 |
| μ, Mean (MPa) | 1740 |
| σ, Standard Deviation (MPa) | 36.29 |
| COV, Coefficient of Variation | 0.021 |
| Bias factor (mean/nominal) | 1.04 |

Mirza determined the statistical parameters of yield strength of prestressing strands (Mirza, 1980). Out of 200 test records to evaluate the mean bias factor of yield strength

as 1.04 and the corresponding coefficient of variation as 0.03. These values are compatible with the values found from the test results according to Argınhan's work (2010). Moreover, the statistical parameters which Mirza determined are common values for reliability approaches in several journals. Therefore, the mean bias factor is taken as 1.00 and coefficient of variation is taken as 0.03.

Frangopol and Al-Harty investigate the physical uncertainties about the pre-stressing strands. In the article 1.01 is used as the mean bias factor and and 0.0125 for the coefficient of variation resulting from the uncertainties according to the cross sectional area of the strands (Harty and Frangopol, 1994).

**Table 39. Statistical Parameters for Prestressing Strands**

| Statistical Parameters | Prestressing Strand | |
|---|---|---|
| | Yield Strength | Cross Section |
| COV, Coefficient of Variation | 0.03 | 0.0125 |
| Bias factor | 1 | 1 |

## 4.2   DIMENSIONS

Mirza defined the cross sectional and dimensional uncertainties for precast beams and post tensioned beams constructed in situ (Mirza, 1979).

**Table 40. Statistical Parameters for Dimensions of In-Situ Beams and Precast Beams (Mirza, 1979)**

| Dimension Description | | In-Situ Beam | | | Precast Beam | | |
|---|---|---|---|---|---|---|---|
| | | Nominal Range | Mean Dev. | Standard Dev. | Nominal Range | Mean Dev. | Standard Dev. |
| Width | Rib | 11-12 | +3/32 | 3/16 | 14 | 0 | 3/16 |
| | Flance | - | - | - | 19-24 | +5/32 | 1/4 |
| Overall Depth | | 18-27 | -1/8 | 1/4 | 21-39 | +1/8 | 5/32 |
| Effective Depth | Top Reinforcement | 1-1/2 | +1/8 -1/4 | 5/8 11/16 | 2-2 1/2 | 0 +1/8 | 5/16 11/32 |
| | Bottom Reinforcement | 3/4-1 | +1/16 -3/16 | 7/16 1/2 | 3/4 | 0 +1/8 | 5/16 11/32 |
| Beam Spacing and Span | | - | 0 | 11/16 | | 0 | 11/32 |
| - Dimensions are in inches | | | | | | | |

According to the Mirza's studies Table 40 is constructed. We can make a reliable assumption for the statistical parameters of in-situ beam dimensions. For instance, if $b_w$ is assumed as 1000mm, then the mean is calculated as 1000 mm + 2.38 mm (3/32 inch). The corresponding standard deviation is calculated as 4.76 mm.

$$\mu_b = b_n + 3.96mm. \qquad [13]$$

$$\delta_b = (6.35)mm./(b_n + 3.96mm.) \qquad [14]$$

Coefficient of variation for flange width is determined as 4.76/1002.38 = 0.00475

Bias factor for flange width calculated as 1002.76/1000 = 1.00276

Applying the same procedure for $d_p$;

$$\mu_{dp} = d_{pn} + 3.18mm \qquad [15]$$

$$\delta_{dp} = 8.73mm/(d_{pn} + 3.18mm) \qquad [16]$$

Effective depth for top post tensioning tendons has a mean deviation as 3.18 mm. Standard deviation for effective depth is stated as 8.73 mm (Mirza, 1979). As a result of this coefficient of variation equals to 8.73/1003.18 = 0.0087 if $d_p$ is assumed as 1000 mm.

The variations from the nominal values for dimensions is quite small. Therefore, nominal values and mean values area assumed to be equal. The bias factor is taken as 1.0 and the coefficient of variation is taken as 0.015, since the dimensions of the post tension beam are bigger when it is compared to the nominal values in Mirza's study.

## 4.4 Statistical Parameters of Resistance Factors

The uncertainty factors of the resistance parameters are given in Table 41. Coefficient of variations, bias factors, type of probability distributions are given in detail for reliability analysis.

Table 41. Statistical Parameters of Resistance Factors

| Parameter | Probability Distribution | Bias Factor | Coefficient of Variation |
|---|---|---|---|
| Concrete Strength | Lognormal | 0.96 | 0.127 |
| Prestressing Tendon Area | Normal | 1 | 0.0125 |
| Prestressing Tendon Strength | Normal | 1 | 0.015 |
| Dimensions | Normal | 1 | 0.015 |

# CHAPTER 5

# MODELLING AND DESIGN OF THE BRIDGES

In this study, LARSA4D (version 7.08.05) was used to model the balanced cantilever bridges and both constructional stage and final stage of the bridges are investigated due to both, temporary and permanent loads. This chapter explains the details and the preferences in the model and comparison of the results. Moreover design of the bridge superstructures according to the corresponding results and also the AASHTO design specification.

## 5.1 PRELIMINARY DESIGN OF THE SUPERSTRUCTURES

To achieve the target reliability index, the cross section dimensions of the superstructure at the pier and mid-span must be determined. Selected cross section dimensions must satisfy the minimum requirements of AASHTO design specifications and Turkish Bridge Design Guideline (TUBITAK, 110G093). According to AASHTO LRFD 2010 5.14.2.3.10d and TUBITAK 110G093 T.3.3 limitations for cross section dimensions are below;

- For variable depth girder with parabolic haunches at pier $1/16 > d_o/L > 1/20$ (optimum 1/18)

- At center of span $1/30 < d_o < 1/50$

- Depth width ratio for a single cell box should be do/b ≥ 1/6

Moreover, the limits for flange, web thickness and other dimensional parameters are determined according to both AASHTO LRFD 5.14.2.3.10 and The Turkish Bridge Design Guideline. The preliminary design for post-tensioned box girders is fulfilled according to part T.3.3. in Turkish Bridge Design Guideline (TUBITAK, 110G093).

Minimum flange thickness is must be more than 1/30 of the distance between webs or haunges. Furthermore, it must be minimum 225 millimeters if transversal post-tensioning is used. Transversal post-tensioning decreases the cracks occurring in top flange and expands the service life of longitudinal post-tensioning tendons.

Minimum web thickness is 200 millimeters, if there is not necessity for vertical post-tensioning. On the other hand, the web thickness must be minimum 300 millimeters. Moreover, if there is both transversal and longitudinal post-tensioning, minimum web thickness cannot be under 400 millimeters.

The cantilever arm for top flange cannot be larger than the 0.45 of the distance between the webs. The cantilever arm for top flange defined as the distance from web center to the end.
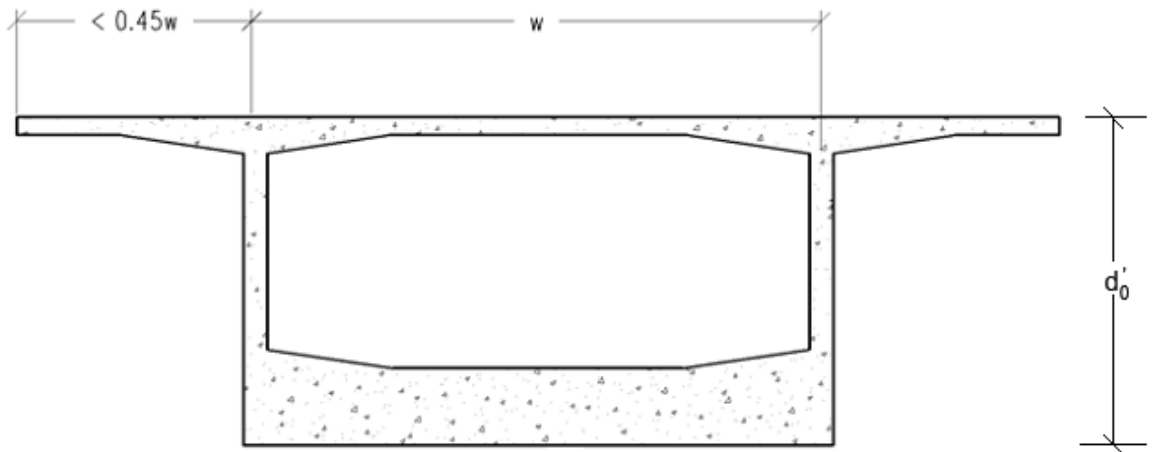
**Figure 82. Top Flange Cantilever Length**

Superstructure depth to span length ratio can be increased up to 1/30 when the bridge depth is constant. If depth is variable between pier and mid-span, then it is suitable to set $d_0/L$ ratio 1/50 at mid-span and 1/20 at piers.
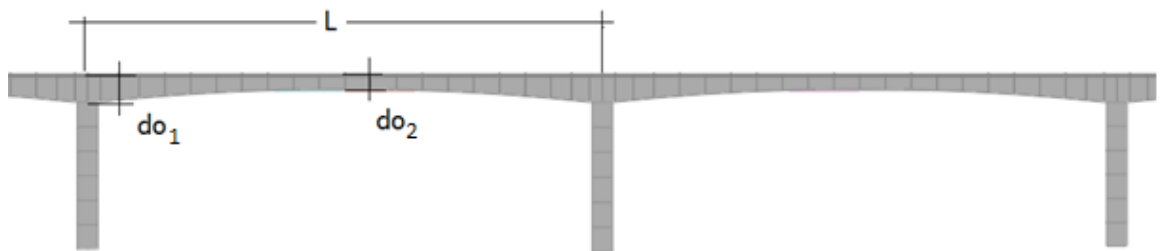


**Figure 83. Superstructure Depth Ratio**
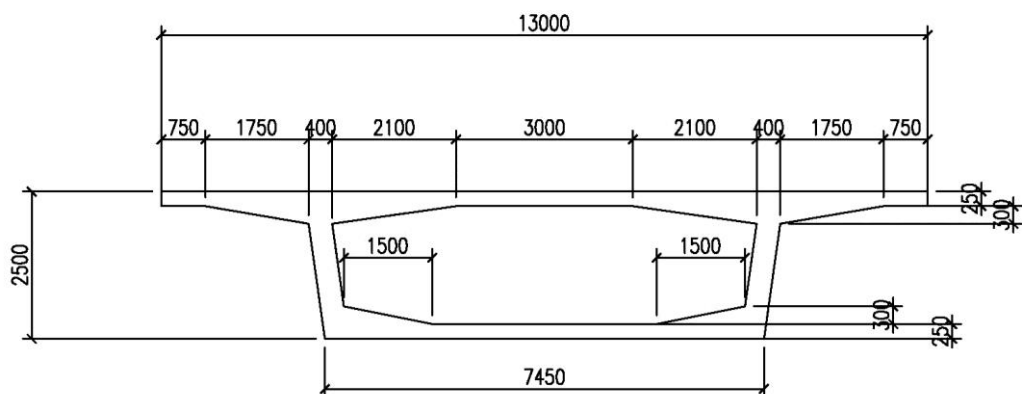


**Figure 84. Superstructure Cross Section for L = 90 meters at Mid-Span**
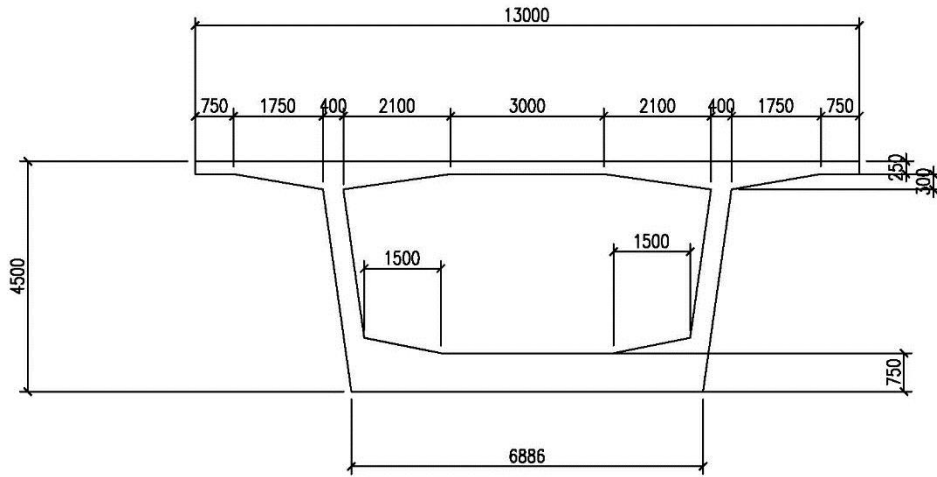
**Figure 85. Superstructure Cross Section for L = 90 meters at Piers**

,
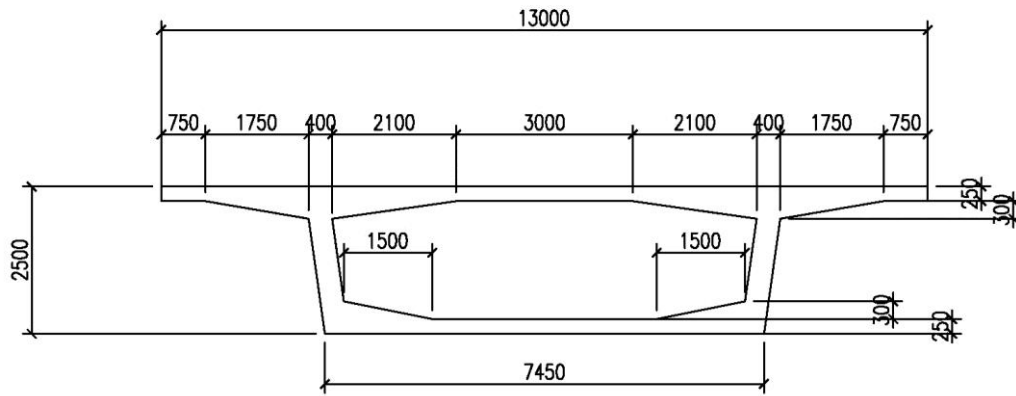


**Figure 86. Superstructure Cross Section for L = 120 meters at Mid-Span**
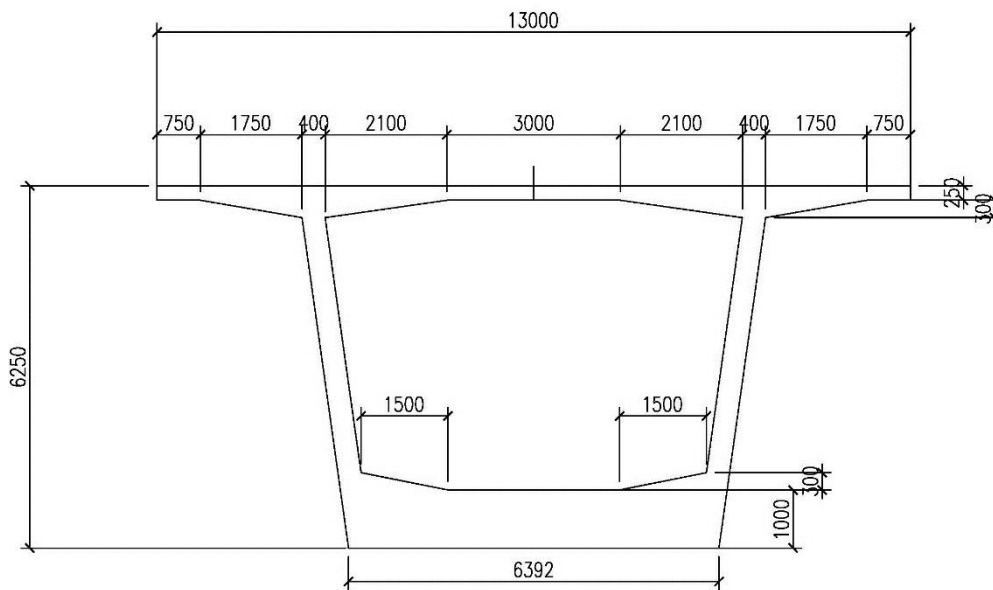


**Figure 87. Superstructure Cross Section for L = 120 meters at Piers**

88
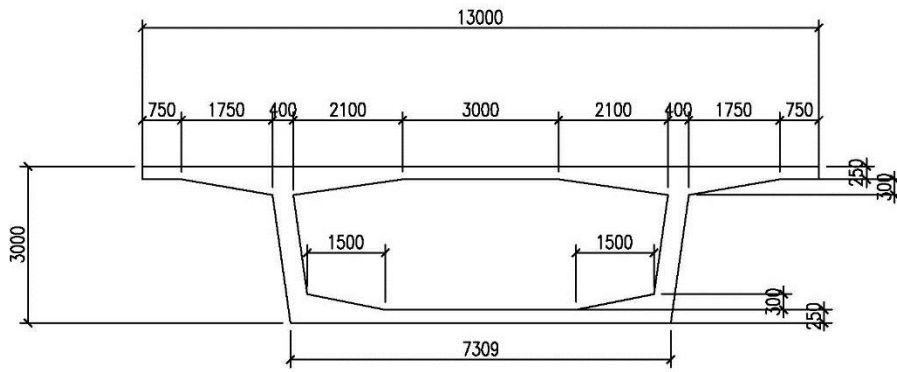
**Figure 88. Superstructure Cross Section for L = 150 meters at Mid-Span**
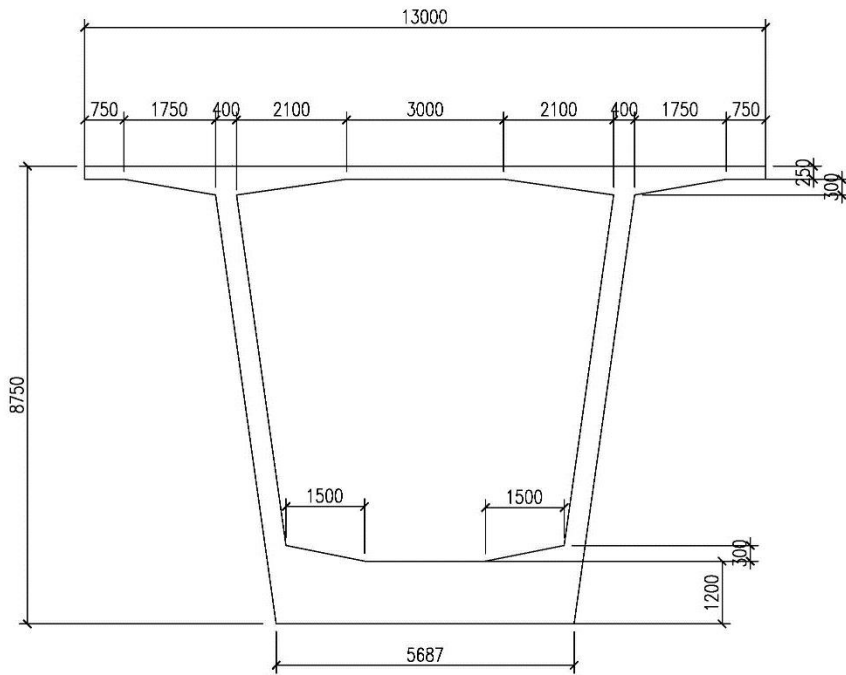


**Figure 89. Superstructure Cross Section for L = 150 meters at Piers**
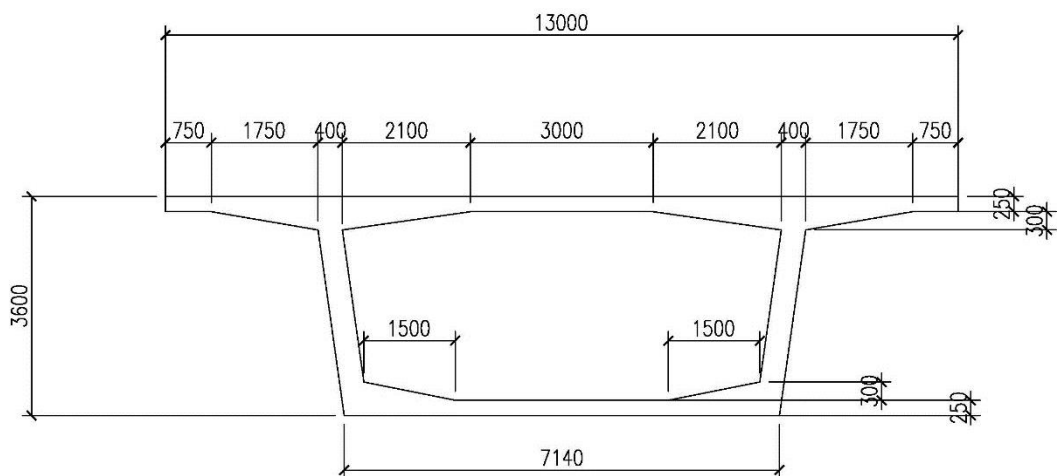


**Figure 90. Superstructure Cross Section for L = 180 meters at Mid-Span**

89
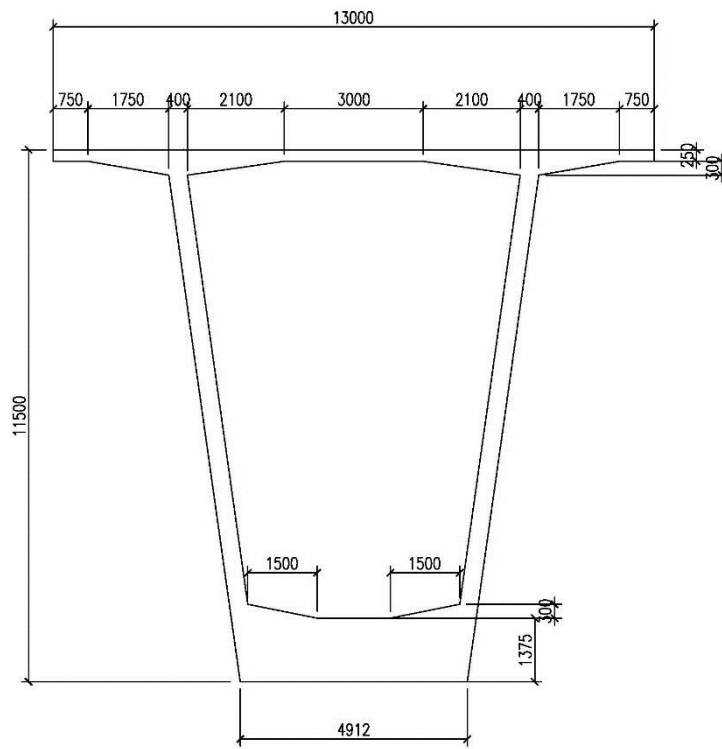
**Figure 91. Superstructure Cross Section for L = 180 meters at Piers**
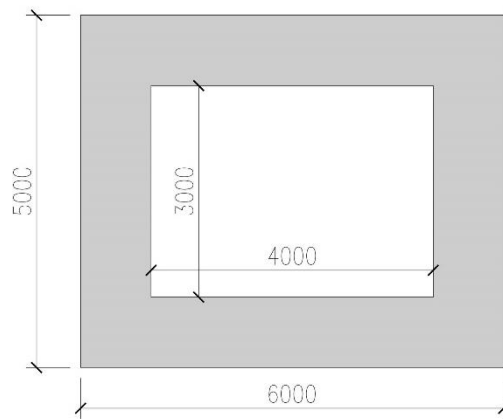


**Figure 92. Pier Cross Section**

## 5.2 DETERMINING THE NUMBER OF POST-TENSIONING DUCTS

To calculate the necessary post tensioning, the bridge is solved without any post-tensioning ducts and the maximum tension stress is obtained. First of all, constructional stage loads are investigated. The maximum flexural tension stress is stated as $f_b$ and the allowable flexural tension stress during stage construction is called as $f_{ri}$. Then the total flexural tension stress is calculated as;

$$f_{pa} = f_b - f_{ri} \qquad [17]$$

Total tension stress must be eliminated in order to complete a proper design for stage construction. To calculate the necessary post-tensioning force the equation below can be used according to TUBITAK 110G093 T.3.4.2

$$-f_{pa} = -\frac{P_p}{A_{section}} - \frac{M_p}{S_a} = -\frac{P_p}{A_{section}} - \frac{P_p e}{S_a} \qquad [18]$$

In this equation Pp stands for the necessary post tensioning force to eliminate the flexural tension stress occurring in stage construction. $A_{section}$ is the area of the section and $S_a$ is the top section modulus for this case. After calculating the Pp force from this equation the number of post tensioning tendons can be calculated.

$$n_{tendons} = \frac{P_p}{f_{pi} A_{tendon} (1 - loss\%)} \qquad [19]$$

$F_{pi}$ is the first jacking force applied to the tendons and it is $0.75f_{pu}$, then the post tensioning loss is effect the first jacking force. %15-20 is good assumption for post tensioning loss, after all the calculation is done if this assumption is not enough then the amount of post-tensioning must be increased. Also Service 3 Load Combination is investigated whether it gives higher tension stress results.

## 5.3 CONSTRUCTIONAL STAGE ANALYSIS

Stress computed during stages must be under the limits defined for the stage construction analyses. In the process of balanced cantilever construction, first step is to construct the piers of the system. After pier construction is done, in order to maintain the balance, both arms of the bridge superstructure are placed equally. An example of balanced cantilever construction is shown in Figure 93 schematically.
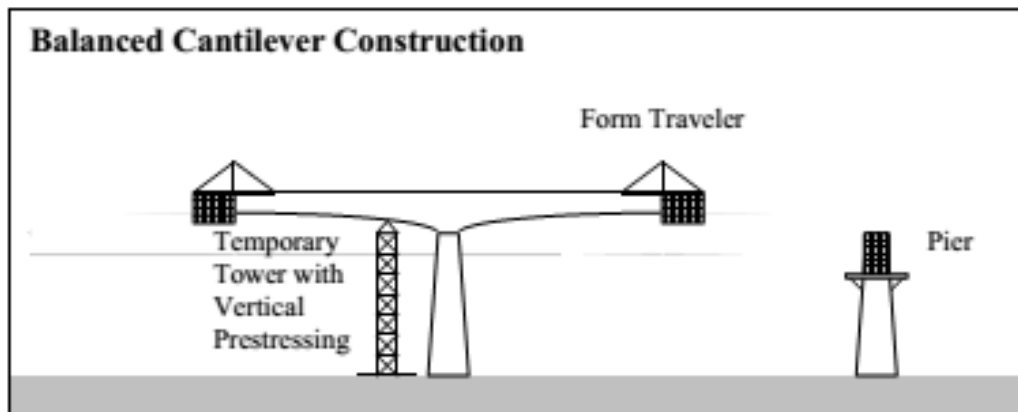


Figure 93. Staged Construction

In addition to the selfweight of the bridge, there is a need of temporary loads for segmentally constructed bridges. Cross section properties and required post-tensioning amount also checked according to constructional stage analyses. Loads taken into account for segmental construction is given below according to AASHTO section 5.14.2.3.2.

DC = Weight of superstructure

DIFF = Differential load: applicable only to balanced cantilever construction taken as 2 percent of the dead load applied to one cantilever.

CLL = Distributed construction live load: an allowance for miscellaneous items of plant, machinery, and other equipment, apart from the major specialized erection equipment; taken as $4.8 \times 10^{-1}$ kPa of deck area; in cantilever construction, this load is taken as $4.8 \times 10^{-1}$ kPa on one cantilever and $2.4 \times 10^{-1}$ kPa on the other.

CE = Specialized construction equipment: the load from segment delivery trucks and any special equipment, including a form traveler launching gantry, beam and winch, truss, or similar major auxiliary structure and the maximum loads applied to the structure by the equipment during the lifting of segments

IE = Dynamic load from equipment: determined according to the type of machinery anticipated. According to Article C5.14.2.3.2 IE may be taken as 10 percent of the segment weight.

Compressive stress in concrete for stage construction shall not exceed 0.50 $f$'c and flexural tension stress limit is $0.58\sqrt{f}$'c.

While modelling the balanced cantilever bridges, three different segment lengths are used; 3, 4 and 5 meters. Therefore, segment lengths are arranged as 1x3+4x3+5x5 to obtain 45 meters of span length. For other bridges, segments which have 5 meters are utilized. Segment weights for 90 meters of span lengths are given below.

**Table 42. Segment Weights for L=90m**

| Segment | Weight(kN) |
|---|---|
| Segment 0 | 1929.33 |
| Segment 1 | 2485 |
| Segment 2 | 2318.68 |
| Segment 3 | 2170.05 |
| Segment 4 | 2533.17 |
| Segment 5 | 2368.35 |
| Segment 6 | 2243.3 |
| Segment 7 | 2159.28 |
| Segment 8 | 2135.05 |
| Segment 9 | 2085.625 |

**Table 43. Load Combinations and Stress Limits for Constructional Stage Analyses**

| Load Combination | LOAD FACTORS | | | | | | | | | | | | | | | STRESS LIMITS | | | | See Note |
|---|---|---|---|---|---|---|---|---|---|---|---|---|---|---|---|---|---|---|---|---|
| | Dead Load | | | Live Load | | | Wind Load | | | Other Loads | | | | | Earth Loads | Flexural Tension | | Principal Tension | | |
| | DC | DIFF | U | CLL | IE | CLE | WS | WUP | WE | CR | SH | TU | TG | WA | EH EV ES | Excluding "Other Loads" | Including "Other Loads" | Excluding "Other Loads" | Including "Other Loads" | |
| a | 1.0 | 1.0 | 0.0 | 1.0 | 1.0 | 0.0 | 0.0 | 0.0 | 0.0 | 1.0 | 1.0 | 1.0 | $\gamma_{TG}$ | 1.0 | 1.0 | $0.50\sqrt{f'_c}$ | $0.58\sqrt{f'_c}$ | $0.289\sqrt{f'_c}$ | $0.331\sqrt{f'_c}$ | — |
| b | 1.0 | 0.0 | 1.0 | 1.0 | 1.0 | 0.0 | 0.0 | 0.0 | 0.0 | 1.0 | 1.0 | 1.0 | $\gamma_{TG}$ | 1.0 | 1.0 | $0.50\sqrt{f'_c}$ | $0.58\sqrt{f'_c}$ | $0.289\sqrt{f'_c}$ | $0.331\sqrt{f'_c}$ | — |
| c | 1.0 | 1.0 | 0.0 | 0.0 | 0.0 | 0.0 | 0.7 | 0.7 | 0.0 | 1.0 | 1.0 | 1.0 | $\gamma_{TG}$ | 1.0 | 1.0 | $0.50\sqrt{f'_c}$ | $0.58\sqrt{f'_c}$ | $0.289\sqrt{f'_c}$ | $0.331\sqrt{f'_c}$ | — |
| d | 1.0 | 1.0 | 0.0 | 1.0 | 0.0 | 0.0 | 0.7 | 1.0 | 0.7 | 1.0 | 1.0 | 1.0 | $\gamma_{TG}$ | 1.0 | 1.0 | $0.50\sqrt{f'_c}$ | $0.58\sqrt{f'_c}$ | $0.289\sqrt{f'_c}$ | $0.331\sqrt{f'_c}$ | 1 |
| e | 1.0 | 0.0 | 1.0 | 1.0 | 1.0 | 0.0 | 0.3 | 0.0 | 0.3 | 1.0 | 1.0 | 1.0 | $\gamma_{TG}$ | 1.0 | 1.0 | $0.50\sqrt{f'_c}$ | $0.58\sqrt{f'_c}$ | $0.289\sqrt{f'_c}$ | $0.331\sqrt{f'_c}$ | 2 |
| f | 1.0 | 0.0 | 0.0 | 1.0 | 1.0 | 1.0 | 0.3 | 0.0 | 0.3 | 1.0 | 1.0 | 1.0 | $\gamma_{TG}$ | 1.0 | 1.0 | $0.50\sqrt{f'_c}$ | $0.58\sqrt{f'_c}$ | $0.289\sqrt{f'_c}$ | $0.331\sqrt{f'_c}$ | 3 |

The balanced cantilever bridge is a type of segmental bridge. In this study, while modelling the balanced cantilever bridge, two segments each has 3 meters length are used for above piers whereas three segments with 4 meters are used on each side of the balanced cantilever. Remaining segments are arranged as five meters and for larger span lengths, the number of the three and for meter segments will remain same, increasing the usage of five meter segments. Pier sections are same for all of the bridges as illustrated in Figure 92.

The detailed stage construction and final position results will be given for the span length of 90 meters bridge. As explained before the dynamic load for constructional stage is directly related to segments weights, as the segment weights were given in Table 42. Balanced cantilever post tensioned bridges are modelled using LARSA 4D. Stress values occurring in stage construction will be given below and stress results are given for the most critical two points of the superstructure to prevent the any kind of failure during stage construction. Since the zero segments are fully supported by the piers, there is no need to investigate the results from it.

Results for constructional stage analyses for the span length of 90, 120, 150 and 180 meters are given below. Results are given for Stress Point 1, which shows the tension stresses for negative moment in MPa. For Figures from 94 to 111, step 1 represents the concrete casting and, in step 2 constructional live loads are applied to the bridge;

**Table 44. Maximum Compression and Tension Stresses for Constructional Stages of 90 meters Span Length Bridge**

| 90 meter | Stage 1 | Stage 2 | Stage 3 | Stage 4 | Stage 5 |
|---|---|---|---|---|---|
| Maximum Compression(MPa) | - | 2.033 | 2.714 | 4.305 | 4.273 |
| Maximum Tension(MPa) | 0.608 | 0.144 | 0.153 | 0.255 | 0.276 |
| **90 meter** | **Stage 6** | **Stage 7** | **Stage 8** | **Stage 9** | |
| Maximum Compression(MPa) | 4.024 | 4.866 | 4.041 | 3.912 | |
| Maximum Tension(MPa) | 0.296 | 0.316 | 0.331 | - | |

**Table 45. Maximum Compression and Tension Stresses for Constructional Stages of 120 meters Span Length Bridge**

| 120 meter | Stage 1 | Stage 2 | Stage 3 | Stage 4 |
|---|---|---|---|---|
| Maximum Compression(MPa) | - | 1.944 | 2.666 | 4.266 |
| Maximum Tension(MPa) | 0.101 | 0.108 | 0.116 | 0.195 |
| **120 meter** | **Stage 5** | **Stage 6** | **Stage 7** | **Stage 8** |
| Maximum Compression(MPa) | 4.432 | 4.453 | 5.552 | 5.241 |
| Maximum Tension(MPa) | 0.213 | 0.232 | 0.253 | 0.275 |
| **120 meter** | **Stage 9** | **Stage 10** | **Stage 11** | **Stage 12** |
| Maximum Compression(MPa) | 4.82 | 5.469 | 4.658 | 4.449 |
| Maximum Tension(MPa) | 0.297 | 0.316 | 0.332 | - |

**Table 46. Maximum Compression and Tension Stresses for Constructional Stages of 150 meters Span Length Bridge**

| 150 meter | Stage 1 | Stage 2 | Stage 3 | Stage 4 | Stage 5 |
|---|---|---|---|---|---|
| Maximum Compression(MPa) | - | 2.879 | 3.577 | 4.036 | 5.457 |
| Maximum Tension(MPa) | 0.071 | 0.076 | 0.081 | 0.137 | 0.149 |
| **150 meter** | **Stage 6** | **Stage 7** | **Stage 8** | **Stage 9** | **Stage 10** |
| Maximum Compression(MPa) | 5.602 | 5.649 | 5.6 | 6.569 | 6.292 |
| Maximum Tension(MPa) | 0.161 | 0.174 | 0.188 | 0.203 | 0.218 |
| **150 meter** | **Stage 11** | **Stage 12** | **Stage 13** | **Stage 14** | **Stage 15** |
| Maximum Compression(MPa) | 5.966 | 5.544 | 6.101 | 5.406 | 5.249 |
| Maximum Tension(MPa) | 0.234 | 0.249 | 0.262 | 0.271 | - |

**Table 47. Maximum Compression and Tension Stresses for Constructional Stages of 180 meters Span Length Bridge**

| 180 meter | Stage 1 | Stage 2 | Stage 3 | Stage 4 | Stage 5 |
|---|---|---|---|---|---|
| Maximum Compression(MPa) | - | 1.685 | 2.372 | 3.852 | 4.18 |
| Maximum Tension(MPa) | 0.052 | 0.056 | 0.059 | 0.101 | 0.109 |
| **180 meter** | **Stage 6** | **Stage 7** | **Stage 8** | **Stage 9** | **Stage 10** |
| Maximum Compression(MPa) | 4.426 | 4.565 | 4.619 | 5.601 | 5.468 |
| Maximum Tension(MPa) | 0.117 | 0.126 | 0.136 | 0.146 | 0.156 |
| **180 meter** | **Stage 11** | **Stage 12** | **Stage 13** | **Stage 14** | |
| Maximum Compression(MPa) | 5.301 | 5.069 | 4.78 | 5.397 | |
| Maximum Tension(MPa) | 0.167 | 0.178 | 0.189 | 0.2 | |
| **180 meter** | **Stage 15** | **Stage 16** | **Stage 17** | **Stage 18** | |
| Maximum Compression(MPa) | 4.927 | 4.423 | 3.829 | 3.703 | |
| Maximum Tension(MPa) | 0.21 | 0.218 | 0.225 | - | |
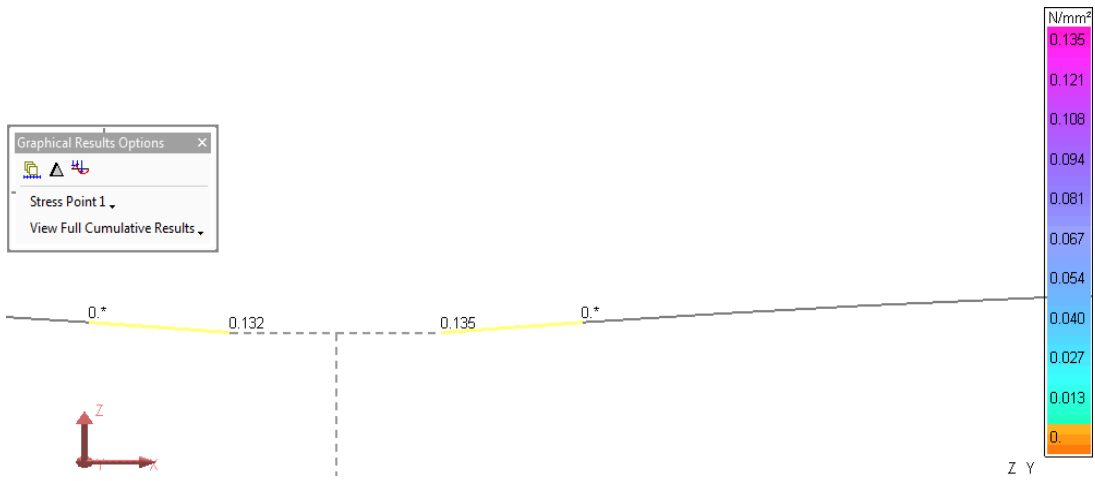
**Figure 94. Stage 1 Step 1 Stress Results for L = 90**
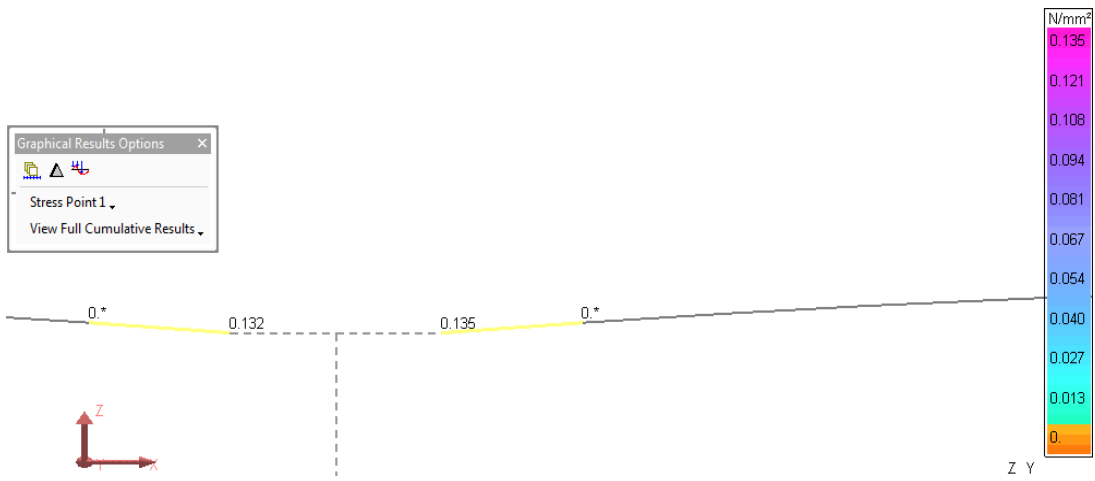


**Figure 95. Stage 1 Step 2 Stress Results for L = 90**
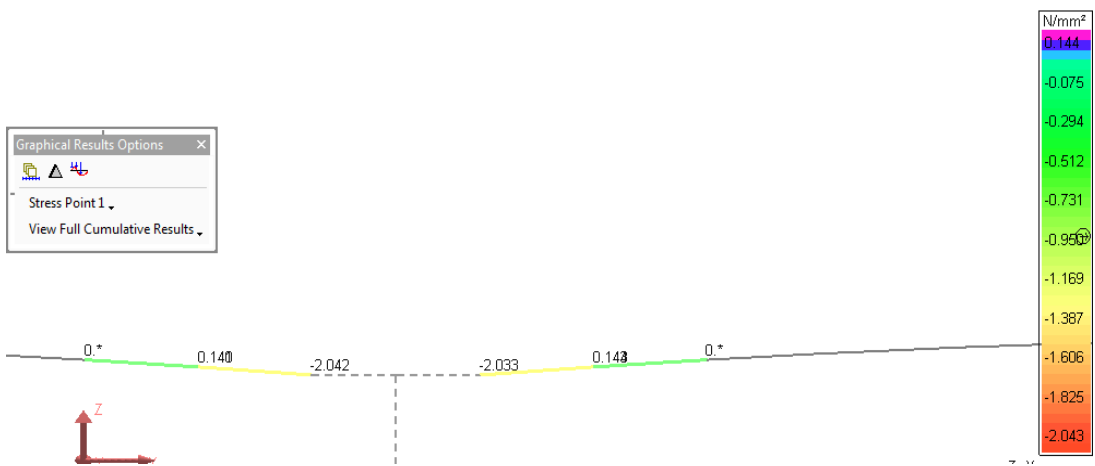


**Figure 96. Stage 2 Step 1 Stress Results for L = 90**
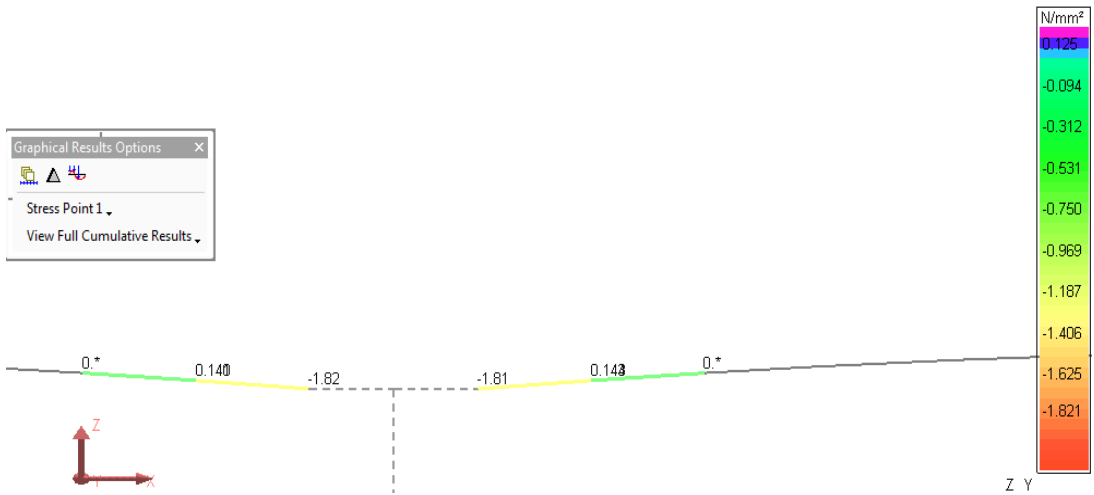
**Figure 97. Stage 2 Step 2 Stress Results for L = 90**
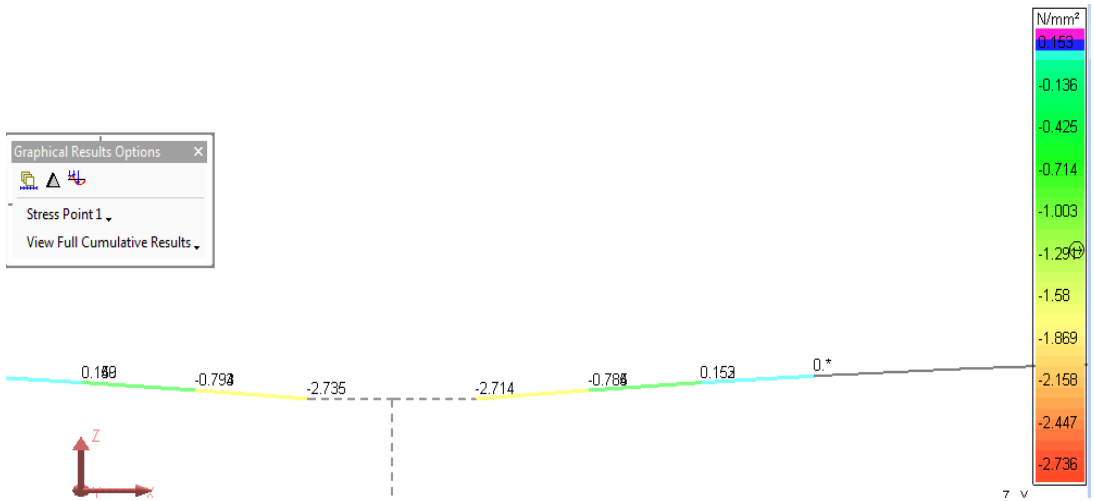


**Figure 98. Stage 3 Step 1 Stress Results for L = 90**
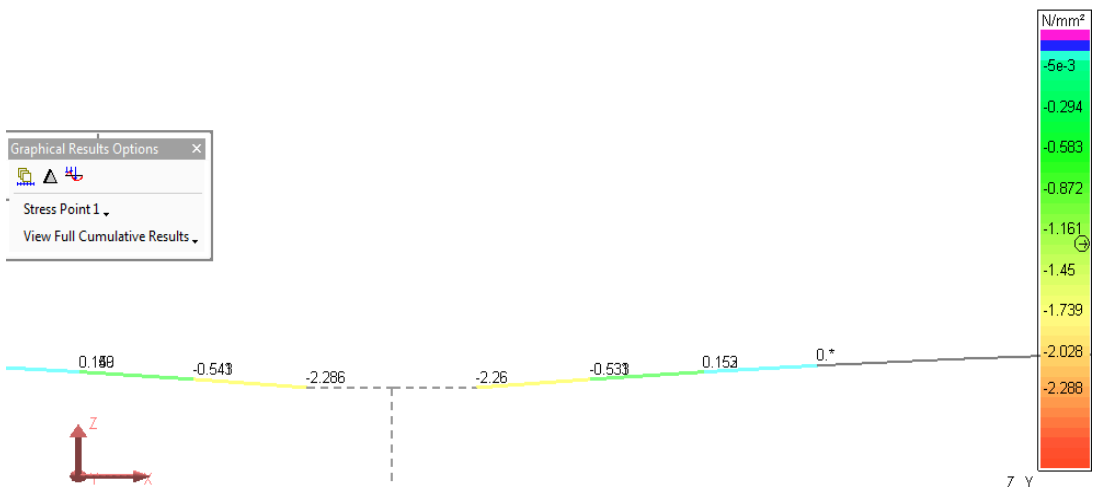


**Figure 99. Stage 3 Step 2 Stress Results for L = 90**
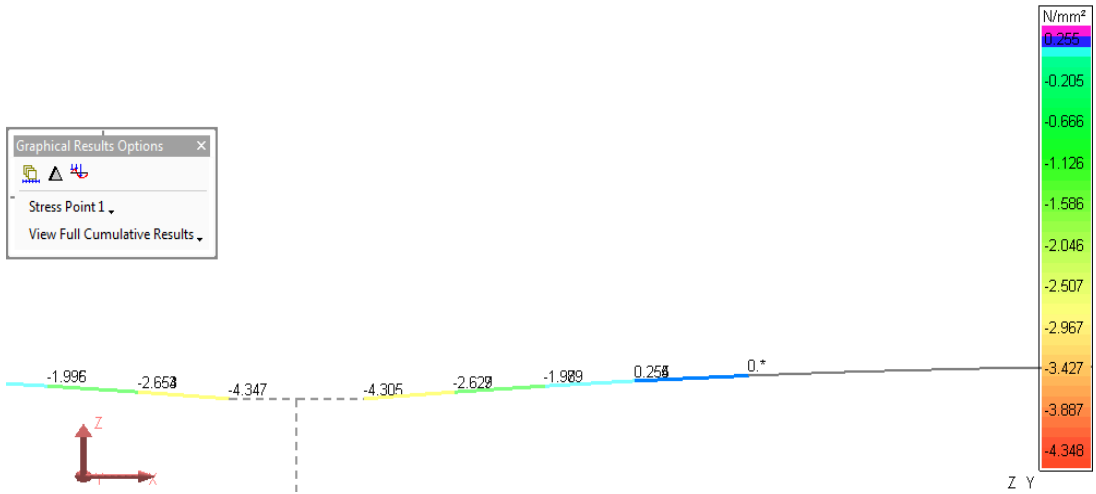
**Figure 100. Stage 4 Step 1 Stress Results for L = 90**
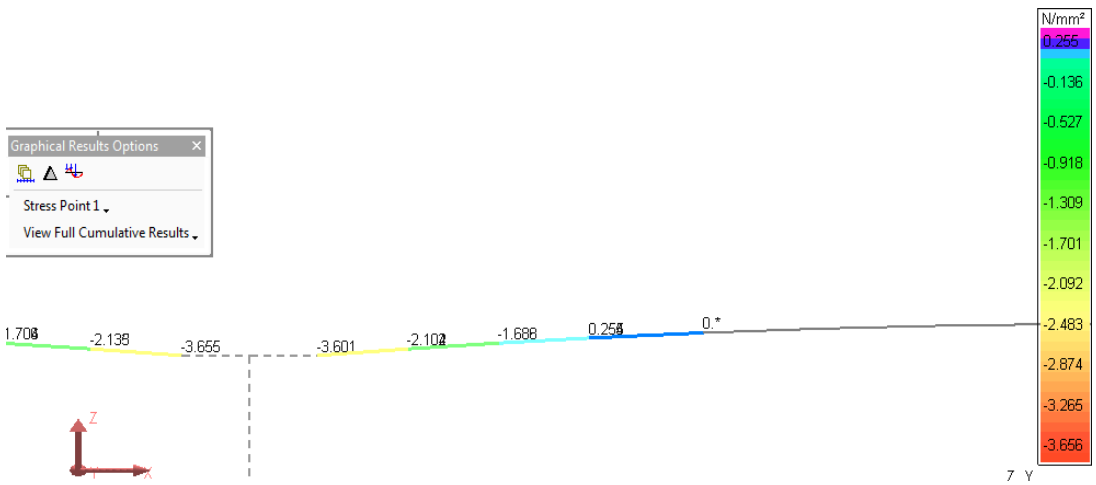


**Figure 101. Stage 4 Step 2 Stress Results for L = 90**
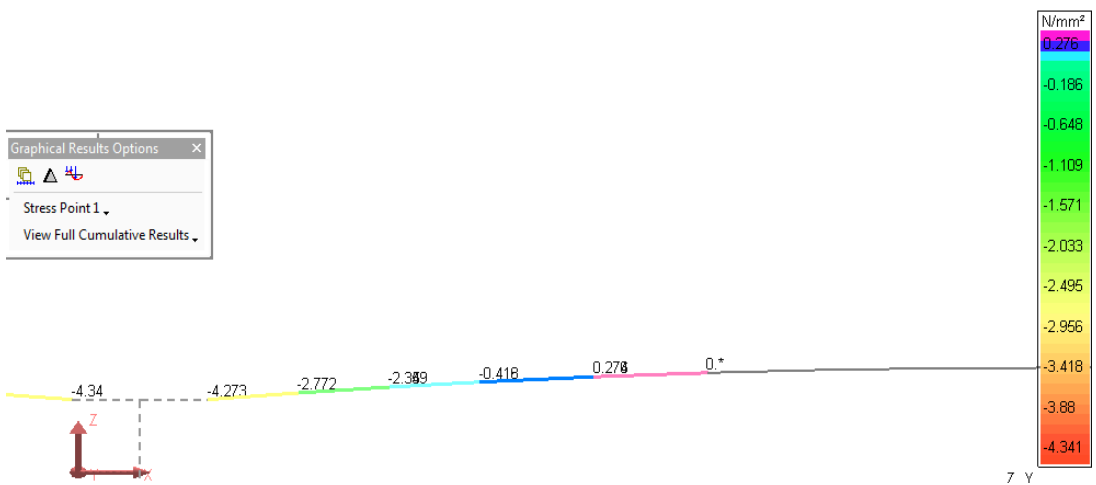


**Figure 102. Stage 5 Step 1 Stress Results for L = 90**
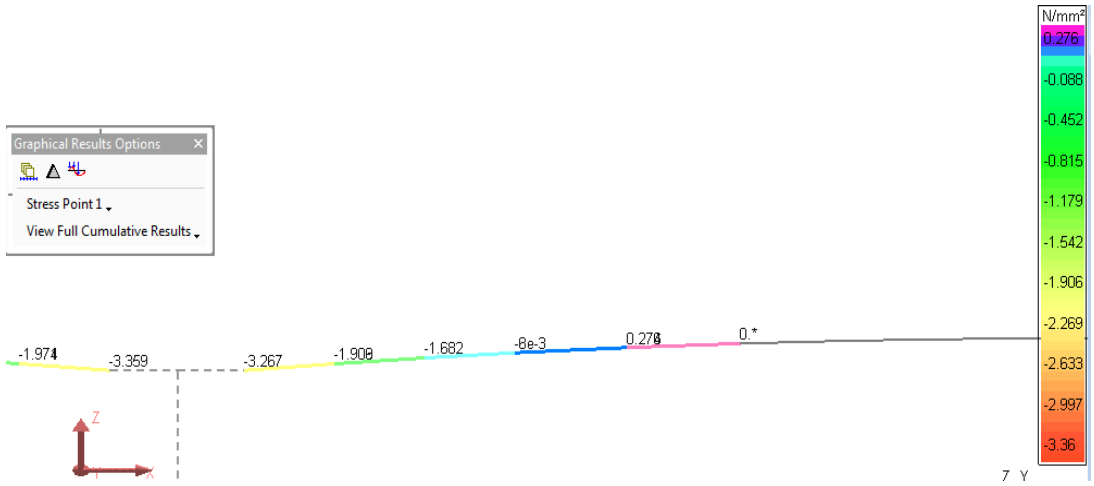
**Figure 103. Stage 5 Step 2 Stress Results for L = 90**
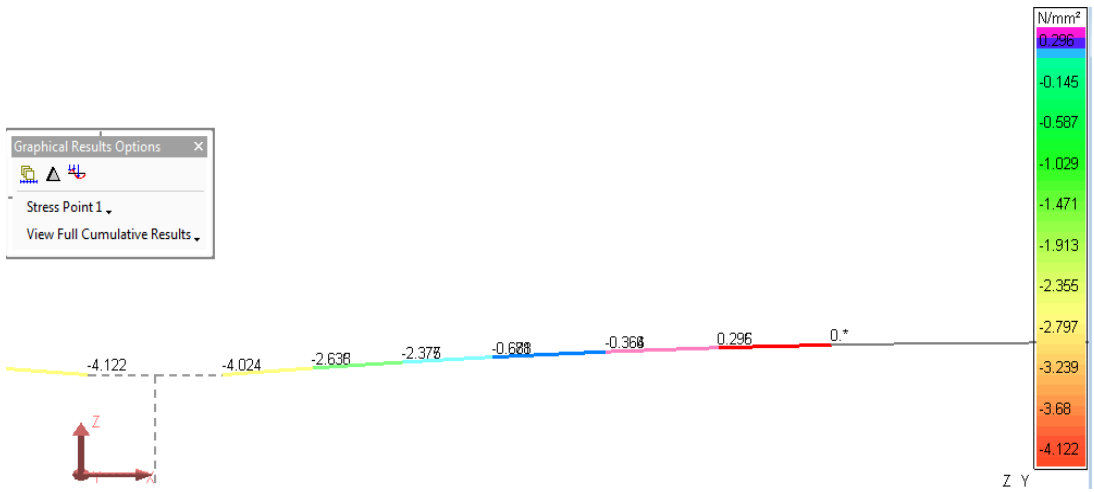


**Figure 104. Stage 6 Step 1 Stress Results for L = 90**
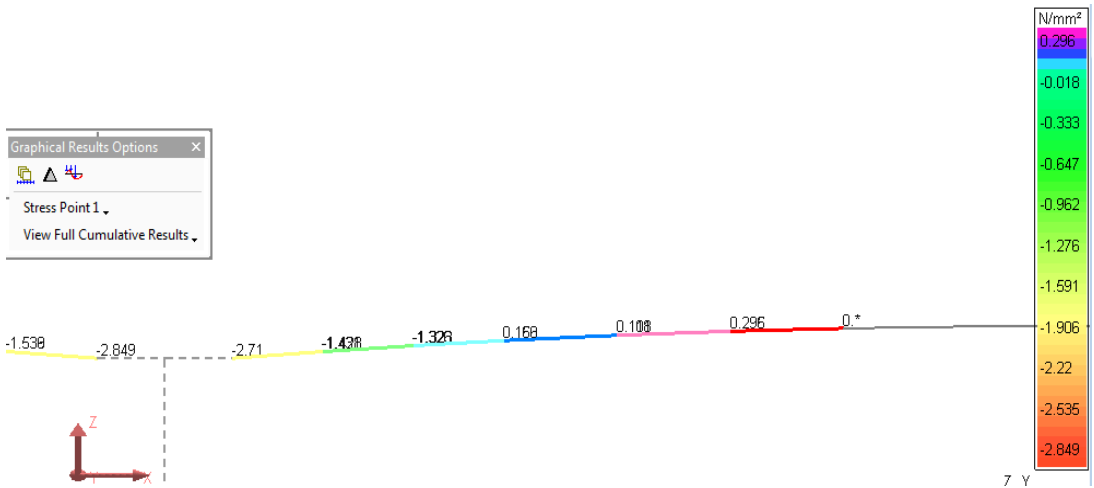


**Figure 105. Stage 6 Step 2 Stress Results for L = 90**

101
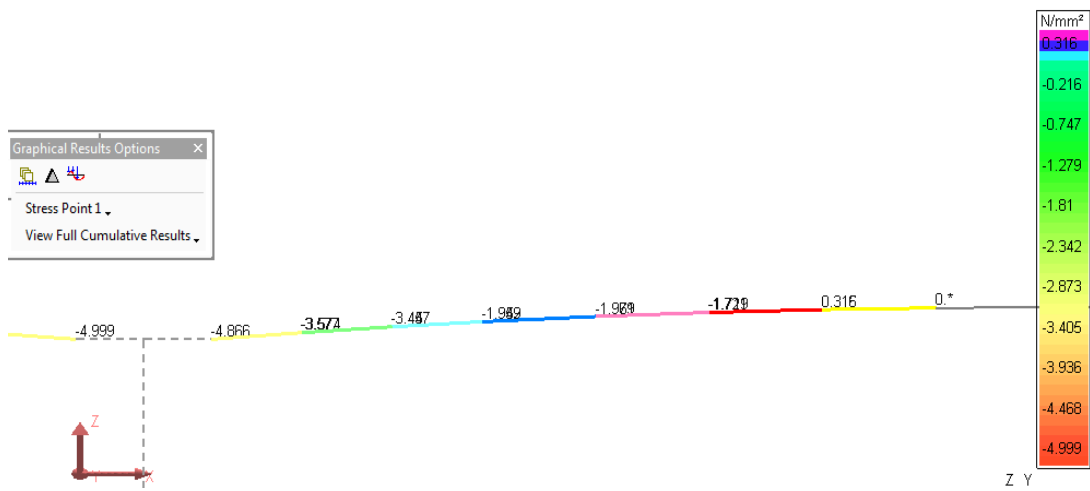
**Figure 106. Stage 7 Step 1 Stress Results for L = 90**
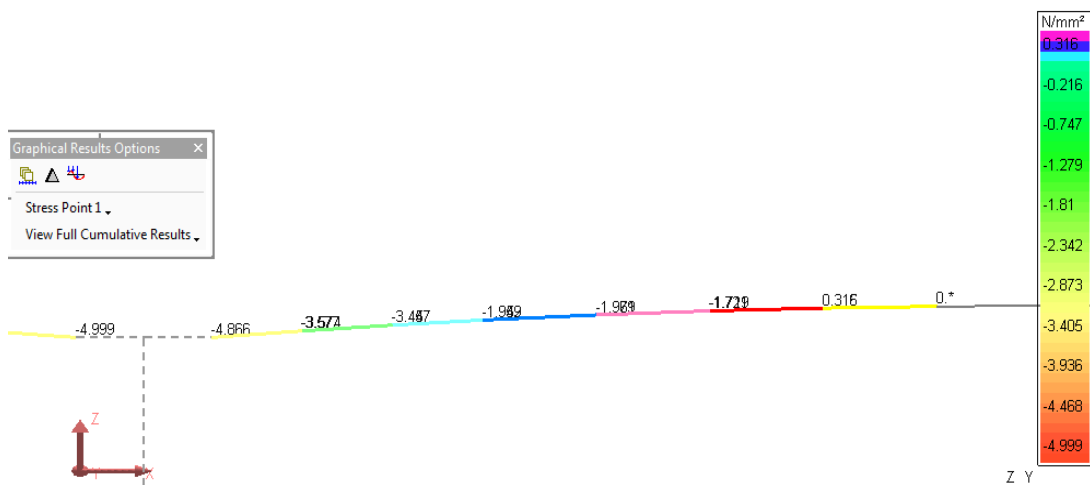


**Figure 107. Stage 7 Step 2 Stress Results for L = 90**
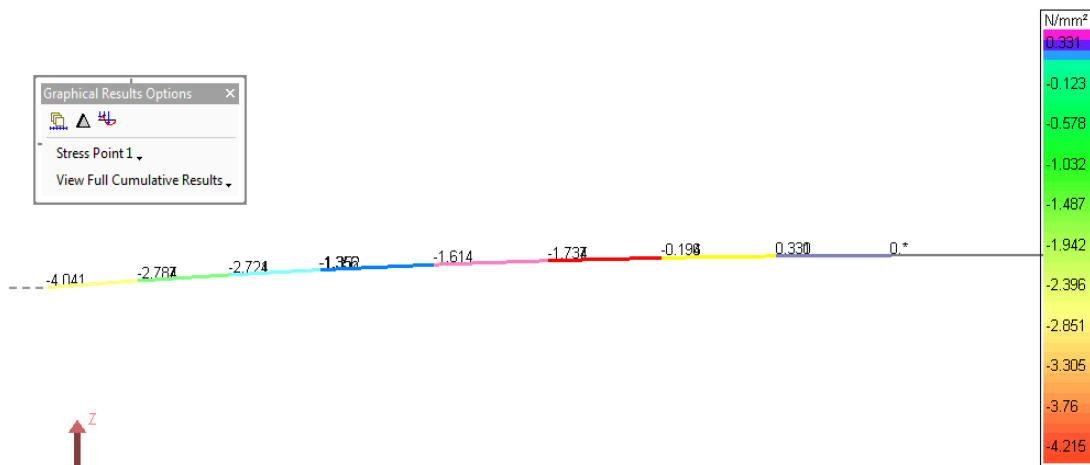


**Figure 108. Stage 8 Step 1 Stress Results for L = 90**
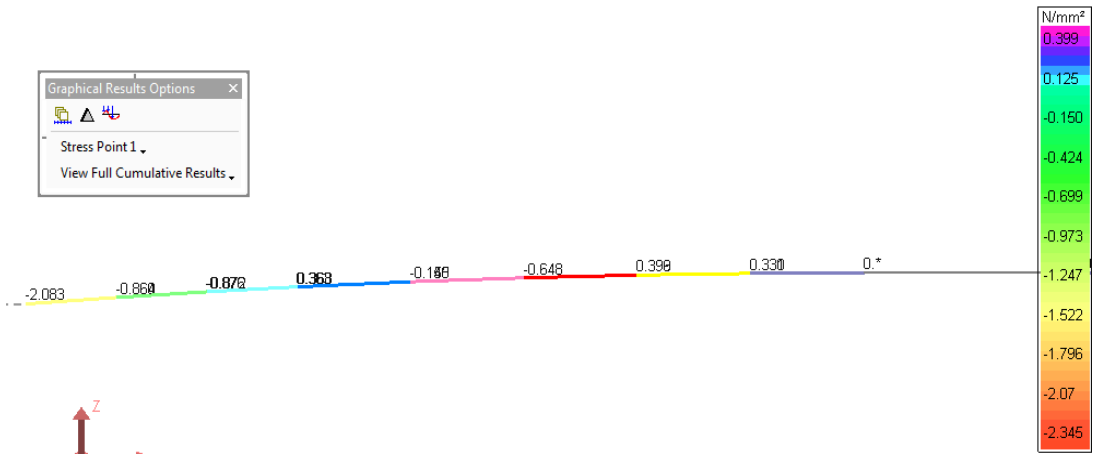
**Figure 109. Stage 8 Step 2 Stress Results for L = 90**
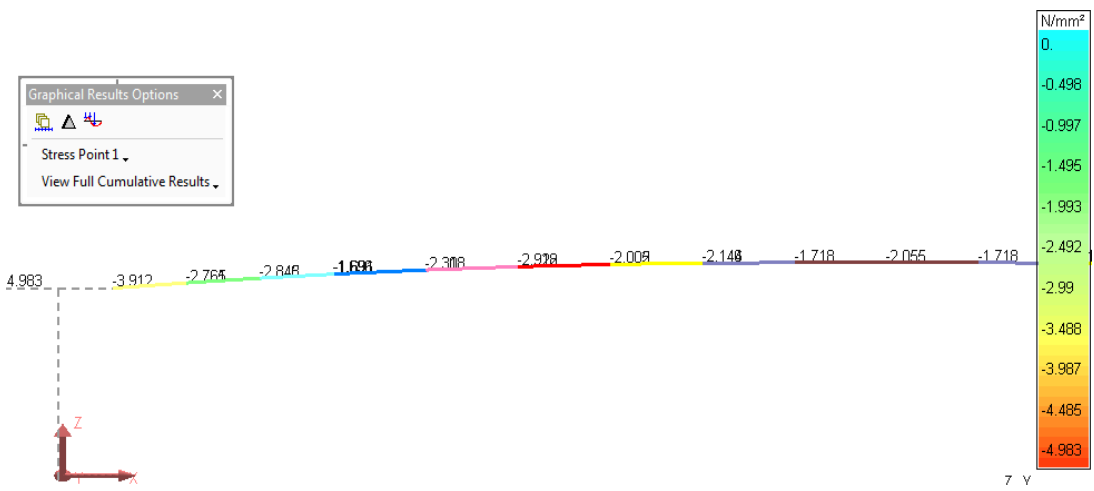


**Figure 110. Stage 9 Step 1 Stress Results for L = 90**
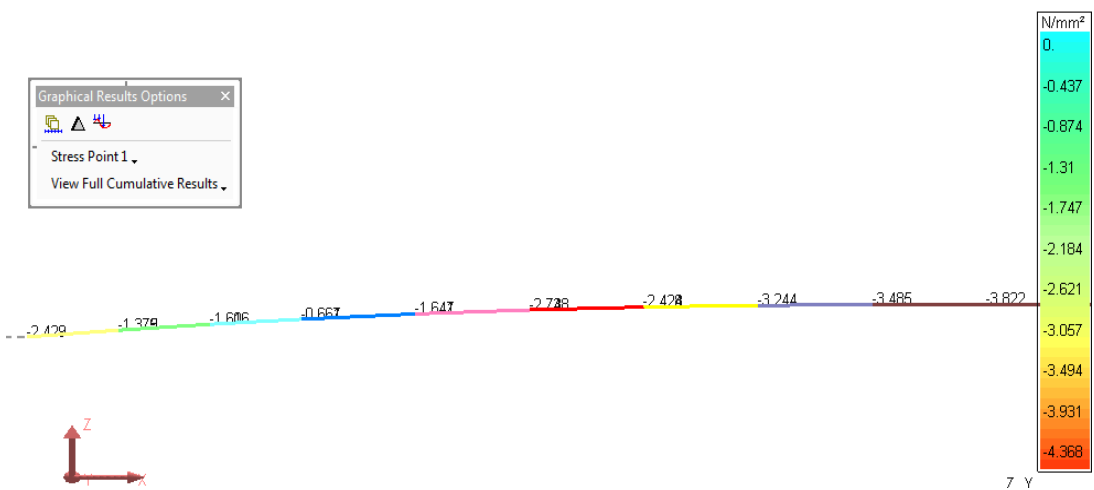


**Figure 111. Stage 9 Step 2 Stress Results for L = 90**

## 5.4 ULTIMATE FLEXURAL RESISTANCE OF POST-TENSIONED ELEMENTS

Flexural resistance capacity equations are based on the design specification AASHTO LRFD for bonded tendons. In chapter 5.7.3.1.1 AASHTO gives the proper equations for fully bonded tendons.

$$f_{ps} = f_{pu} \left( 1 - k \frac{c}{d_p} \right) \tag{[20]}$$

$$k = 2 \left( 1.04 - \frac{f_{py}}{f_{pu}} \right) \tag{[21]}$$

To determine the k values instead of the formula in AASHTO LRFD 5.7.3.1.1-2 according to the table C5.7.3.1.1-1 k is taken as 0.28 for low relaxation strand.

**Table 48. The Values for k according to different types of prestressing strands**

| Type of Tendon | $f_{py}/f_{pu}$ | Value of k |
|---|---|---|
| Low relaxation strand | 0.9 | 0.28 |
| Stress relieved strand and Type 1 high-strand bar | 0.85 | 0.38 |
| Type 2 high strand bar | 0.8 | 0.48 |

To calculate the neutral axis for post tensioned box girders the formula in AASHTO LRFD 5.7.3.1.1-3. This formula for T shape behaviour of post tensioned beams.

$$c = \frac{A_{ps}\, f_{pu} + A'_s\, f'_s - 0.85 f'_c (b - b_w) h_f}{0.85 f'_c\, \beta_1\, b_w + k A_{ps} \dfrac{f_{pu}}{d_p}} \qquad [22]$$
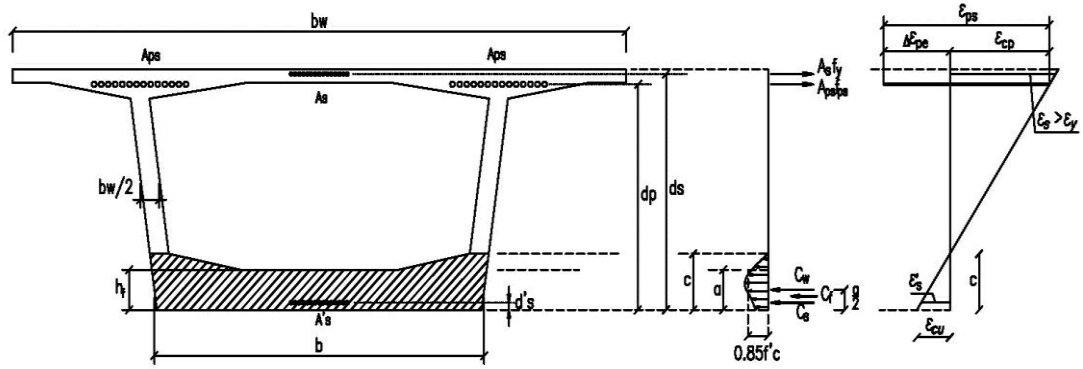


**Figure 112. Forces on Post-Tensioned Concrete Box Girder**

For determining the behaviour of post tensioned beam whether it is T shaped or rectangular, first the neutral axis shall be calculated according to the rectangular shape formula. After calculating c, a will be determined as $\beta_1$*c which is compression block and it is compared to compression flange thickness to determine the post tensioned beam whether it behaves T shaped or rectangular. The stress block factor for compression zone $\beta_1$, calculated according to the concrete class. If the concrete class is C28 or lower than the $\beta_1$ is 0.85 and $\beta_1$ degrades 0.05 for every 7 MPa increase.

$$c = \frac{A_{ps}\, f_{pu} + A_s\, f_s - A'_s\, f'_s}{0.85\, f'_c\, \beta_1\, b + k\, A_{ps} \dfrac{f_{pu}}{d_p}} \qquad [23]$$

$A_{ps}$ = Area of prestressing steel (mm$^2$)

$f_{pu}$ = Specified tensile strength of prestressing steel (MPa)

$f_{py}$ = Yield strength of strand (MPa)

105

$A_s$ = Area of mild steel reinforcement (mm$^2$)

$A'_s$ = Area of compression reinforcement (mm$^2$)

$f_s$ = Stress in the mild steel reinforcement at nominal flexural resistance (MPa)

$f'_s$ = Stress in the mild steel compression reinforcement at nominal flexural resistance(MPa), as specified in Article 5.7.2.1 AASHTO LRFD 2010

b = width of compression flange (mm)

$b_w$ = width of web (mm)

$h_f$ = depth of compression flange(mm)

dp = distance from extreme compression fiber to the centroid of the prestressing tendons (mm)

c = distance between the neutral axis and the compressive face (mm)

$\beta_1$ = stress block factor specified in Article 5.7.2.2 AASHTO LRFD 2010

$$M_n = A_{ps}f_{ps}\left(d_p - \frac{a}{2}\right) + A_s f_s \left(d_s - \frac{a}{2}\right) - A'_s f'_s \left(d'_s - \frac{a}{2}\right)$$
$$+ 0.85 f'_c (b - b_w) h_f \left(\frac{a}{2} - \frac{h_f}{2}\right)$$

[24]

Mn = The nominal moment capacity

ds = Distance from extreme compression fiber to the centroid of non prestressed tensile reinforcement

d's = Distance from extreme compression fiber to the centroid of non prestressed compression reinforcement

a = $\beta_1$c depth of equivalent stress block

The flexural nominal moment capacity of a section which has a rectangular stress distribution and no mild reinforcement is given below.

$$M_n = A_{ps}f_{ps}\left(d_p - \frac{a}{2}\right) \qquad\qquad [25]$$

## 5.4.1 Shear Lag Effect

The effective flange width shall be taken equal to physical flange width if;

- $b \leq 0.1\ l_i$
- $b \leq 0.1\ d_o$

Unless, the cross section dimensions are not appropriate for these effective flange width may be calculated and used in case of physical width for ultimate moment capacity. On the other hand, the effective flange width cannot be larger than the physical flange width (AASHTO LRFD 4.6.2.6.2 and TUBITAK 110G093 T.4.2).

$d_o$ = depth of superstructure (mm)

b = physical flange width on each side of the web, e.g. $b_1$, $b_2$ and $b_3$, as shown in Figure 115.

$b_e$ = effective flange width corresponding to the particular position of the section of interest in the span as specified Figure 113.

$b_m$ = effective flange width for interior portions of a span as determined from Figure 114(mm).

$b_s$ = effective flange width at interior support or for cantilever arm as determined from Figure 114(mm).

a = portion of span subject to a transition in effective flange width taken as the lesser of the physical flange width on each side of the web shown in Figure 115 or one quarter of the span length(mm).

$l_i$ = a notional span length specified in Figure 113 for the purpose of determining effective flange widths using Figure 114 (mm).



| System | | Pattern of $b_m/b$ |
|---|---|---|
| Single-Span Girder<br>$\ell_i = 1.0\ell$ | | |
| Continuous Girder | End Span<br>$\ell_i = 0.8\ell$ | |
| | Interior Span<br>$\ell_i = 0.6\ell$ | |
| Cantilever Arm<br>$\ell_i = 1.5\ell$ | | |

**Figure 113. Pattern of Effective Flange Width, $b_e$, $b_m$, and $b_s$**

108

For $\dfrac{b}{l_i} \geq 0.7$ : $b_m = 0.173\, l_i$

$b_s = 0.104\, l_i$

$\dfrac{\text{effective width}}{\text{physical width}}$
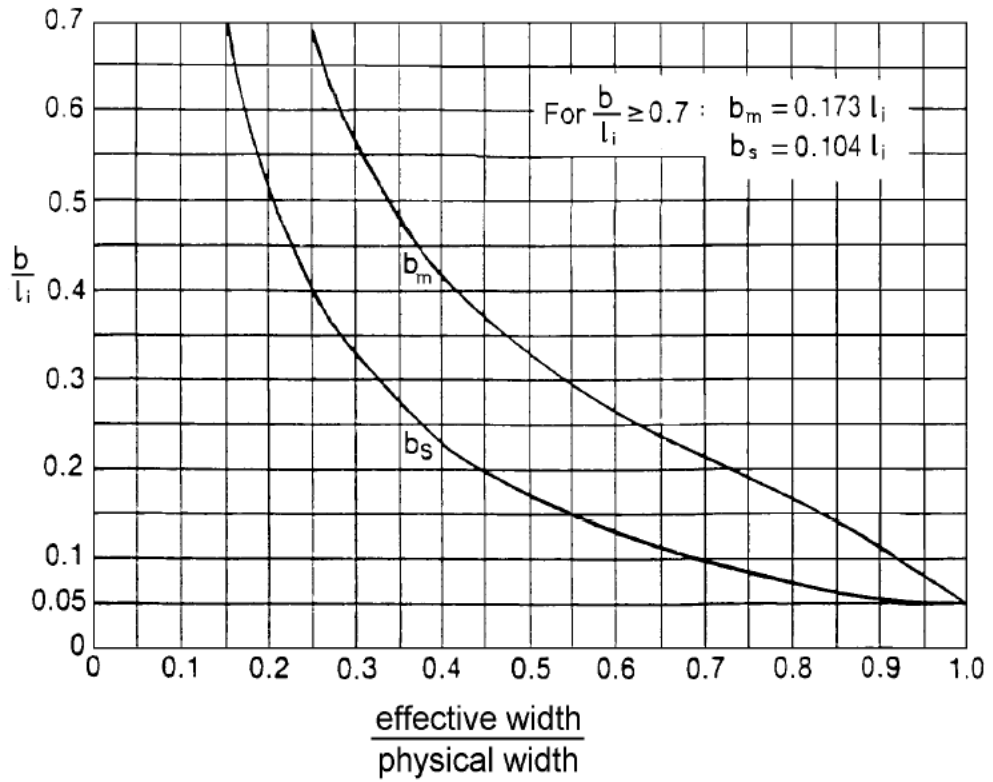
**Figure 114. Values of the Effective Flange Width Coefficients for $b_m$ and $b_s$ for the Given Values of $b/l_i$**
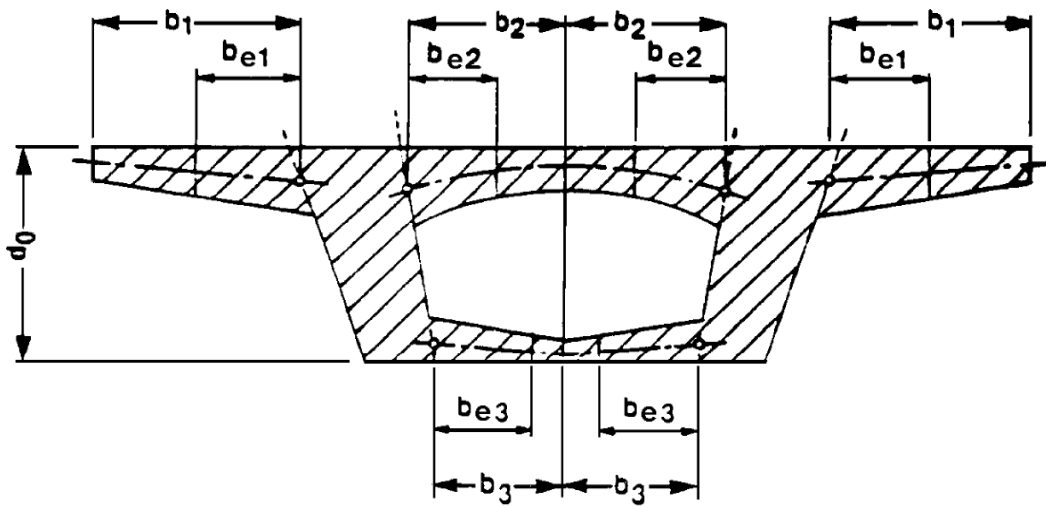


**Figure 115. Cross Sections and Corresponding Effective Flange Widths, $b_e$**

### 5.4.2 Ultimate Flexural Capacity Calculation for 90m Span Length

In this section, the ultimate flexural capacity calculation for span length of 90 meters will be illustrated. 90 meters span length is chosen because shear lag effects the capacity calculation for only this bridge. The related results are given below;

**Table 49. Material Properties for Concrete Prestressing Strands**

| | | |
|---|---|---|
| $f_{py}$ | 1674 | MPa |
| $f_{pu}$ | 1860 | MPa |
| $\beta_1$ | 0.764 | |
| $f'_c$ | 40 | MPa |

Choosing the material properties of the bridge components, $f_{py}$ and $\beta_1$ values determined according to material specifications. Then, according to the amount of pre-stressing tendons and beam section dimensions compression block distance, c is determined. To convert the compression block as rectangular distribution c is multiplied by $\beta_1$ and the result is compared with compression flange thickness to decide the cross section behaviour rectangular or T-shaped.

**Table 50. Section Parameters of Cross Section and Strand Area**

| | | |
|---|---|---|
| $A_{ps}$ | 69160 | mm$^2$ |
| $d_p$ | 4300 | mm |
| b | 6220 | mm |
| $b_w$ | 800 | mm |
| $h_f$ | 750 | mm |

**Table 51. Compression Block Calculation for Cross Section of 90 meters Span Length**

| | | |
|---|---|---|
| $A_{ps}$ | 69160 | mm$^2$ |
| $f_{pu}$ | 1860 | MPa |
| $f'_c$ | 40 | MPa |
| $\beta_1$ | 0.764 | |
| b | 6220 | mm |
| k | 0.28 | |
| $d_p$ | 4300 | mm |
| c | 756.9272 | mm |
| a | 578.2924 | mm |

The ultimate moment capacity formula $M_n$, is calculated according to AASHTO LRFD 5.7.3.2.2-1 or TUBITAK 110G093 T.3.5.1.3. If the cross section behaviour is rectangular, then $b = b_w$ and concrete contribution is eliminated in the capacity formula. In this study, mild reinforcement is not used as a result of this the ultimate moment capacity was defined in Equation 23 the results are given in Table 52.

**Table 52. Ultimate Flexural Moment Capacity for Cross Section of 90 meters Span Length**

| | | |
|---|---|---|
| **$M_n$** | **490516.5** | **kN.m** |
| $A_{ps}$ | 69160.0 | mm$^2$ |
| $f_{ps}$ | 1768.3 | MPa |
| $d_p$ | 4300.0 | mm |
| $f'_c$ | 40.0 | MPa |
| b | 6220.0 | mm |
| $b_w$ | 800.0 | mm |
| $\beta_1$ | 0.764 | |
| $h_f$ | 750.0 | mm |
| a | 578.3 | mm |

## 5.5 SHEAR STRENGTH CHECK

In designing process of concrete decks for AASHTO LRFD Bridge Design Specifications, shear behaviour for ultimate state. Box girder bridges has the similar working principle when the shear forces taken into consideration. On the other hand, principal stresses should be investigated according to the existing longitudinal, vertical and shear stresses. For balanced cantilever post-tensioned bridges, the most critical location is near the interior piers at the top the web for service condition. Moreover, neutral axis zone will be also investigated to see the effect of maximum shear stress with a higher level of compression. To check the principal stresses in webs Service 3 load combination is used. The details for calculating the principal stresses for the span length of 90 meters is given and the rest is illustrated in tabular form.

M = The moment resulting from externally applied loads

$M_{Pp}$ = Post tensioning moment according to the eccentricity of the strands

P = Total axial force occurring on the investigated section

V = Vertical shear force

Q = First moment of area with respect to gravitational center of the section

I = Moment of inertia about gravitational center of the section

t = Perpendicular web thickness

| | | |
|---|---|---|
| M = 235916 kN.m | $M_{Pp}$ = 160675 kN.m | P= 78278 kN |
| A = 12.929 m$^2$ | I = 41.436 m$^4$ | t = 0.4 m |

$\sigma_M$ = 235916 kN.m x 1.746 m / 41.436 m$^4$ / 1000 = 9.94 MPa

$\sigma_{MPp}$ = 160675 kN.m x 1.746 m / 41.436 m$^4$ / 1000 = 6.77 MPa

$P/A = 78278$ kN / $12.929$ m$^2$ / $1000 = 6.104$ MPa

Total compressive stress $= 6.104 + 6.77 - 9.94 = 2.394$ MPa
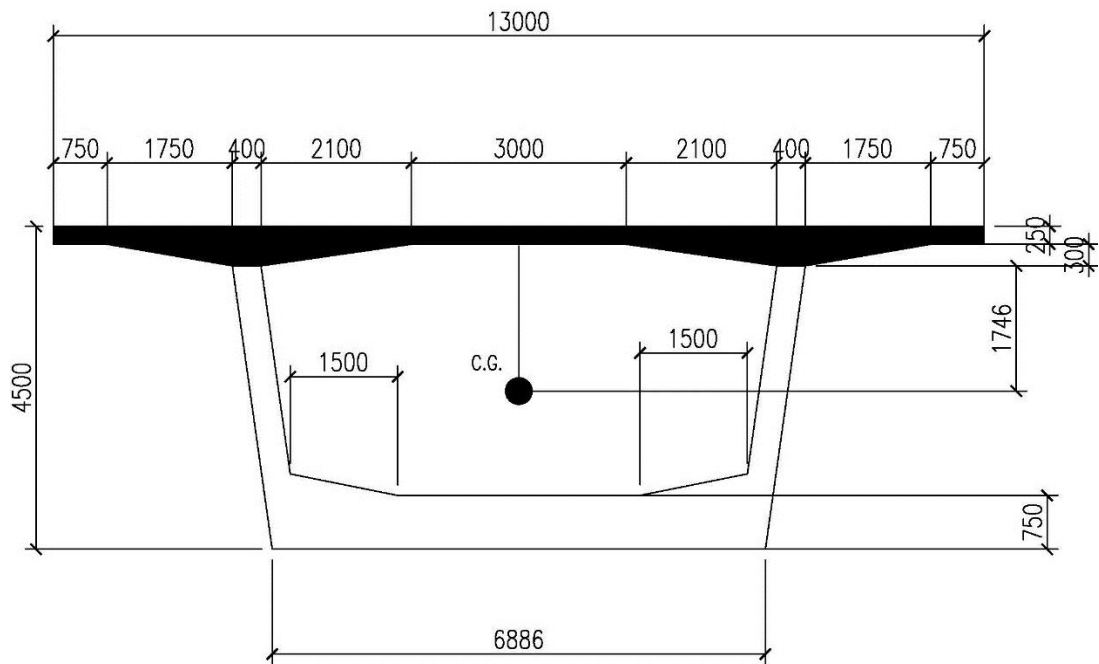


**Figure 116. Cross Section Properties for Shear Stress Calculations**

$V = 7847$ kN

$Q = 4.645$ m$^2$ x $2.101$ m $= 9.387$ m$^3$

$I = 41.436$ m$^4$

$t = 0.8$ m

$\tau = 7847$ kN x $9.76$ m$^3$ / $41.436$ m$^4$ / $0.8$ m / $1000 = 2.31$ MPa
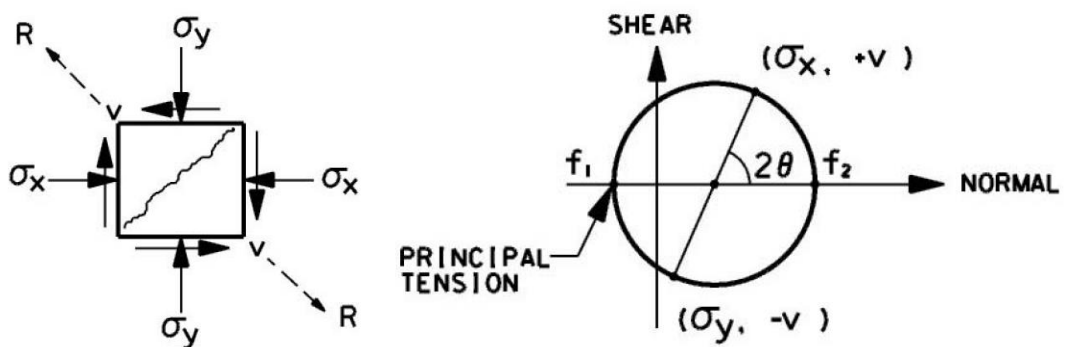


**Figure 117. Principal Tension at the Webs of Box Girders**

113

$$f_1 = \frac{\sigma_x + \sigma_y}{2} - \frac{1}{2}\sqrt{4v^2 + (\sigma_x - \sigma_y)^2} \qquad [26]$$

$\sigma_x$ = 2.934 MPa

$\sigma_y$ = 0 (If there is no vertical post-tensioning, then $\sigma_y$ zero)

$\tau$ = 2.31 MPa

$f_1$ = 2.934 / 2 – ½(4 x 2.31² + 2.934²) ^½ = -1.27 MPa

The limit stress for principal tension is 0.289 x √40 = 1.827 MPa

**Table 53. Principal Tensile Stress Control of Top Web**

| Span Length(m) | σ(MPa) | V(kN) | Q(m³) | I(m⁴) | t(m) | τ(MPa) | $f_1$(MPa) | Limit (MPa) |
|---|---|---|---|---|---|---|---|---|
| 90 | 2.934 | 7847 | 9.75 | 41.44 | 0.8 | 2.31 | -1.27 | 1.827 |
| 120 | 1.202 | 10525 | 14.67 | 93.64 | 0.8 | 2.06 | -1.55 | 1.827 |
| 150 | 1.48 | 13467 | 21.13 | 207.55 | 0.8 | 1.71 | -1.13 | 1.827 |
| 180 | 2.4 | 17283 | 27.05 | 389.26 | 0.8 | 1.50 | -0.72 | 1.827 |

**Table 54. Principal Tensile Stress Control of Web Neutral Axis**

| Span Length(m) | σ(MPa) | V(kN) | Q(m³) | I(m⁴) | t(m) | τ(MPa) | $f_1$(MPa) | Limit (MPa) |
|---|---|---|---|---|---|---|---|---|
| 90 | 6.054 | 7847 | 10.95 | 41.44 | 0.8 | 2.59 | -0.96 | 1.827 |
| 120 | 5.899 | 10525 | 17.81 | 93.64 | 0.8 | 2.50 | -0.92 | 1.827 |
| 150 | 6.471 | 13467 | 28.10 | 207.55 | 0.8 | 2.28 | -0.72 | 1.827 |
| 180 | 7.25 | 17283 | 39.70 | 389.26 | 0.8 | 2.20 | -0.62 | 1.827 |

## 5.5.1 Mohr's Circle for Principle Tension Check

In previous section, the most critical section for bending stresses and shear stresses are investigated separately and tabulated. Corresponding Mohr's Circle drawings will be given to get a more clear view for the principal tension and comparison of the two cases.

114
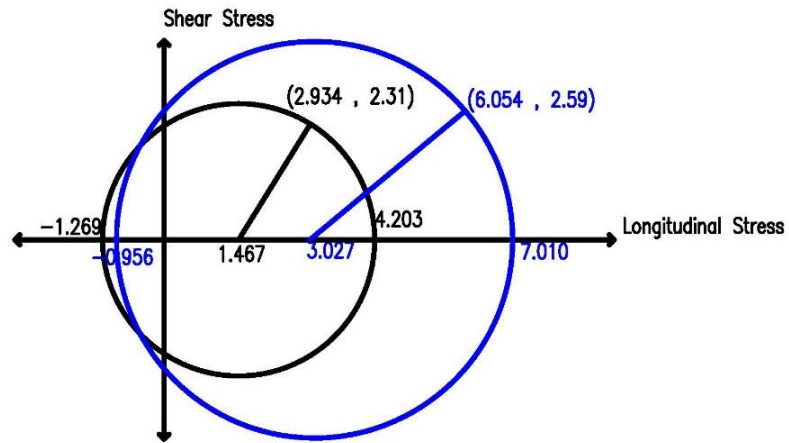
**Figure 118. Principle Stress Control for L = 90 Box Section (Units in MPa)**
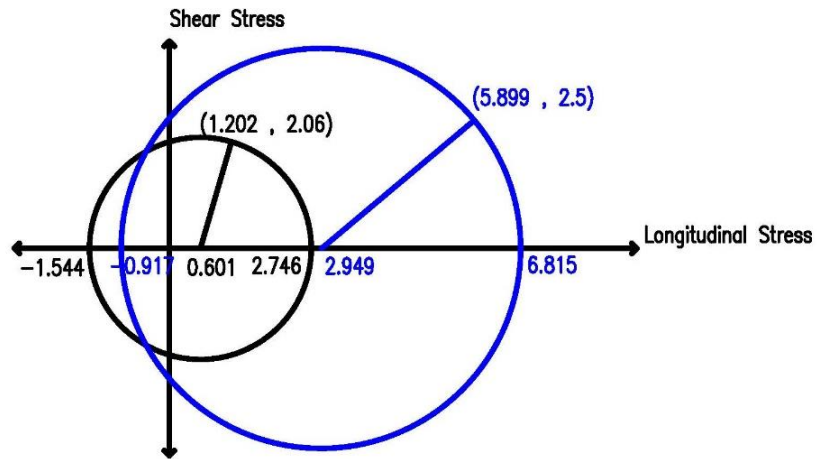


**Figure 119. Principle Stress Control for L = 120 Box Section (Units in MPa)**
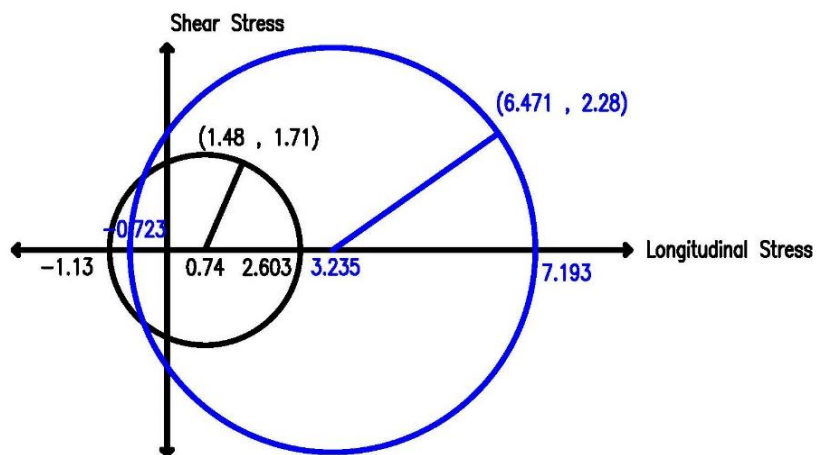


**Figure 120. Principle Stress Control for L = 150 Box Section (Units in MPa)**

115
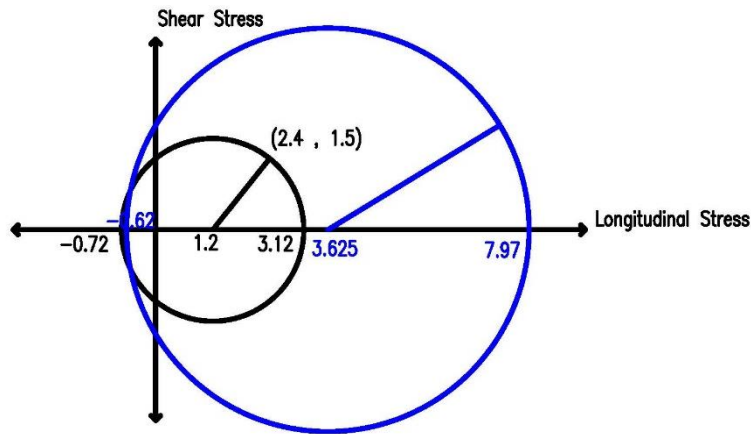
**Figure 121. Principle Stress Control for L = 180 Box Section (Units in MPa)**

## 5.6    FATIGUE CHECK

Truck passages creates cyclic loading for the prestressing tendons. Due to this cyclic loading, fatigue limits of prestressing tendons should be investigated. Endurance limit is the fatigue stress limit which is independent from fatigue life cycles. According to ASM Handbook, the endurance stress limit of high strength steel is around 650 MPa for the specimen which has 1950 MPa of ultimate tensile strength. Moreover, "Elements and Engineering Alloys" states the minimum endurance limit of high strength steel (1860 MPa) as 0.35 times the ultimate tensile strength (651 MPa). Stress deviations which are caused by truck passages is 2 MPa at maximum. As a result of this, there is no need to consider the fatigue strength for prestressing tendons. Moreover, according to AASHTO LRFD 2010 5.5.3.1, if Service 3 Limit State is fulfilled then there is no need to check the reinforcement for fatigue.
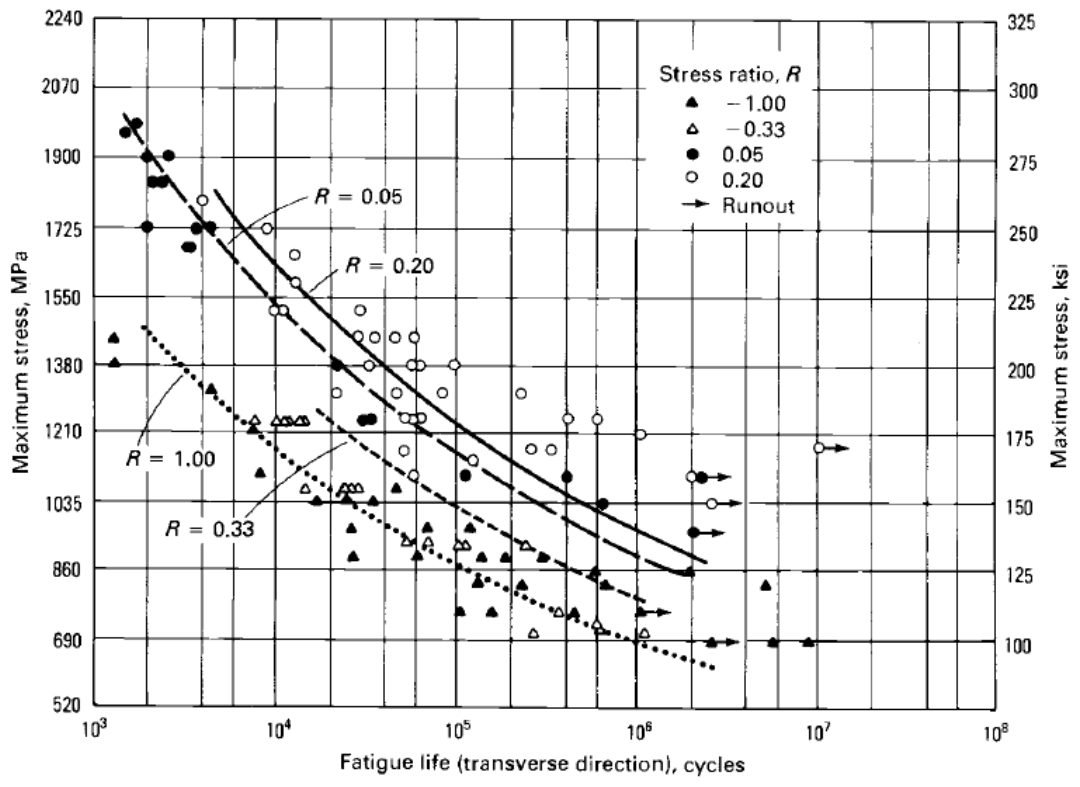
**Figure 122. Best Fit S-N Curves for an Ultimate Tensile Strength of 1930 MPa (ASM Handbook, Volume 1)**

# CHAPTER 6

# RELIABILITY INDEX

## 6.1 RELIABILITY METHOD

In every design process, the aim is to obtain higher resistance compared to resultant reactions. Both resistance and reaction forces includes uncertainty according to the parameters which they are calculated from. To illustrate the calculation in simpler state, the capacity (the ultimate moment or stress capacity) is shown as R and the demand (resultant moment or stress) is shown as Q. Finally, the limit state function is illustrated as $f_s = R - Q$

There are several ways for failure modes of bridges such as ultimate moment capacity, shear forces, excessive stress values and etc. In this study, three modes of failure taken into account to reach the target reliability indices. For the first step, the relevant analysis are completed for construction stage through the stress values. Then, the Service 3 load combination is controlled for closed position of the bridge. Finally, target reliability index is calculated for ultimate limit state and targeted as 4.5. Moreover, the corresponding moment capacity and resultant moment values are calculated and the reliability evaluation is completed. The reliability indices and Service 3 stress values are compared to arrange the tension stress limit for Service 3 load combination. Furthermore, the reliability evaluation for different types of live load models are completed and the results are compared for the same span lengths.

Probability of failure is defined as;

$$P_F = P(R - Q < 0) \qquad [27]$$
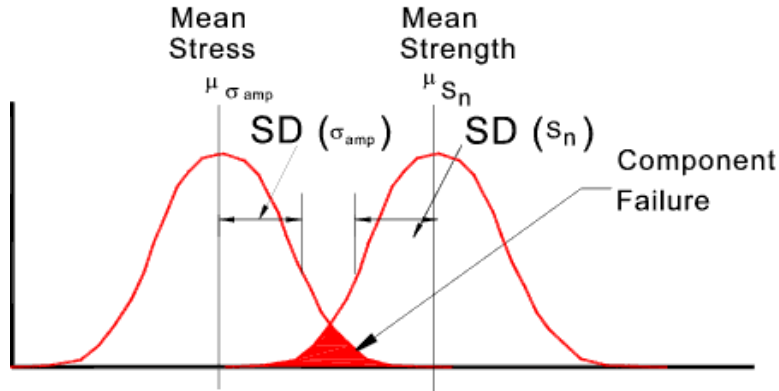


**Figure 123. Probability of Failure**

As it seen from Figure 123, even if the mean strength or resistance is much higher than demand there is an always a failure probability resulting from the uncertainties of parameters. Demand and capacity parameters are not independent parameters, uncertainties of these variables are changing depending on each other.

If the M is defined as safety margin and X is the random variables, then M should be calculated as;

$$M = R - S = g(X) = g(X_1, X_2, \dots, X_n) \qquad [28]$$

To obtain the failure boundary or limit state the M should be equal to zero. When M = R − S = 0 is zero it creates an equilibrium state between success and failure zones. Figure 124 shows the survival boundary for limit state function on two dimensional graph.
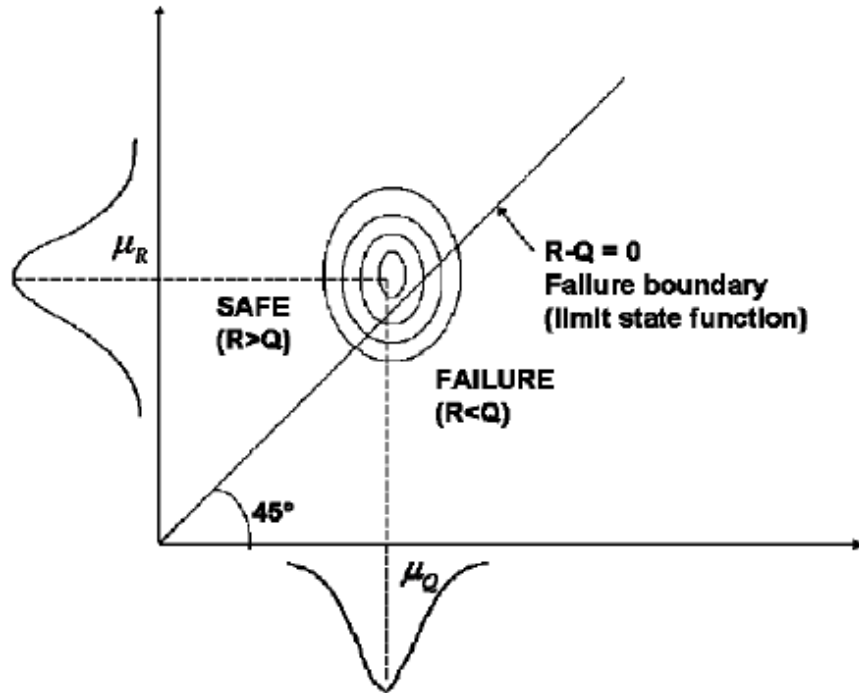
**Figure 124. Failure Boundary for Limit State Function**

# 6.1   MEAN VALUES FIRST ORDER SECOND MOMENT METHOD

The reliability index is defined as the survival or failure probability of the structure considering the parameters that effects both capacity and demand. The Mean Value First Order Second Moment was derived from the Taylor series approximation. The statistical parameters such as mean and coefficient of variation is calculated through this approximation. The mean is shown as μ, the coefficient of variation is defined as σ and the finally the reliability index is calculated as;

$$\beta = \frac{\mu}{\sigma} \tag{[29]}$$
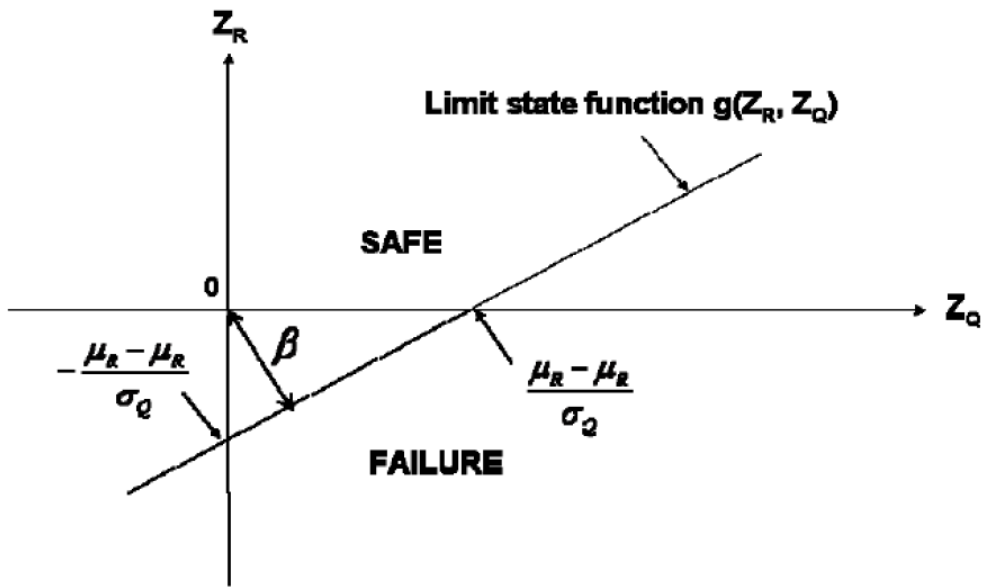
**Figure 125. Graphically Illustration of Reliability Index for Limit State Function**

Failure probability can be obtained according to the reliability index using the following formula if the distribution type is normal.

$$P_f = \phi(-\beta) = 1 - \phi(\beta) \tag{30}$$

$\phi$ = Standard normal cumulative distribution

Failure function is illustrated as below if the function is assumed to be linear.

$$g(X) = a_0 + a_1 X_1 + \cdots + a_n X_n \tag{31}$$

To calculate the mean value for failure function $\mu_x$ is used instead of variable X and the formula becomes;

$$\mu_g = g(\mu_X) = a_0 + a_1 \mu_{X_1} + \cdots + a_n \mu_{X_n} \tag{32}$$

Corresponding variance equation is expressed as;

$$\sigma_g^2 = a_1^2 \sigma_{X_1}^2 + \cdots + a_n^2 \sigma_{X_n}^2 + \sum_{i=1}^{n} \sum_{j=1, j \neq i}^{n} \frac{\partial g}{\partial X_i} \frac{\partial g}{\partial X_i} Cov(X_i, X_j) \qquad [33]$$

The linearized function is illustrated as follows according to Koç, 2013

$$g(X) = g(\mu_X) + \sum_{i=1}^{n} \frac{\partial g}{\partial X_i} (X_i - \mu_{X_i}) \qquad [34]$$

To obtain the $\mu_g$ and $\sigma_g$ following formulas are used;

$$\mu_g \cong g(\mu_{x1}, \dots, \mu_{xn}) \qquad [35]$$

$$\sigma_g^2 \cong \sum_{i=1}^{n} \sum_{j=1}^{n} \frac{\partial g}{\partial X_i} \frac{\partial g}{\partial X_i} Cov(X_i, X_j) \qquad [36]$$

To illustrate the failure probabilities of the reliability indices varying from 0 to 6, Table 55 is constructed.

**Table 55. The Reliability Indices and the Corresponding Failure Probabilities**

| Reliability Index, $\beta$ | Probability of Failure, $P_f$ |
|---|---|
| 0 | 0.5 |
| 1 | 0.159 |
| 2 | 0.0228 |
| 3 | 0.00135 |
| 4 | 0.0000317 |
| 5 | 0.000000287 |
| 6 | 0.000000000987 |

## 6.2 FAILURE FUNCTION

The survival function which is illustrated in Chapter 6.1 contains resistance and demand parts. The demand, Q, is classified as the total moment for ultimate state and the equation to calculate the total Q values are given in this section.

$D_1$ = Dead Load – Cast in Place Concrete

$D_2$ = Dead Load – Wearing Surface

$D_3$ = Dead Load – Miscellaneous

LL = Live Load – Truck Load

DF = Dynamic Factor

$$Q = D_1 + D_2 + D_3 + LL*(1+DF) \qquad [37]$$

## 6.3    TARGET RELIABILITY INDEX

Up to this point, there are a many different approaches to determine the target reliability index. The reliability index approach are explained in details in several bridge design specifications. In Annex C part of the Eurocode (EN 1990:2002) Basis of Structural Design, probability based design details are given. β is the reliability index, ϕ is the cumulative distribution function and $P_f$ is the failure probability of corresponding reliability index. The reliability index for related failure probabilities are given below.

**Table 56. Reliability Index for Related Failure Probabilities (Eurocode, 1990:2002)**

| Relation between β and $P_f$ | | | | | | | |
|---|---|---|---|---|---|---|---|
| Pf | $10^{-1}$ | $10^{-2}$ | $10^{-3}$ | $10^{-4}$ | $10^{-5}$ | $10^{-6}$ | $10^{-7}$ |
| β | 1.28 | 2.32 | 3.09 | 3.72 | 4.27 | 4.75 | 5.20 |

In serviceability life of bridges, there are many possible conditions to satisfy the necessary safety conditions considering reliability aspects. According to the Eurocode, there are several target reliability index for various design situations. Different consequences classes has been developed to illustrate the variation of reliability indices and these consequences are given in tabular form below.

**Table 57. Consequences Classes and Descriptions (Eurocode, 1990:2002)**

| Consequences Class | Description | Examples of buildings and civil engineering works |
|---|---|---|
| CC3 | High consequence for loss of human life, economic, social or environmental consequences very great | Grandstands, public buildings where consequences of failure are high (e.g. a concert hall) |
| CC2 | Medium consequence for loss of human life, economic, social or environmental consequences very great | Residential and office buildings, public buildings where consequences of failure are medium(e.g. an office building) |
| CC1 | Low consequence for loss of human life, economic, social or environmental consequences small or negligible | Agricultural buildings where people do not normally enter (e.g. storage buildings), greenhouses |

Three consequence classes of CC1, CC2 and CC3 are linked with three reliability classes such as RC1, RC2 and RC3. Table 58 shows the reliability indices for RC1, RC2 and RC3.

Table 58. Reliability Indices of Different Reliability Indices for 1 and 50 years of time periods (Eurocode, 1990:2002)

| Reliability Class | Minimum Values for $\beta$ | |
| --- | --- | --- |
| | 1 year reference period | 50 years reference period |
| RC3 | 5.2 | 4.3 |
| RC2 | 4.7 | 3.8 |
| RC1 | 4.2 | 3.3 |

According to the Eurocode 1990:2002 and TUBITAK 110G093 the reliability index for ultimate flexural strength cannot be less than 4.5. This values is obtained by considering the maximum reliability index values for 50 year reference period. As a result of the values from Eurocode, target reliability index is arranged as 4.5 for stage ultimate capacity.

## 6.4 RELIABILITY INDEX ACCORDING TO DIFFERENT TRUCKS IN ULTIMATE LIMIT STATE

Design procedures of the post-tensioned balanced cantilever bridges are performed according to the AASHTO LRFD bridge design specifications. Moreover, number of ducts are determined by aiming target reliability indices. In addition, necessary calculations are completed to check the design if it is satisfying the corresponding principal stresses at webs. Finally, when the whole design is completed, the reliability indices for different trucks at strength limit state are computed and compared. The contribution of truck moments to total moments are very limited, truck moment is changing 20 percent to 12 percent when it is compared to total moment. As a result of this, variation between the reliability indices of live load models are considerably low

except H30-S24 Truck Load. Span length of designed bridges are very high to normal bridges so, H30-S24 Truck Load gives significantly higher reliability index values comparing other load models. As the span length increases, H30-S24 Lane Load becomes more critical than KGM-45, due to the fact that H30-S24 Lane Load has 15 kN/m lane loading while lane loading of KGM-45 is 10.
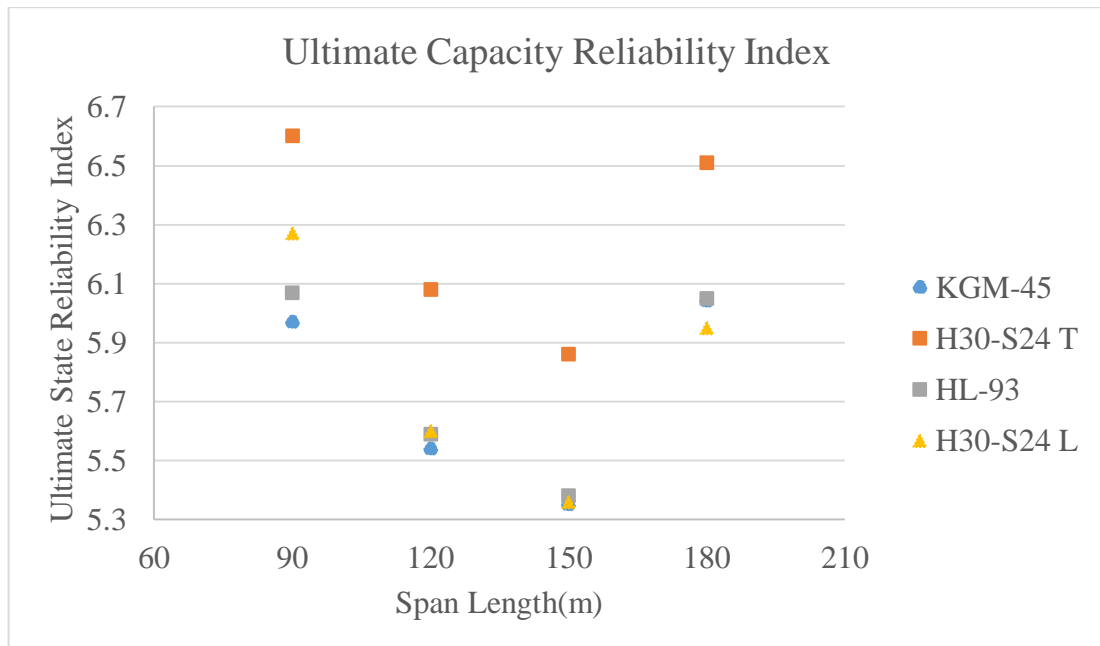


**Figure 126. Ultimate Capacity Reliability Index For Different Live Load Models**

## 6.5 RELIABILITY INDEX VS SUPERSTRUCTURE STRESS

Among the world, there are several bridge design codes with different specifications and load models. Load factors and permissible tension stresses for this codes, are determined through reliability analyses with the local conditions of the country. As a results of this, there are several variable to set a target reliability index for different limit states. AASHTO LRFD is arranged the reliability index around 3.5 for ultimate limit state. In this study, the resulting stresses from Service 3 load combination and corresponding ultimate state reliability indices are calculated and correlated. As a

127

result of this correlation the graphs are constructed from the Figure 127 to 131. There are different tension stress limits for varied target reliability indices.
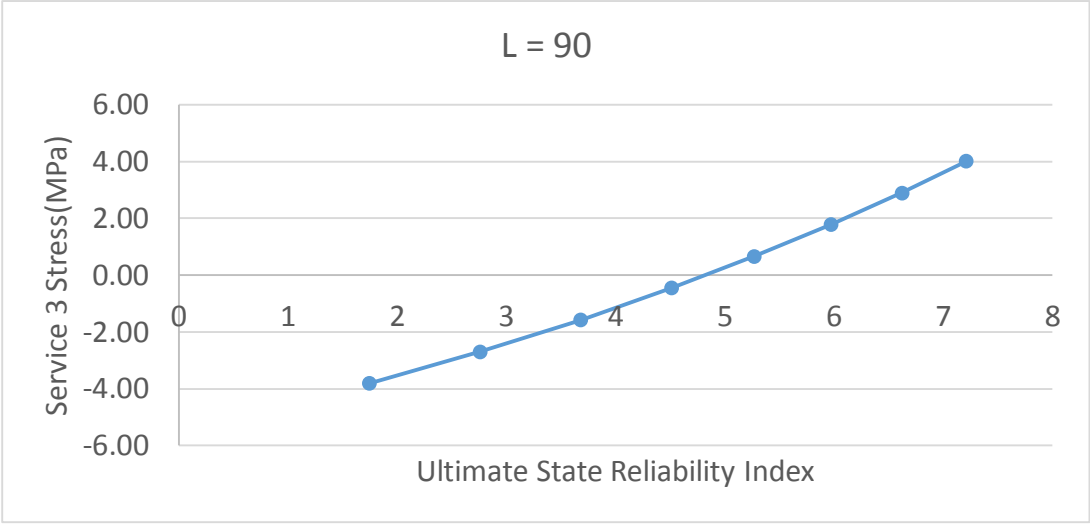


**Figure 127. Service 3 Stress vs Ultimate State Reliability Index L = 90**
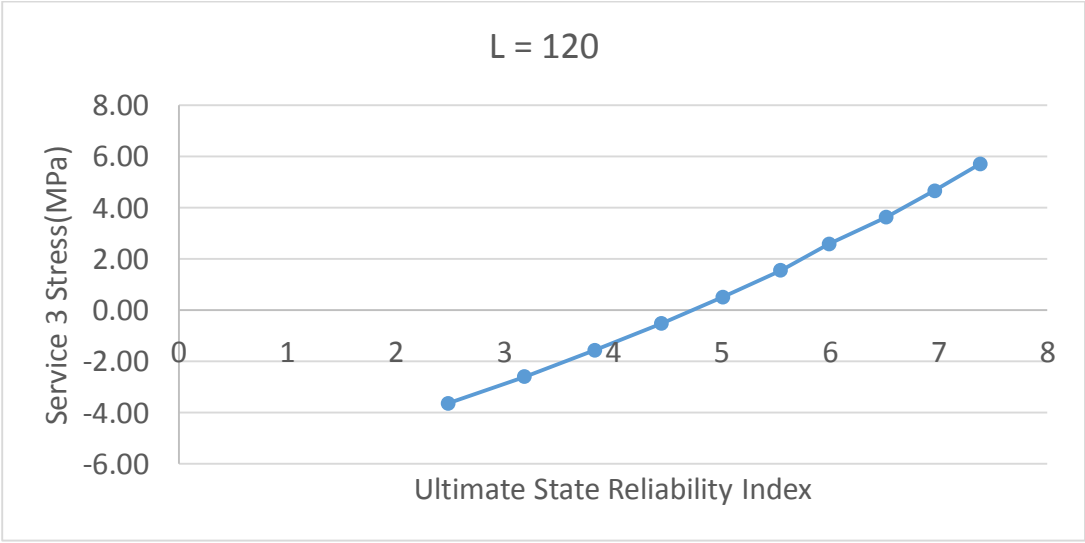


**Figure 128. Service 3 Stress vs Ultimate State Reliability Index L = 120**
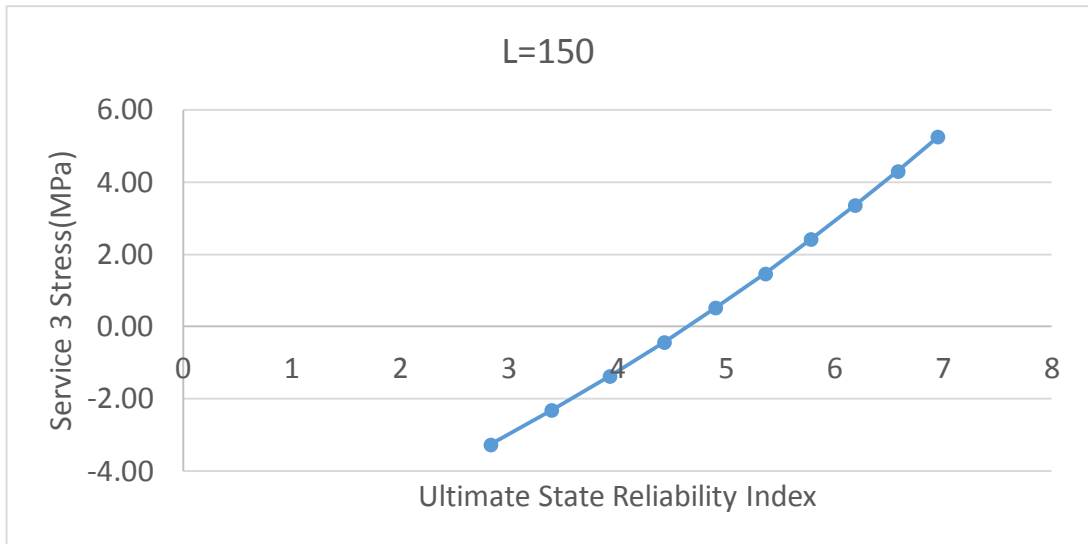
**Figure 129. Service 3 Stress vs Ultimate State Reliability Index L = 150**
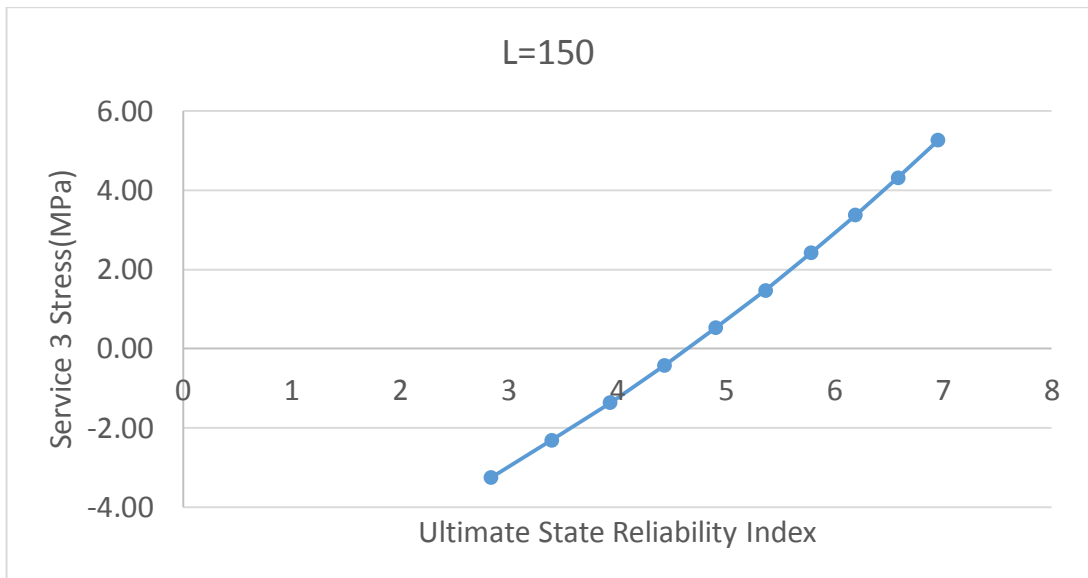


**Figure 130. Service 3 Stress vs Ultimate State Reliability Index L = 180**
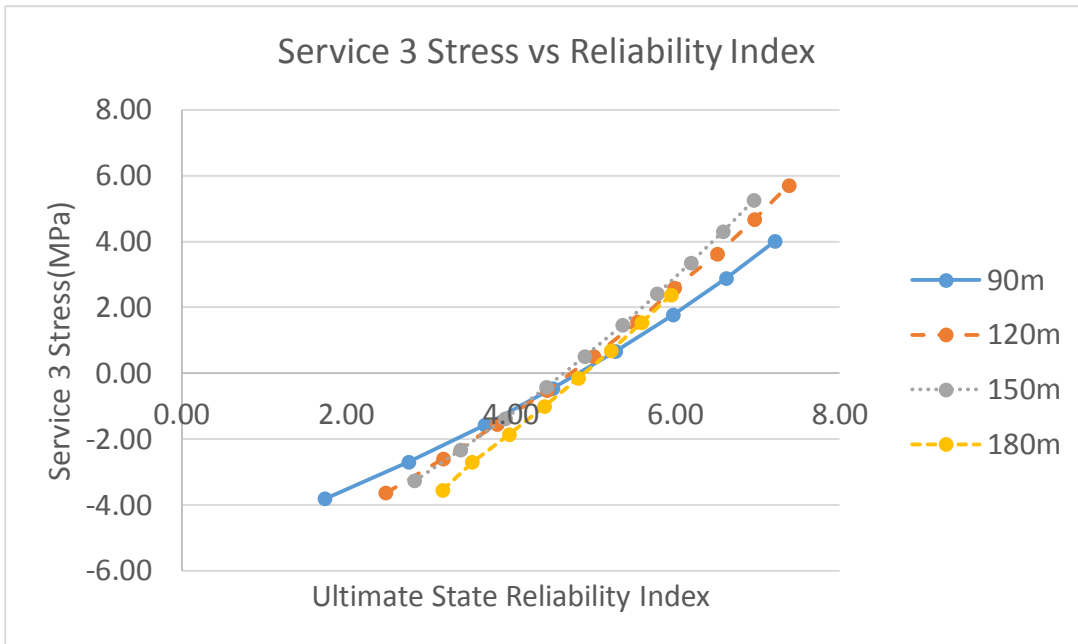
**Figure 131. Correlation Between the Reliability Indices and Service 3 Stresses for Different Span Lengths**

# CHAPTER 7

# CONCLUSION

## 7.1    SUMMARY AND COMMENTS

In designing highway bridges, AASHTO LFD Bridge Design Specifications were used in Turkey. On the other hand, design methods are evolved into probabilistic-based design which is named as Load Resistance Factor Design (LRFD). As a result of this, General Directorate of Highways of Turkey conducted a study with METU to complete a design guide similar to Load Resistance Factor Design of AASHTO. Within these studies a new live load model is created in this specification named as AYK-45, later General Directorate of Highways adopted the AYK-45 and convert its' name as KGM-45.

In this study, balanced cantilever post-tensioned bridge models are investigated. The bridges are composed of 3 spans and span length arrangement is designed as L/2 + L + L/2 and L is the main span length. Four different main span lengths are 90, 120, 150 and 180 meters. Negative moment regions are investigated due to the fact that it is the most critical criteria for balanced cantilever post-tensioned bridges. Moreover, constructional stage and ultimate moment capacity cases investigated separately. The most critical principal tensile stresses calculated to check the adequacy of design. KGM-45, H30-S24 Truck Load and HL-93 Live Load Models are investigated and

compared. The target reliability index for constructional stages is targeted as 4.5 and the corresponding reliability indices for ultimate moment capacity are calculated.

Uncertainties for load and resistance parameters such as bias factor and coefficient of variation are determined to complete the reliability calculations. To compute the reliability indices Mean Value First Order Second Moment Method is used. This study is performed to see the reliability indices of post-tensioned balanced cantilever bridge in Turkey. As a result of this, the statistical parameters of material and load variables are calculated according to conditions in Turkey. On the other hand, uncertainties of some parameters such as dead load, are adopted from Nowak's Calibration Report (1999).

Statistical parameters are determined for live loads according to the truck loads for Turkey. Truck database contains data from the years 2005, 2006 and 2013. There are 28054 truck data which contains axle distance and axle weights. Argınhan's study (2010) and Koç's study (2013) contains data from 2005 and 2006, moreover Dönmez (2015) expand this database with the truck data from 2013. To obtain the future effect of truck loads, this database is used to determine the statistical parameters and extrapolate truck data for 75 years. In extrapolation of truck loads, three different cases are investigated; overall, upper-tail and extreme cases. On the other hand, only the extreme case is used to calculate the reliability indices to evaluate the most critical truck loads in reliability approach.

Reliability index approaches are concluded with the computation of all span lengths according to live load models for Strength 1. Moreover, the resulting stresses of Service 3 and Stage Construction are matched with the reliability indices are expanded by trying different number of tendons and calculating different final stresses. As a result of this study, flexural tension limit stresses are defined for the reliability indices of 3.5 and 4.5. AASHTO LRFD defines the ultimate state reliability index as 3.5, on the other hand it should be 4.5 according to TUBITAK 110G093.

**Table 59. Service 3 Tension Limit**

| Reliability Index | Turkish Design Code | | AASHTO |
|---|---|---|---|
| | 4.5 | 3.5 | 3.5 |
| 90 | $0.07\sqrt{f_c}$ | $0.28\sqrt{f_c}$ | $0.24\sqrt{f_c}$ |
| 120 | $0.06\sqrt{f_c}$ | $0.33\sqrt{f_c}$ | $0.24\sqrt{f_c}$ |
| 150 | $0.05\sqrt{f_c}$ | $0.34\sqrt{f_c}$ | $0.24\sqrt{f_c}$ |
| 180 | $0.13\sqrt{f_c}$ | $0.52\sqrt{f_c}$ | $0.24\sqrt{f_c}$ |

In this study, reliability index for the ultimate flexural capacity is targeted as 4.5 for the construction per TUBITAK 110G093(2014). To achieve the target reliability index, it is suggested that the tension limit of the concrete should be less than $0.05 * \sqrt{f_c}$ for Service 3 Load Combination. The same limit recommended in AASHTO is $0.24\sqrt{f_c}$ and unconservative for designs in Turkey. This difference is mainly believed to develop due to use of a different design truck and a lower target reliability index for US designs.

The AASHTO LRFD specification targets a reliability index of 3.5 and results in a tension limit of $0.3*\sqrt{f_c}$ that is 600 percent more than the recommendation for the new Turkish Design System.

The KGM-45, HL-93 and H30-S24L almost resulted in similar reliabilities for the given four different bridges. The H30-S24T Truck generates much less force effects on the bridge that results in higher safety for the fix design of each bridge.
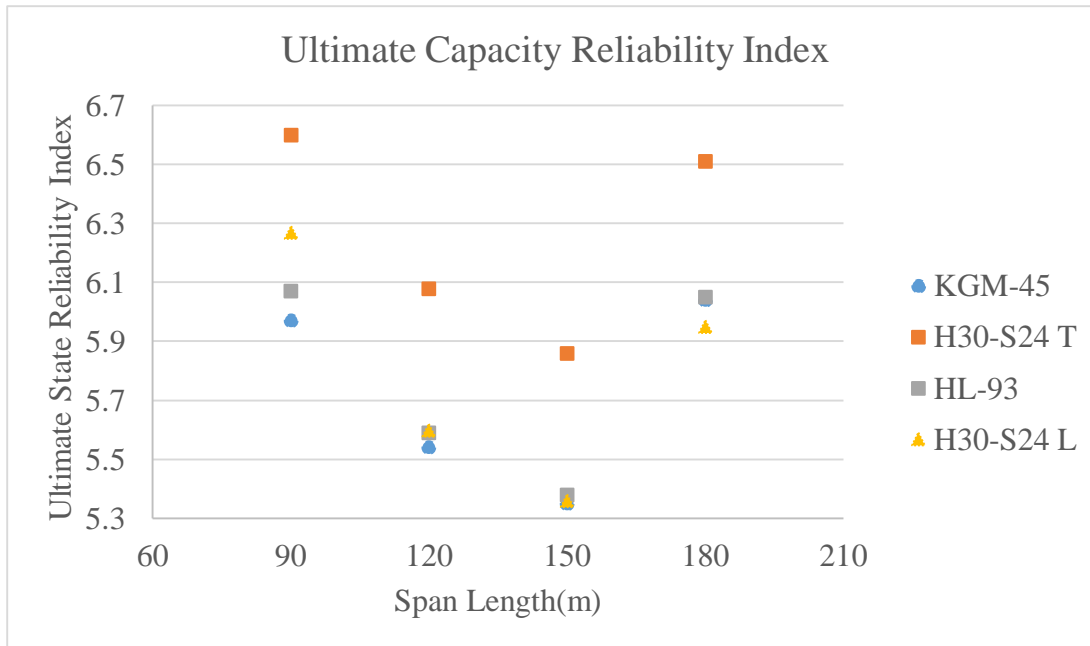
**Figure 132. Ultimate Capacity Reliability Index For Different Live Load Models**

## 7.2 FUTURE STUDIES

In this study, the reliability indices are investigated for post-tension bridges which is built by balanced cantilever method. Both constructional stages and ultimate conditions are considered. Reliability analyses is performed for the negative moment region of superstructure. Shear failure is also investigated according to the most critical case for web of box section.

The target reliability index is arranged as 4.5 for the ultimate state and the corresponding Service 3 stresses are calculated according to KGM-45, H30-S24 Truck, H30-S24 Lane Loading and HL-93 live load models. In future, there can be a necessity for load factor calibration of KGM-45 live load model due to the fact that it is a new one. Moreover, the reliability process is only consists live loads for this study, other parameters can be also studied.

To conclude, there are several bridge components such as pier, pier caps, abutments, foundations and piles that are likely fail for different conditions and each of them can be studied separately. Moreover, a cost optimization can be performed for reliability index approach to evaluate the necessity for higher or lower level of target reliability index.

# REFERENCES

American Association of State Highway and Transportation Officials. (2007). AASHTO LRFD Bridge Design Specifications. Washington DC.

American Association of State Highway and Transportation Officials. (2010). AASHTO LRFD Bridge Design Specifications. Washington DC.

Ang, A . H.-S.,Tang, W. H. (1984). Probability Condepts in Engineering Planning and Design, Vol. 2: Decision, Risk, and Reliability. John Wiley & Sons Inc.

Argından, O. (2010). Reliability Based Safety Level Evaluation of Turkish Type Precast Prestressed Concrete Bridge Girders Designed in Accordance with the Load and Resistance Factor Design Method, M.Sc. Thesis. Ankara: The Graduate School of Natural and Applied Sciences, METU.

Caner, A.(2011). Highway and Railroad Infrastructure Lecture Notes

Castillo, E. (1988). Extreme Value Theory in Engineering. Academic Press Inc.

Fırat, F.K. (2006). Türkiye'de Kullanılan Betonun Kalitesinin İstatistiksel Olarak İncelenmesi. Yedinci Uluslararası İnşaat Mühendisliğinde Gelişmeler Kongresi, 11-13 Ekim 2006. İstanbul: Yıldız Teknik Üniversitesi.

Fırat, F.K. (2007). Development of Load and Resistance Factors for Reinforced Concrete Structures in Turkey, Phd. Thesis. Ankara: The Graduate School of Natural and Applied Sciences, METU.

Koç, A.F. (2013). Calibration of Turkish LRFD bridge Design Method for Slab on Steel Plate Girders, M.Sc. Thesis. Ankara: The Graduate School of Natural and Applied Sciences, METU.

T.C. Bayındırlık Bakanlığı, Karayolları Genel Müdürlüğü, (1982). Yol Köprüleri için Teknik Şartname. Ankara: Karayolları Genel Müdürlüğü Matbaası.

Dönmez, Y. (2015). Turkish LRFD Live Load Design Parameters for Cable Stayed Bridge with Concrete Deck on Steel Girder, M.Sc. Thesis. Ankara: The Graduate School of Natural and Applied Sciences, METU.

Xie H.- Wang Y.-Zou R.(2013). Reliability Analysis of RC-T-Beam Highway Bridges in China Based on a Virtual Bridge Dataset

Nowak, A.S.-Park, C.H-Casas, J.R.(2001). Reliability Analysis of Prestressed Concrete Bridge Girders: Comparison of Eurocode, Spanish Norma IAP and AASHTO LRFD

Ministry of Communications of PRC.JTG D62-2004, code for design of highway reinforced concrete and prestressed concrete bridges and culverts. Beijing: China Communications Press; 2004 [in Chinese]

Nowak, A. S. (1999).NCHRP Report 368: Calibration of LRFD Bridge Design Code. Washington, DC: National Academy Press

Norma IAP-98, "Actions in Highway Bridfes", Road Directorate, Spanish Ministry of Public Works, Madrid, 1998.

Nassih, H. H., Nowak, A. S. (1995). Dynamic Effect of Truck Loads on Girder Bridges. Road Transport Technology – 4 (pp. 383-387). Ann Arbor: University of Michigan Transportation Research Institute.

Karakule, F.-Akakın, T.(2005). Hazır Beton Sektörünün Gelişimi. Deprem Sempozyumu Kocaeli 2005.

Akakın, T.-Kılınç, C.-Işık, A.-Zengin, H.(2013). Hazır Beton Kongresi 2013. Türkiye Hazır Beton Birliği.

Mirza, S.A., Hatzinikolas, M. And MacGregor J.G., Statistical Description of the Strength of Concrete, Journal of the Structural Division, ASCE, Vol 105, No ST6, pp.1021 – 1037, 1979.

Kömürcü, A.M., A Probabilistic Assessment of Load and Resistance Factors for Reinforce Concrete Structures Considering the Design Practice in Turkey, M.Sc. Thesis, Department of Civil Engineering, METU, Ankara, 1995

Al-Harty AS, Frangopol DM. Reliability Assessment of Prestressed Concrete Beam. J Struct Eng 1994; 120(1): 180-99

Mirza SA, Kikuchi DK, MacGregor JG. Flexural Strength Reduction Factor for Bonded Prestressed Concrete Beams. J ACI 1980;77(4):237-46

Mirza, S. A. And MacGregor, J.G. Variations in Dimensions of Reinforced Concrete Members, Journal of Structural Divisions, ASCE Vol. 105, NO. ST4, pp. 921-937, 1979

BS EN 1991-2:2003 Eurocode 1: Actions on Structures-Part 2: Traffic Loads on Bridges

TUBITAK 110G093(2014), Türkiye Köprü Mühendisliğinde Tasarım ve Yapıma İlişkin Teknolojilerin Geliştirilmesi Teknik Kılavuzu

Barker R. M., Puckett J.A. Design of Highway Bridges An LRFD Approach. Second Edition. John Wiley and Sons INC. 2007

Larsa 4D v7.08.05 : LARSA, Inc., New York, USA

BS EN 1990:2002 Eurocode – Basis of structural design

ASM Handbook, Volume 1: Properties and Selection: Irons, Steel, and High-Performance Alloys, pp 673-688, 1990

Elements of Metallurgy and Engineering Alloys, 2008